



*Alma Mater Studiorum - Università di Bologna*

---

**DOTTORATO DI RICERCA IN BIOCHIMICA**

SETTORE DISCIPLINARE MED/03 (GENETICA MEDICA)

**ANALYSIS OF *TNFRSF5* GENE MUTATIONS  
AND SPLICING VARIANTS IN CD40 RECEPTOR  
REGULATION**

Tesi di Dottorato di:

Dott. *Stefano Caraffi*

Relatore:

*Chiar.mo Prof. Giovanni Romeo*

Correlatore:

*Dott.ssa Simona Ferrari*

Coordinatore:

*Chiar.mo Prof. Giorgio Lenaz*

*XIX ciclo*

---

Anno Accademico 2005-2006



*Alma Mater Studiorum - Università di Bologna*

---

**DOTTORATO DI RICERCA IN BIOCHIMICA**

SETTORE DISCIPLINARE MED/03 (GENETICA MEDICA)

**ANALYSIS OF *TNFRSF5* GENE MUTATIONS  
AND SPLICING VARIANTS IN CD40 RECEPTOR  
REGULATION**

Tesi di Dottorato di:

Dott. *Stefano Caraffi*

Relatore:

*Chiar.mo Prof. Giovanni Romeo*

Correlatore:

*Dott.ssa Simona Ferrari*

Coordinatore:

*Chiar.mo Prof. Giorgio Lenaz*

*XIX ciclo*

---

Anno Accademico 2005-2006

*This is just for you.*

Stefano Caraffi

19

RESILIENCE

# CONTENTS

<b>1. INTRODUCTION</b>	<b>1</b>
1.01 CD40 plays a key role in the immune system	1
1.02 CD40 gene and protein structure	3
1.03 CD40-CD40L interactions	5
1.04 Intracellular signalling events	7
1.05 Biological effects of CD40 activation on B cells	10
1.06 Biological effects of CD40 activation on other cells	14
1.07 CD40-CD40L signalling defects cause Hyper-IgM syndromes	16
<b>2. MATERIALS AND METHODS</b>	<b>20</b>
2.01 Human <i>TNFRSF5</i> gene analysis	20
2.02 Cell cultures	21
2.03 B cells separation and stimulation	22
2.04 Flow Cytometry	23
2.05 Human CD40 transcripts analysis	23
2.06 Construction of recombinant vectors from CD40 transcript variants	25
2.07 Transient transfections and stable transfectants	26
2.08 Western Blot	27
2.09 Cell fractionation	28
2.10 Immunofluorescence staining and confocal microscopy	28

<b>3. RESULTS AND DISCUSSION</b>	<b>30</b>
3.01 Characterization of HIGM-3 patients	30
3.02 Identification of CD40 transcript variants in B-LCLs	33
3.03 Detection of CD40 splicing variants in subpopulations of human B lymphocytes	38
3.04 Detection of CD40 transcript variants in several different human tissues	42
3.05 Six CD40 splicing variants are conserved throughout different cell types	44
3.06 Detection of the CD40 protein	48
3.07 Recombinant constructs and stable cell lines expressing CD40 and its variants allow considerations on protein stability	51
3.08 Exposure of the CD40 variants on the plasma membrane	53
3.09 Localization of the CD40 protein variants within cell compartments	56
3.10 Analysis of CD40 splicing in neuroblastoma cell lines	60
<b>4. CONCLUSIONS</b>	<b>63</b>
<b>APPENDIX A</b>	<b>65</b>
<b>ANALYSIS OF CD45 ISOFORMS VALIDATES A RAPID AND SENSITIVE METHOD FOR THE SCREENING OF TRANSCRIPT VARIANTS.</b>	
<b>REFERENCES</b>	<b>72</b>
<b>ACKNOWLEDGEMENTS</b>	<b>85</b>

# 1. INTRODUCTION

## **1.01 - CD40 PLAYS A KEY ROLE IN THE IMMUNE SYSTEM**

The immune system is a sophisticated organization of molecules, cells and tissues devoted to defend the host against infection. It can act through innate immunity, which serves as a first line of defence but lacks the ability to recognize certain pathogens and to provide the specific protective immunity that prevents reinfection, and through adaptive immunity, based on clonal selection from a repertoire of lymphocytes bearing highly diverse antigen-specific receptors that enable the immune system to recognize any foreign antigen. Host defense requires many different recognition systems and effector mechanisms to seek out and destroy the wide variety of pathogens in their various habitats within the body and at its surface.

Cytokines are small proteins that play a central role in the regulation of many aspects of both innate and adaptive immunity, including cell maturation, proliferation, recruitment at the site of infection and activation of the effector functions; they also control the development and organization of peripheral lymphoid tissues. They are produced by various cells in the body, usually in response to an activating stimulus, and induce responses through binding to specific receptors. They can act in an autocrine manner, affecting the behavior of the cell that releases the cytokine, or in a paracrine manner, affecting the behavior of adjacent cells. Some cytokines can act in an endocrine manner,

affecting the behavior of distant cells, although this depends on their ability to enter the circulation and on their half-life. One of the major structural families of cytokines, the tumor necrosis factor (TNF) family, are trimeric proteins that are often associated with the cell surface. They all bind members of the tumor necrosis factor receptor (TNFR) superfamily, a group of integral membrane glycoproteins that trigger multiple signal transduction pathways with functions in both innate and adaptive immunity [1].

**CD40** is a member of the TNFR superfamily and was first identified in 1984 on the surface of B lymphocytes [2]. Therefore, research on CD40 was initially focused around the regulation of humoral immune responses. CD40 was identified as a molecule expressed during all stages of B cell development and differentiation, whereas its ligand, **CD40L** (CD154), was mainly expressed on activated CD4<sup>+</sup> T cells. The pivotal role of CD40-CD40L in T cell-dependent B cell responses was proven by the finding that individuals with mutations in the gene encoding CD40L suffered from a severe immune deficiency, the X-linked hyper-IgM syndrome (XHIGM or HIGM-1) [3-7]. CD40-CD40L interactions were found essential to elicit a specific, adaptive humoral immune response from B cells through immunoglobulin (Ig) isotype switching and affinity maturation, and to promote germinal center formation and memory B cell development [8]. Similar deficiencies in mounting immune responses were observed in genetically modified mice with inactivation of either the CD40 or CD40L gene [9-10]. After this breakthrough finding, research on CD40-CD40L has expanded in various directions. It was found that CD40 expression was much broader than initially thought, encompassing B cells, basophils, eosinophils, monocytes, dendritic cells (DC), and even non-hematopoietic cells such as endothelial cells, keratinocytes, smooth muscle cells, epithelial cells and fibroblasts [8, 11]. In addition, CD40L, though mainly expressed in mature CD4<sup>+</sup> T cells, was also found on basophils, eosinophils, monocytes, macrophages, dendritic cells, NK cells, B lymphocytes, platelets, mast cells, endothelial cells, smooth muscle cells and

epithelial cells [11]. A common feature of all these cells is that CD40L expression is non-constitutive, but can be rapidly induced upon activation.

## **1.02 - CD40 GENE AND PROTEIN STRUCTURE**

A cDNA encoding human CD40 was isolated by expression cloning from a library of the Burkitt lymphoma Raji [12]. The murine cDNA was cloned from lipopolysaccharide (LPS) + Interleukin-4 (IL-4) stimulated murine B cells by cross-hybridization with the human cDNA probe [13]. Southern blot analysis demonstrated that the mouse CD40 gene is a single copy gene located on the distal region of chromosome 2, which is syntenic to human chromosome 20q11-q13 [14]. Accordingly, the human CD40 gene, *TNFRSF5*, was mapped to chromosome 20 by using human-rodent somatic cell hybrids and to 20q12-20q13.2 by in situ hybridization [15]. *TNFRSF5* spans a 11.5 Kb region of genomic DNA and consists of nine exons, initially thought to be expressed as a single 1.5 Kb mRNA. It has been demonstrated that the murine CD40 homolog is expressed through alternative splicing as five different transcripts, at least two of which productively translated into functional proteins [16]. In the present work we propose that a similar complex splicing pattern also concerns the human transcript.

The 1.5 Kb mRNA encodes a protein of 277 amino acid (aa) residues [17]. Although its crystal structure has not yet been resolved, a model has been built through the use of homology modeling, mutagenesis, X-ray structures of TNFR, and alignment of the TNFR family [19]. According to this model, CD40 comprises a 193 aa N-terminal extracellular domain, including a 21 aa leader sequence (encoded by exon 1), a 22 aa transmembrane domain (entirely encoded by exon 7), and a 62 aa C-terminal intracellular tail (Genbank no. X60592). Therefore, CD40 has the structure of a typical type I transmembrane

protein. Biochemical characterization suggests that the mature CD40 protein is a phosphorylated glycoprotein that migrates in sodium dodecyl sulfate (SDS) polyacrylamide gel electrophoresis as a 43-48 kDa polypeptide under both reducing and non-reducing conditions. It is hydrophobic, with an acidic pI of 3.2. It has two (Asn153, Asn180) conserved N-linked glycosylation sites (Swissprot no. P25942) [8].

The extracellular segment of CD40 contains 20 cysteine residues which are thoroughly conserved in its murine and bovine homologs. Like all other TNF receptors, it is organized in a number of Cysteine-Rich Domains (CRD), in which disulfide bonds between the Cys residues are critical for correct folding. Initially it was suggested that CD40 would form 4 CRDs of about 40 aa each. More recently the modularity of the TNFR family has been refined, suggesting that every domain is actually built of two modules, with five different forms of modules being identified, each one stabilized by one or two disulfide bonds (Figure 1.01) [19].

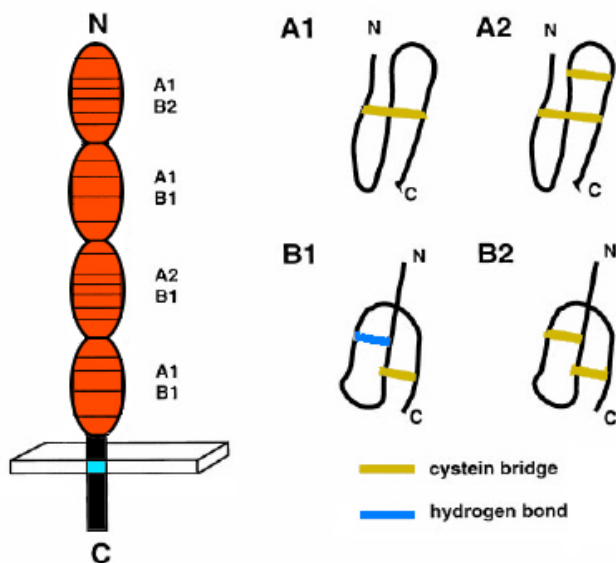


**Fig. 1.01** - Schematic representation of the CD40 protein. The extracellular region of CD40 is cysteine-rich (20 residues), as indicated by the horizontal lines. Each of the four CRDs can be subdivided into two cysteine modules, chosen among the A1, A2, B1, B2 TNFR-homology building blocks. Chains are connected by one or two cysteine bridges as indicated in red, whereas in the B1 module, an additional hydrogen bond (in blue) is formed.

The intracellular region of CD40 does not bear a close relationship to any other characterized molecule. Unlike most other TNFRs, it has no death domain; instead, it is linked to proteins called TRAFs (TNF-receptor-associated factors), a recently identified class of cytoplasmic messengers that interact in ways still largely unknown [1].

### **1.03 - CD40-CD40L INTERACTIONS**

The structure of the TNF-like extracellular region of human CD40L (spanning from Gly116 to Leu261) has been resolved by X-ray crystallography at a resolution of 2 Å [20]. CD40L is a sandwich of two  $\beta$ -sheets with jelly-roll topology and forms a threefold symmetric homotrimer (Brookhaven no. 1ALY). The three-dimensional organization is similar to that described for the TNF- $\alpha$  and LT $\alpha$  proteins, as predicted by initial modeling studies. Combining these data with the proposed structural model for the CD40 receptor, it has been suggested that each CD40L trimer recruits three CD40 molecules on the surface of the target cell, and forms polar interactions based on three acidic residues (D84, E114, E117) on CD40 and three basic residues (K143, R203, R207) on CD40L. These results are mostly compatible with earlier mutagenesis studies identifying CD40: E74, Y82, D84, N86, E117 and CD40L: K143, Y145, Y146, R203, Q220 as the residues involved in CD40-CD40L interactions [21]. Thus the CD40L binding site has been shown to be located in the second and third CRD of CD40.

The exact mechanism through which the extracellular binding of CD40L can elicit a response within the cytoplasm of target cells is still controversial. While it has been demonstrated that the stimulatory capacity of different anti-CD40 antibodies depends on the location of the epitope on CD40 [22-23] and it has been suggested that binding of CD40L induces a conformational change in CD40 necessary for signal transduction [24-26], recent experiments in a murine B cell line with a series of deletion constructs showed that none of the extracellular domains are essential for signalling via human CD40 [27]. Some functions, like proliferation induction, are more epitope dependent, whereas others, like rescue from apoptosis, are essentially epitope independent and probably rely simply on the cross-linking of the receptors [26].

By comparing the ability of soluble monomeric, dimeric and trimeric CD40 variants to activate transcription factors in the cytosol, it has been shown that the minimal requirement to induce a signal through CD40 is the formation

of a receptor dimer [28], although trimerization generates a stronger signal. According to Haswell et al. [29] increasing valency of the extracellularly applied ligand correlates with the strength of the receptor-mediated signal. Furthermore, it has been shown that the type and differentiation stage of the target cell determines not only the functional consequences of CD40 signalling [8], but also the level of cross-linking required to initiate a certain signalling pathway [25]. Accordingly, ligation via trimeric CD40L expressed on a cell membrane was shown to be essential for the activation of some particular signalling pathways, such as IL-6 production in naive B cells [30].

Several members of the TNFR superfamily spontaneously form oligomers on the cell surface even in the absence of a ligand. It has been demonstrated that oligomerization of Fas, TNFR1 and TNFR2 depends on a conserved domain within the distal extracellular CRD [31-32]. The domain that mediates this interaction has been named pre-ligand assembly domain (PLAD) [33]. Though the PLAD seems to be physically distinct from the ligand contact domains, its presence is required for ligand binding [32]. It has been known for a long time that CD40 purified from resting B cells, under nonreducing conditions, forms dimers and multimers [17]; recently, FRET analysis confirmed pre-ligand association of CD40 in the plasma membrane [33]. Although it has not yet been shown which CD40 domain is responsible for pre-ligand assembly, homology studies suggest that PLAD is feasibly located in CRD1 [34], and it has been demonstrated that this domain is in fact required for CD40L-CD40 interaction, even though it does not contain any of the residues that are known to be important for ligand binding [35]. It ensues from this evidence that ligand-induced signalling cannot result from simple oligomerization of the receptor. It rather implies that ligand binding produces a change in the arrangement of the receptor that allows adapter molecules to bind. The advantages this pre-assembly system provides to the TNFRSF are, however, not fully understood. It may be a route to down-regulate the susceptibility for ligand-induced signalling by assembly of functional receptors together with non-functional receptors lacking the intracellular domain [31]. As

an alternative explanation, ligand binding might promote the formation of a super cluster [32-34], which in turn initiates intracellular signalling events. Though pre-ligand association seems to be dispensable in CD40-mediated B cell proliferation [27], it cannot be excluded that some of the CD40 signalling pathways require the PLAD.

It was recently found that CD40 depends on the microenvironment of lipid rafts to function optimally [36-38], although one group reported conflicting results [39]. Lipid rafts (also denominated membrane rafts) are cholesterol- and glycosphingolipid-enriched micro-domains that serve as an assembly site for several receptor complexes of central importance in the immune system. For instance, the B cell receptor can be recruited in rafts after stimulation [40]; likewise, engagement of CD40 results in the translocation of CD40, as well as of its downstream signalling mediators TRAF2 and 3, to lipid rafts [36, 38]. Active formation of CD40L clusters is required for subsequent formation of CD40 clusters, which in turn is central for initiation of CD40 signalling [41].

#### **1.04 - INTRACELLULAR SIGNALLING EVENTS**

Studies on CD40 signal transduction have resulted in a complex picture of the different mediators and pathways involved. Although CD40 has no kinase domain, CD40 ligation activates several second messenger systems. Among the earliest detectable events after CD40 engagement are the activation of protein tyrosine kinases (PTKs, including lyn, syk, and Jak3), activation of phosphoinositide-3 kinase (PI-3 kinase) and phospholipase C $\gamma$ 2 [8]. Activation of protein kinase A (PKA) has been controversial, but it has been shown that cAMP can modulate both positive and negative CD40-induced responses [42]. In recent years many studies have concentrated on the involvement of

serine/threonine kinases: stress-activated protein kinase/c-jun amino-terminal kinase (JNK/SAPK), p38 MAPK, and extracellular signal-regulated mitogen-activated protein kinase (ERK). Contrasting results have been obtained regarding JNK, p38, or ERK activation [43-45]. However, general conclusions should be taken with care because these studies often have used different cellular models. For instance activation of different B cell subsets results in opposite biological effects, depending on the differentiation/activation stage of the cells, which is probably a reflection of different routes of signal transduction.

Coupling of the CD40 receptor to different signalling pathways has been better understood by the identification of TRAFs. With the two-hybrid system, such protein-protein interactions have been demonstrated for several members of the TNFR family. At present six different members of the TRAF family have been identified. It is interesting that, although there is little cross reactivity between the extracellular ligands of the TNFR family, the intracellular ligands seem to be much more promiscuous and form a complex network of homo- and heterodimers. Mutagenesis of the intracellular part of CD40 has provided more insight into the coupling to different signal transduction pathways.

The first member identified as a protein associated with CD40 has been TRAF3, a 62 kDa intracellular protein that is expressed in almost all cell types [46]. It contains several functional domains involved either in signal transduction (RING finger domain, isoleucine zipper, zinc finger) or in protein-protein interactions either to associate with CD40 or to form homo-/heterodimers. TRAF3 knockout mice show an apparently normal signaling in B cells, whereas T cell activation is impaired, already pointing at the redundancy of the TRAF molecules [47].

CD40 also associates with TRAF2, a molecule that interacts with TNFR2. Induction of NF- $\kappa$ B activation after CD40 cross-linking can in large part be attributed to TRAF2 signaling. Crystallography of the TRAF domain of TRAF2 showed a spontaneous trimeric self-association, suggesting that the need for receptor trimerization might be based on the avidity for the TRAF2

trimer [48]. Finally, two other TRAF proteins, TRAF5 and TRAF6, were also demonstrated to associate with the CD40 receptor [49]. Inactivation of the TRAF5 gene resulted in hampered B cell proliferation and up-regulation of various surface receptors [50]. Using wild-type CD40 and a cytoplasmic tail deletion mutant only containing the binding site for TRAF6 (CD40d246), it was demonstrated that CD40 activates ERK both by a ras-dependent pathway and a ras-independent pathway involving TRAF6 [51].

Early mutagenesis studies also suggested a critical role for the Thr residue at position 254 (complete coding sequence), implicated in TRAF3 binding [52]. TRAF3 was cloned by screening for proteins that can interact with the Epstein-Barr virus (EBV) transforming gene product LMP1 (latent infection membrane protein-1) [53]. Physiologically, TRAF-mediated signals will be launched by trimerization of surface receptors. After EBV transformation, it is likely that the oligomerization of these molecules is obtained by the spontaneous aggregation capacity of the LMP1 molecule. This indicates that EBV utilizes the CD40 signaling pathway to activate and immortalize B lymphocytes. Continuous expression of LMP1 is essential for the proliferation of the EBV-immortalized B cells [54]. Generation of chimeric proteins suggest that CD40-induced and LMP1-induced pathways are completely overlapping [55].

After early biochemical changes, these signals are translated into the activation of specific transcription factors that drive further gene activations. Cross-linking of CD40 on B cells and other cells results in activation of NF- $\kappa$ B and NF- $\kappa$ B-like transcription factors. Gel retardation assays showed the presence of, at least, the NF- $\kappa$ B family members p50, p65 (relA), and c-Rel. Activation of NF- $\kappa$ B has been described as a downstream effect of various members of the TRAF family (TRAF2, 5, 6) [56]. CD40-induced NF- $\kappa$ B activation is at least partially mediated by a dramatic decrease in the half life of both I $\kappa$ B- $\alpha$  and I $\kappa$ B- $\beta$  in a proteasome-dependent manner [57].

Next to NF- $\kappa$ B, CD40 cross-linking results in the expression/activation of AP1 and NF-AT transcription factors, as well as members of the Jak-STAT pathway, an important route in the signaling of many cytokines. CD40 is associated with Jak3, and activation leads to phosphorylation of STAT3 [58]. In addition, CD40 triggering can activate the STAT6 transcription factor [59].

### **1.05 - BIOLOGICAL EFFECTS OF CD40 ACTIVATION ON B CELLS**

Extensive studies on CD40 activation of B cells have demonstrated that CD40 activation has major effects on many steps of the B cell natural history [8]. Some CD40 functions are mediated through a cross-talk with the B cell antigen receptor (BCR) complex [60], which consists of the membrane-bound immunoglobulins generated in the bone marrow during B cell maturation and relies on association with small transmembrane proteins, Ig- $\alpha$  and Ig- $\beta$ , for intracellular signal transduction. *In vitro* studies have shown direct effects of CD40 activation on cytokine production (IL-6, IL-10, TNF- $\alpha$ , LT- $\alpha$ ), expression of adhesion molecules and costimulatory receptors (ICAM, CD23, B7.1/CD80, B7.2/CD86), and increased expression of Major Histocompatibility Complex (MHC) class I, MHC class II, and TAP transporter [61]. These molecules, which all contribute to the biological function of the B cells, have also provided the tools to study signal transduction pathways in more detail. CD40 usually acts in concert with either cytokines or other receptor-ligand interactions to guide B lymphocytes through their differentiation program, and it was shown to induce re-expression of telomerase activity in memory B cells, thereby contributing to an expanded lifespan of these cells [62].

*In vivo*, most of these processes take place in germinal centers, specialized microenvironments within secondary lymphoid organs. The inner

region consists of rapidly proliferating mature B cells, which progressively migrate outwards and make contact with follicular dendritic cells (FDC) and with T cells in the outer mantle zone. Upon entering the germinal center, B cells are inherently prone to die. Simultaneous cross-linking of their BCRs by antigens and engagement of their cell-surface CD40 by CD40L must occur in order to rescue B cells from apoptosis and initiate proliferation, thus forming the germinal center. Antigen can be provided in the form of immune complexes on follicular dendritic cells, or by live pathogens themselves which are carried to the lymphoid tissues and multiply there until eliminated by the immune response, after which the germinal center decays. CD40L is provided by contact with activated or 'armed'  $T_H2$  cells, a subclass of  $CD4^+$  T helper cells. Additional signals required for survival are also delivered by direct contact with T cells. One such signaling system, involving the TNF family member BlyS (B lymphocyte stimulator) on T cells and TACI (its receptor) on B cells, has recently been found to be essential for the maintenance of germinal centers. How these signals exert their effects on B cells is not completely understood. The combined signals from the B-cell receptor and CD40 seem to upregulate a protein called Bcl- $X_L$ , a relative of Bcl-2, which promotes B-cell survival.

Armed  $T_H2$  cells activate B cells when they recognize the appropriate peptide:MHC class II complex on the B-cell surface. As with armed  $T_H1$  cells acting on macrophages, recognition of peptide:MHC class II complexes on B cells triggers armed helper T cells to synthesize both cellbound and secreted effector molecules that synergize in activating the B cell. Other than CD40L, secretion of the cytokine interleukin-4 (IL-4) is required to drive the resting B cell into the cell cycle. After several rounds of proliferation, two additional cytokines secreted by helper T cells, IL-5 and IL-6, contribute to the differentiation of B cells into antibody-secreting plasma cells, which provide Ig-mediated immune responses against extracellular pathogens (such as bacteria) and many viruses, and memory B cells, ready to respond rapidly during re-infection situations [1].

The primary antibody repertoire is generated in the bone marrow by means of the V(D)J recombination process that allows genomic rearrangement between variable (V), diversity (D), and joining (J) elements of the Ig heavy (CH) and light (LH) chain genes. As a result of this process, IgM and IgD antibodies are generated largely in an antigen-independent way. However, to produce potent and specific antibody responses to foreign antigens, CD40 acts in concert with either cytokines or other receptor-ligand interactions to shape a secondary antibody repertoire in peripheral lymphoid organs, by means of class switch recombination (CSR) and somatic hypermutation (SHM) [63].

CSR or isotype switching determines the effector function of antibodies produced by specific B cell clones via replacement of the Ig  $\mu$  heavy chain ( $C_\mu$ ) with other constant ( $C_X$ ) heavy chains, derived from genomic elements located downstream from  $C_\mu$  in the immunoglobulin heavy chain (IGHC) gene cluster. It is a 'region-specific' DNA recombination mechanism consisting in the formation of a DNA double-strand break (dsb) by an as yet unidentified nuclease, the excision of the intervening sequences as a circularized episomal fragment, and the subsequent DNA repair by nonhomologous end-joining (NHEJ) mechanisms, though there is some evidence that mismatch repair (MMR) is also involved [64-65]. Recombination occurs within the 1-10 Kb switch (S) region sequences located upstream of each  $C_X$  gene and tends to occur for the same S region on both productive and nonproductive alleles. Since S regions consist of repetitive elements (either pentameric tandem repeats or 49 bp repeats) but lack specific signal sequences, it has been argued that the site of DNA rearrangement depends on the secondary structure assumed by the S region upon transcription and possibly on the formation of a DNA-RNA hybrid [66]. In fact, transcription of both  $S_\mu$ - $C_\mu$  and the target  $S_X$ - $C_X$  gene involved in the recombination process are required for CSR to commence [67]. CD40 signalling cooperates with other cytokines to trigger the specific I promoters located 5' of the target  $C_X$  gene and initiate synthesis and splicing of these so-called germline transcripts. This process is regulated by

iE $\mu$  (B-cell specific transcriptional enhancer) and by control elements located 3' of the IgH locus [68].

Though CSR is initiated by CD40 engagement, the isotype specificity is determined by cytokines. IL-4/IL-13 induce the switch to IgE and IgG4, which is fine-tuned by other cytokines. IL-7 might enhance class switching to IgE and IgG4 [70], whereas addition of IL-10 inhibits IgE, but promotes IgG4 production [71]. Switch to IgG1 and IgG3 is induced by IL-10, whereas IgG2 is induced by an as yet unidentified T cell factor. Finally, the switch to IgA production is promoted by a combination of IL-10 plus transforming growth factor beta (TGF $\beta$ ). More recently, it has become clear that other molecular interactions, like interaction with DC, also might enhance the level of Ig production [72], or even directly promote the switch to a specific isotype (IgA) [73]. In contrast, CD30, another member of the TNFR family, seems to be a CD40-inducible negative regulator of isotype switching [74].

SHM expands the antibody repertoire by introducing point mutations specifically in immunoglobulin V genes of activated B cells at an extraordinarily high frequency ( $10^{-3}$  bases per generation, one million higher than during normal DNA replication) [75-76]. Interestingly, not all IgG or IgA undergo SHM, whereas some IgM are somatically mutated, indicating that CSR and SHM are independent. Similar to what was observed for CSR, CD40-induced transcription is essential for initiating SHM. Mutations are commonly found within a 1.5-2 Kb region that lie 3' to the promoter of the rearranged V gene, where TAA and RGYW motifs (R=G or A, Y=T or C, W=A or T) act as mutational hot spots. During SHM, both single- and double-strand DNA breaks are scattered along the DNA target sequence [77]. NHEJ is dispensable for this process, whereas error-prone DNA polymerases are required [76, 78]. Through clonal selection, SHM allows B cells to increase antibody affinity to a specific antigen [63].

For the regulation of selection of high-affinity memory B cells, a complex network of interactions exists involving CD40, Fas, BCR, and cytokines. CD40 cross-linking induces Fas expression and sensitivity for Fas-

mediated apoptosis. However, the simultaneous triggering of the BCR increases the resistance to Fas-induced apoptosis [79]. In contrast, apoptosis of germinal center B cells can be induced by prolonged cross-linking of the BCR, an effect that can be prevented by the addition of IL-4 [80]. The interplay of these various signaling pathways has been confirmed *in vivo* using HEL transgenic mice [81]. It is interesting that BCR activation also seems to block the induction of CD30, thereby providing a safeguard to prevent not only expansion of non-antigen-selected B cells, but also their unwanted isotype switching [74].

Recently, Brodeur et al. identified a 23-kD protein that bound CD40 as C4BP-alpha (C4BPA). Immunohistochemical analysis showed that C4BP colocalized with CD40 on B cells in tonsillar germinal centers, while competitive binding assays showed that CD40L and C4BP bound distinct sites on CD40. C4BP induced proliferation, upregulation of ICAM1 and CD86 surface expression, and, together with IL-4, IgE synthesis in normal B cells. Therefore, it was proposed that C4BP is an activating ligand for CD40 and represents an interface between complement and B cell activation [82].

### **1.06 - BIOLOGICAL EFFECTS OF CD40 ACTIVATION ON OTHER CELLS**

The expression of CD40 on Antigen Presenting Cells (APCs) like **monocytes** and **DCs** is now well established [83-84]. CD40 ligation results in an enhanced survival of these cells, in the secretion of cytokines (such as IL-1, IL-6, IL-8, IL-10, IL-12, TNF- $\alpha$ , MIP-1 $\alpha$ ) and enzymes such as matrix metalloproteinase (MMP), in enhanced monocyte tumoricidal activity, and in the synthesis of nitric oxide (NO), which plays an important part in inflammatory responses. The interaction between CD40 and CD40L has important reciprocal consequences for both APC and T cell function.

Activation of the CD40 receptors is one of the critical signals that allows the full maturation of DCs into the most powerful APCs [85]. In turn, CD40 ligation considerably alters these APCs' phenotype by upregulating the expression of costimulatory molecules such as ICAM-1, LFA-3, CD80, and CD86, which contribute to the processes of T cell priming, proliferation, differentiation and effector functions, especially increasing T<sub>H</sub>2 responses [84, 86, 87]. CD40-CD40L interactions themselves proved to be bidirectional: cross-linking of CD40L contributes to the generation of helper function and germinal centers [88] and considerably enhances T cell cytokine production [89]. There has been some controversy as to whether antigen presentation in the absence of CD40-CD40L interaction leads to tolerance [90]. In some models, like the cellular immunity against Vesicular Stomatitis Virus (VSV), T cell priming seems to be independent of CD40L [91], although differences might exist between the induction of the cytotoxic T lymphocyte (CTL) response and maintenance of CTL memory [92].

The expression of CD40 has now been observed on many **non-hematopoietic cell lineages**: vascular endothelial cells and vascular smooth muscle cells; keratinocytes, thymus and kidney epithelial cells; lung, dermal, thyroid, gingival fibroblasts; hepatocytes [8]. Although the expression is generally low in these tissues, the molecule is clearly up-regulated under various pathological conditions. Accordingly, expression can be observed in **carcinomas** and in many cultured cell types including endothelial cells, epithelial cells, fibroblasts. Increased expression of CD40 is observed after *in vitro* activation, notably after stimulation with IL-1 or interferon- $\gamma$  (IFN- $\gamma$ ). The functional relevance of the CD40 molecule on these cells is relatively less investigated. In patients suffering from the HIGM syndrome, as well as in CD40 and CD40L knock-out mice, no gross abnormalities are observed in these organs. However, it has been suggested that the inability to ligate CD40 on biliary epithelial cells may contribute to a defective defence against intracellular pathogens [93], whereas on some cell types, including carcinomas, it has been demonstrated that CD40 activation results in an induction of cell

death [94-96]. Most likely, CD40 expression on non-hematopoietic cells is relevant to inflammatory responses: *in vitro* CD40 cross-linking increases the production of cytokines, chemokines and other inflammatory mediators [97].

Detection of CD40 within the **thymus** pointed out a possible role of CD40-CD40L interactions in the selection of the T cell repertoire [98]. Clonal deletion of thymocytes bearing T cell receptors of low affinity/avidity is altered by the functional blockade of CD40L by anti-CD40L antibodies [99]. A useful consequence of this observation is the development of mouse models to test anti-CD40L antibodies in the treatment of autoimmunity [100].

Another possible therapeutic lead derives from the suggestion that CD40-CD40L interactions in T cell priming might inhibit tolerance induction. Interference with CD40 activation has been extensively investigated in murine models to prolong the survival of experimentally transplanted organs, including heart, skin, aorta and pancreatic islets allografts [101]. Although treatment with anti-CD40L alone prolongs survival, better results have been obtained by combined treatment either with donor splenocytes or CTLA4-Ig. Simultaneous blocking of CD40 and CD28, a main target of APC costimulatory activity, resulted in long-term acceptance of skin and cardiac allografts [102]. These findings might open the way to new therapeutic intervention strategies to prevent transplant rejection and induce long-term tolerance.

### **1.07 - CD40-CD40L SIGNALLING DEFECTS CAUSE HYPER-IGM SYNDROMES**

Defects in CD40L, CD40 and some of the downstream targets of their signalling cause hereditary immune deficiencies known as Hyper-IgM syndromes (HIGM) due to their peculiar clinical features.

HIGM type 1 (**HIGM-1**) depends on defective expression of CD40L and is inherited as an X-linked trait [3-7]. It accounts for 65-70% of all cases

with the HIGM phenotype. Affected males suffer not only from recurrent bacterial, but also from opportunistic infections (e.g., *Pneumocystis carinii* pneumonia/PCP and watery diarrhea due to *Cryptosporidium parvum*) since early in life. Severe liver/biliary tract disease, increased occurrence of gastrointestinal tumors, and neutropenia are additional typical hallmarks of the disease. Immunologic features include very low serum levels of IgG, IgE and IgA, with normal to increased IgM levels [103]. While primary follicles are present in the lymph nodes, germinal centers are characteristically absent or abortive. In keeping with the defect of CSR, switched (IgD<sup>-</sup>, CD27<sup>+</sup>) circulating B cells are missing, and in general the number of circulating memory (CD27<sup>+</sup>) B cells is markedly reduced, while the rate of SHM is only marginally affected [104]. In spite of the severe clinical features, which are suggestive of combined immune deficiency, the number and distribution of T cell subsets are normal, as are proliferative responses to mitogens, although *in vitro* proliferation to T-dependent antigens is often reduced. Bone marrow transplantation from matched related or unrelated donors is the treatment of choice [105]. When none of these options are available, clinical management is based on regular administration of intravenous immunoglobulins (IVIG) and antibiotic prophylaxis.

Defects in CD40 cause **HIGM-3**, a rare autosomal recessive form of HIGM, was first described by our group in 2001 and recognized to date in only five patients from four unrelated families [106-108]. Similar to CD40L deficiency, patients with CD40 mutations present during infancy with severe clinical symptoms, including opportunistic infections and failure to thrive, suggestive of combined immunodeficiency. The lack of activation of monocytes and dendritic cells in the absence of CD40 may account for opportunistic infections in both CD40L and CD40 deficiencies. CD40-deficient patients were found to lack CD40 expression on the surface of B lymphocytes and monocytes. *In vitro* B cell stimulation with anti-CD40 and IL-10 failed to induce IgA or IgG production [106], in contrast with B cells from XHIGM patients who do [3-4]. Similar to XHIGM patients, CD40 deficient infants have

decreased numbers of IgD<sup>-</sup> CD27<sup>+</sup> memory B cells. Treatments include IVIG infusions every 3-4 weeks, PCP prophylaxis, and attention to nutrition. Stem cell transplantation is expected to be less successful [109], since it restores CD40 expression only for hematopoietic stem cell-derived cell lineages and not for other CD40-expressing cell types [110].

Another autosomal recessive form of HIGM, **HIGM-2**, presents with mild, recurrent bacterial sinorespiratory and gastrointestinal tract infections, but without increased susceptibility to opportunistic pathogens [111-112]. It is caused by mutations within Activation-Induced Cytidine Deaminase (*AICDA*), the gene encoding AID, a DNA editing enzyme [113]. AID expression is induced by CD40 and physiologically restricted to germinal center B cells [114], where it was shown to be the only B cell specific component necessary and sufficient for both CSR and SHM to occur [115]. Accordingly, AID-deficient patients have markedly diminished levels of IgG and IgA coupled with normal or elevated IgM, but unlike HIGM-1 or 3 the numbers of CD19<sup>+</sup> B cells and CD27<sup>+</sup> memory B cells are normal, and T cell immunity is universally intact [113]. A characteristic clinical finding, present in half of the patients with AID deficiency, is lymphoid hyperplasia due to the presence of giant germinal centers filled with proliferating B lymphocytes co-expressing IgM, IgD, and CD38. Treatment with regular infusions of IVIG is effective in reducing infections but does not affect lymphoid hyperplasia [116].

A further autosomal recessive form of HIGM is caused by defects in Uracyl-DNA-Glycosylase (*UNG*), a DNA-editing enzyme involved in CSR and SHM. The clinical phenotype of *UNG* deficiency closely resembled HIGM-2, but molecular investigations in CD40 activated B cells revealed the presence of SHM, though the rate of transition vs tranversion was biased for certain residues, probably reflecting failure to remove uracil residues from DNA after AID deamination [117-118].

Recently, another form of X-linked HIGM characterized by the association of hypogammaglobulinemia with hypohydrotic ectodermal dysplasia (**HIGM-ED**) was identified [119-120]. This condition is caused by

hypomorphic mutations of the gene encoding for NEMO-IKK $\gamma$ , a scaffolding protein for the IKK $\alpha$  and IKK $\beta$  kinases, which regulate activation of the NF- $\kappa$ B transcription factor. In HIGM-ED, engagement of CD40 or BCR is unable to produce NF- $\kappa$ B-dependent reactions. It is not a pure humoral deficiency since defects of T and natural killer (NK) cells have been also reported [121].

It has already been remarked that the study of HIGM-affected individuals was invaluable in elucidating many of the inter- and intracellular mechanisms involved in the immune response, like CSR and SHM. Future investigations of these models will certainly provide further insights on the delicate regulation of the immune system, as well as on new possible targets for the treatment of immune deficiency, autoimmunity, graft-vs-host disease and tumorigenesis.

## 2. MATERIALS AND METHODS

### 2.01 - HUMAN *TNFRSF5* GENE ANALYSIS

The human CD40 gene structure was determined by alignment of the CD40 mRNA sequence (accession no. NM 001250) with a contig derived from assembled genomic sequence data (accession no. AL035662.60). The nine exons of human CD40 gene were amplified by Polymerase Chain Reaction (PCR) with the following primers. Primers for exon 1: 5'-ATAGGTGGAC-CGCGATTGGT-3' (fwd); 5'-TCCCAACTCCCGTCTGGT-3' (rev). Primers for exon 2: 5'-GCTGAAGAAGTTGCAACGGA-3' (fwd); 5'-AAAGCAAAG-GGGGACTCCA-3' (rev). Primers for exon 3: 5'-GTTAGTGTCTGACTCAT-GGA-3' (fwd); 5'-AATGGCTGCATTGTCGGGA-3' (rev). Primers for exon 4: 5'-GGTCTGAGGAAGAAAGAGCA-3' (fwd); 5'-CTTGGGCCCTAAGC-TCCT-3' (rev). Primers for exon 5: 5'-GTGGTCCACTGTGATGGTTA-3' (fwd); 5'-GAGGCCACTCTGCAGATGCT-3' (rev). Primers for exon 6: 5'-GTTGTGTGCTCAGTGAACCT-3' (fwd); 5'-ACCTTCCTAGGCTTTCT-CCA-3' (rev). Primers for exon 7: 5'-GTAGGGAGAACTGCAGGT-3' (fwd); 5'-CCAGATAAGAAACAGGTGGT-3' (rev). Primers for exon 8: 5'-GTAGGGAGAACTGCAGGT-3' (fwd); 5'-GTTTTACTGCCCCATAG-GCA-3' (rev). Primers for exon 9: 5'-AGGGGCTCCTCAGAGGCA-3' (fwd); 5'-CTCTCTGGCCAACTGCCT-3' (rev). For exons 1, 2, 4, 5, and 9, PCR was performed with 2.5 units of AmpliTaq Gold DNA polymerase (Roche

Molecular Systems): 1 cycle at 95°C for 10 min, and 35 cycles at 94°C for 30 s, at 65°C for 30 s, and at 72°C 30 s. For exons 3, 6, 7, and 8, PCR was performed with 1 unit of AmpliTaq Gold DNA polymerase: 1 cycle at 94°C for 5 min, and 35 cycles at 94°C for 30 s, at 58°C for 30 s, and at 72°C for 30 s. PCR products were gel purified by using MultiScreen 96-well Filtration System (Millipore), sequenced with BigDye® Terminator v1.1 Cycle Sequencing Kit (Applied Biosystems), and analyzed with the ABI Prism 3730 DNA Analyzer (Applied Biosystems) with the assistance of *Sequencher 4.5* software (Gene Codes Corporation).

## **2.02 - CELL CULTURES**

B lymphoblastoid cell lines (B-LCLs) were established from patients and healthy donors via transformation of B cells with EBV by our partners at the Pediatric Clinic of the University of Brescia. Human Embryonic Kidney cells HEK-293 were kindly provided by Dr M. Vargiolu (Azienda Ospedaliera Universitaria di Bologna Policlinico S. Orsola-Malpighi, Dipartimento di Patologia Clinica, Microbiologia, Medicina Trasfusionale e Genetica Medica, Unità Operativa di Genetica Medica Microbiologia, Bologna, Italy). LAN-1, SH-SY5Y, SK-N-SH, IMR-32 and SK-N-BE neuroblastoma cell lines were a kind courtesy of Prof. G. Della Valle (Università di Bologna, Facoltà di Scienze Matematiche, Fisiche e Naturali, Dipartimento di Biologia Evoluzionistica e Sperimentale, Bologna, Italy), while AF and LAP-35 cells were donated by Prof. G.P. Bagnara (Università di Bologna, Facoltà di Medicina e Chirurgia, Dipartimento Di Istologia, Embriologia e Biologia Applicata, Bologna, Italy). All cells were grown in RPMI-1640 medium (Cambrex) supplemented with 10% complement-inactivated Fetal Bovine Serum (FBS) (Gibco), 0.3 mg/ml L-Glutamine (Euroclone, CelBio), 1 U/ml

Penicillin (Euroclone, CelBio) and 0.1 mg/ml and Streptomycin (Euroclone, CelBio).

### **2.03 - B CELLS SEPARATION AND STIMULATION**

Normal human peripheral blood mononuclear cells (PBMC) were prepared from healthy donors' buffy coat diluted in 1 vol of PBS (10 mM potassium/sodium phosphate buffer with 136 mM NaCl, pH 7.4) by density centrifugation over Ficoll-Paque Plus (Stem Cell Technologies Incorporated). B lymphocytes were purified from PBMC by negative selection using MACS® magnetic cell sorting human B Cell Isolation Kit II (Miltenyi Biotec) as per the manufacturer's specifications, and were >95% CD19<sup>+</sup> as determined by flow cytometry analysis. CD27<sup>+</sup> and CD27<sup>-</sup> B cells were subsequently isolated with MACS® CD27 Microbeads (Miltenyi Biotec).

Purified CD19<sup>+</sup>, CD27<sup>+</sup>, and CD27<sup>-</sup> B lymphocytes were seeded at  $1 \times 10^6$  cells/ml in a flat-bottom 96-well plate in the presence of  $1 \times 10^4$  irradiated L4.5 cells per ml. B lymphocytes were cultured in Iscove's medium supplemented with 50 µg/ml human transferrin, 5 µg/ml bovine insulin, 0.5% Bovine Serum Albumin (BSA) and 50 µM 2β-Mercaptoethanol (2β-ME), all from Sigma-Aldrich, and additioned with either mouse anti-human CD40 [EA-5] monoclonal antibody (MAb) (Calbiochem) and IL-4 (R&D Systems), or with SAC (*Staphilococcus aureus* Cowan I protein; Sigma-Aldrich) and IL-2 (R&D Systems) for 24 hours, as described by Marconi et al. [122].

## **2.04 - FLOW CYTOMETRY**

Peripheral blood lymphocytes, B-LCLs and HEK-293 cells resuspended in PBS at a concentration of  $5 \times 10^5$  cells/ml were incubated at 4°C for 30 min with 5 µl of FITC (Fluorescein isothiocyanate)-labeled anti-human CD40 (5C3 mAb) and PE (Phycoerythrin)-labeled anti-human CD19 (HIB19 mAb) antibodies (BD PharMingen). Pt.1 B-LCLs were also stained with anti-CD40 [EA-5] antibody and a secondary PE-conjugated anti-mouse IgG antibody (Caltag). After staining, the cells were washed twice with PBS, fixed with 2% paraformaldehyde (Sigma-Aldrich) in PBS and analyzed by FACSCalibur (Beckton Dickinson).

## **2.05 - HUMAN CD40 TRANSCRIPTS ANALYSIS**

Analysis of CD40 transcripts in human tissues was performed on pre-normalized, serial diluted cDNAs from a Human Rapid-Scan Gene Expression Panel (OriGene Technologies). For all other samples, total RNA was extracted from aliquots of  $2 \times 10^6$  cells with the RNeasy Mini Kit (QIAGEN) following the manufacturer's specifications, and was then subjected to Reverse Transcription (RT) PCR. RT reactions to obtain the cDNAs were performed on a GeneAmp PCR System 2700 thermal cycler (Applied Biosystems) according to the following protocol: addition of 500 ng Oligo-d(T) primers to 11 µl of RNA, incubation at 70°C for 5 min and 4°C for 1 min, addition of 1x First-Strand Buffer, 10 mM 1,4-Dithio-DL-threitol (DTT) and 2 mM deoxynucleotide tri-phosphate (dNTP) Mix, incubation at 42°C for 2 min, addition of 1 unit Superscript II Reverse Transcriptase, incubation at 42°C for 30 min, addition of 1 unit RNase H, incubation at 55°C for 5 min. All reagents were from Invitrogen.

In order to set up a screening for CD40 transcript variants, cDNA was amplified with four pairs of oligonucleotides (Applied Biosystems), the forward primer of each couple conjugated with a fluorescent dye at its 5' end yielding amplicons A, B, C and D (Table 2.01). PCR was performed using 1 unit of AmpliTaq Gold DNA polymerase and a final concentration of 1.5 mM MgCl<sub>2</sub>, on a GeneAmp PCR System 2700 thermal cycler set for initial denaturation at 96°C for 10 min, 25-30 cycles with denaturation at 96°C for 30 s, annealing at 60°C for 30 s, extension at 72°C for 30 s, and a final cycle at 72°C for 12 min. Amplicons from the same sample were pooled together at a volume/volume ratio of 1:1:2:3 µl for A, B, C and D respectively to correct for the intensity of each specific fluorescent dye and diluted in 40 µl of double-distilled water (ddH<sub>2</sub>O). 1µl of each pool was added to 9µl of Formaldehyde (Sigma-Aldrich) containing 0.2µl of GeneScan 500 (-250) LIZ size standard (Applied Biosystems) and loaded on the ABI Prism 3730 DNA Analyzer for automated capillary gel electrophoresis, and the results were plotted with the *AbiPrism GeneMapper v3.5* software (Applied Biosystems).

**Table 2.01** - PCR primers used for CD40 transcript analysis.

<b>Amplicon</b>	<b>Primer name</b>	<b>Sequence (5' → 3')</b>	<b>Position</b>
A	CD40trF1, FAM-conjugated	GGTTCGTCTGCCTCTGCAGT	exon 1
	CD40trR1	AGCATGAGCGGTGCAGGA	exon 4
B	CD40trF2, VIC-conjugated	GGTGAGTGACTGCACAGAGT	exon 3
	CD40trR2	GTCCAAGGGTGACATTTTTCGA	exon 5
C	CD40trF3, NED-conjugated	CCTGTGAGAGCTGTGTCCT	exon 4
	CD40trR3	AGCACCAAGAGGATGGCA	exon 7
D	CD40trF4, PET-conjugated	TTGTGCAACAGGCAGGCA	exon 6
	CD40trR4	TTGGAGCCAGGAAGATCGT	exon 9

Nucleotide sequences of all the observed amplicons were validated by repeating the PCRs with 5'-unmodified primers and cloning the products into pcR2.1-TOPO vectors using the TOPO TA Cloning Kit and related protocol (Invitrogen). TOP10F' strain E. coli cells (Invitrogen) were employed as a host for transformation (in these and in all subsequent proceedings), and colonies containing the recombinant plasmids were screened by PCR with the primer pair for the appropriate amplicon and at the same conditions described previously. Nucleotide sequence analysis was then performed on these amplification products as described for the genomic CD40 amplicons (Section 2.01).

To envision the presence of full-length transcripts, cDNAs from neuroblastoma cell lines were also amplified with the primers employed for cloning wild-type CD40 mRNA (primers 40aF and 40a1R; sequence and reaction conditions are detailed in Section 2.06). PCR products were separated on a 2% SeaKem LE Agarose gel (Cambrex) in TAE buffer (40 mM Tris, 20 mM Acetic acid, 1 mM EDTA) alongside a molecular weight marker (GeneRuler 1 Kb DNA Ladder from Fermentas) and visualized with Ethidium Bromide (BIO-RAD) on a Vilber Lourmat transilluminator.

Quantitative Real-Time (QRT) PCR were performed on a BIO-RAD iCycler using Applied Biosystems assay-on-demand TaqMan® probes, primers and protocols.

## **2.06 - CONSTRUCTION OF RECOMBINANT VECTORS FROM CD40 TRANSCRIPT VARIANTS**

Amplicons encompassing the whole ORF of CD40 transcripts were generated using a forward primer overlapping the ATG start codon (40aF: 5'-CACCGCTATGGTTCGTCTGC-3') and a reverse primer positioned

downstream of the stop codon employed by the specific transcript variant we intended to clone (40a2R: 5'-AGGATCCCGAAGATGATGG-3' for the transcript lacking exon 5, 40a1R: 5'-AACTGCCTGTTTGCCAC-3' for all others). PCRs were performed using 1 unit of Platinum *pfx* DNA polymerase (Invitrogen), which ensured high fidelity copies because of its proofreading activity, and the following thermal cycling conditions: 1 cycle at 94°C for 5 min, 35 cycles at 94°C for 15 s, at 58°C for 30 s, and at 68°C for 1 min, 1 cycle at 68°C for 7 min. PCR products were cloned into pcR2.1-TOPO vectors using the TOPO TA Cloning Kit and related protocol as described in the previous section. Plasmid DNA of the recombinant constructs was prepared from the bacterial amplification host with QIAGEN Plasmid Midi Kit. Each product of interest was then subcloned into three expression vectors: pcDNA3 (Invitrogen); pEGFP-N1 (Clontech) and pFLAG-N1. The former two vectors were kindly provided by Dr. A. Ripalti (Azienda Ospedaliera Universitaria di Bologna Policlinico S. Orsola-Malpighi, Dipartimento di Patologia Clinica, Microbiologia, Medicina Trasmfusionale e Genetica Medica, Unità Operativa di Microbiologia, Bologna, Italy); the latter was developed in our laboratory.

pcDNA3-CD40 subclones were constructed by excising the product of interest from pcR2.1-CD40 plasmids with NotI and SpeI restriction enzymes and inserting it into pcDNA3 polylinker at the NotI and XbaI sites. All restrictions were performed with endonucleases from Roche Molecular Systems, gel-purified with Montage DNA Gel Extraction Kit columns (Millipore), and ligated overnight at 16°C at a 1:10 vector:insert molar ratio using 0.5 units/reaction of T4 DNA Ligase from Fermentas.

pCD40-EGFP and pCD40-FLAG constructs were obtained by cloning into the NheI and SalI sites of pEGFP-N1 or pFLAG-N1 the PCR products generated using pcDNA3-CD40 plasmids as templates, a common forward primer (40bF: 5'-ACCGTGCTAGCTATGGTTCGTCTG-3') and reverse primers removing the stop codon depending on the cloned transcript (40b1R: 5'-CTGCGGTGCGACTGTCTCTCCT-3' for wt-CD40 and del5+6-CD40, 40b2R: 5'-TATAGTCGACCCTATTCTGGGGACCACA-3' for del5-CD40,

40b3R: 5'-CTACAGTCGACCCTCCCTGTCTCTCC-3' for Pt.3-CD40 and Pt.4-CD40). PCR was performed using Platinum *pfx* DNA polymerase as described previously in this section.

pFLAG-N1 was developed starting from pEGFP-N1. The sequence encoding EGFP was excised by restriction with SalI and NotI and substituted with a FLAG-encoding oligonucleotide dimer, obtained by resuspending FLAG\_u: 5'-TCGACTGATTACAAGGACGACGATGACAAGTAGC-3' and FLAG\_l: 5'-GCGGCCGCTACTTGTTCATCGTCGTCCTTGTAATCAG-3' (MWG-Biotech AG) in STE buffer (10mM Tris pH 8.0, 50 mM NaCl, 1 mM EDTA) at a concentration of 200  $\mu$ M each and annealing them in a water bath that was gradually left to cool from 95°C to room temperature.

All primers used in the construction of recombinant vectors were synthesized by Sigma-Proligo.

## **2.07 - TRANSIENT TRANSFECTIONS AND STABLE TRANSFECTANTS**

All transfections were performed on 80% confluent cells using Lipofectamine 2000 Reagent (Invitrogen) according to the manufacturer's protocol for plasmid DNA. Stable transfectants HEK-40F and HEK-40G were selected for Neomycin resistance from HEK-293 cells transfected with pwt-CD40-FLAG and pwt-CD40-EGFP, respectively, by adding 500  $\mu$ g/ml G418 (Sigma-Aldrich) to the culture medium every two days for two weeks and subsequent manual isolation of the resulting clones with a sterile micropipette.

Fusion proteins originating from the pEGFP constructs were visualized on an Axiovert 200 inverted microscope (Zeiss) with a 20x objective.

## **2.08 - WESTERN BLOT**

5 x 10<sup>6</sup> B-LCLs, 3 x 10<sup>6</sup> HEK-293 or 5 x 10<sup>6</sup> neuroblastoma cells were lysed with 50 µl lysis buffer (150 mM NaCl/100 mM Tris·Cl pH 7.5, 2 mM EDTA, 0.5% Triton X-100, protease inhibitors) for 30 min on ice and centrifuged for 10 min at 16,000 x g. Protein content of the supernatants was quantified with the DC Protein Assay Kit (BIO-RAD) on a DU530 UV/Vis Spectrophotometer (Beckman Coulter), 1 volume of SDS gel-loading buffer (50mM Tris-HCl, pH 6.8 with 20% Glycerol, 2% SDS, 2% 2β-ME, 0.02% Bromophenol Blue) was added to 20 µg of total protein, and the samples were boiled for 3 min. For B-LCLs and HEK-293 cells transfected with the FLAG constructs, pellets were also resuspended in 50 µl of DNase I buffer (200 mM TrisH·Cl, 20 mM MgCl<sub>2</sub>), treated with 1 µl di DNase I (Invitrogen) at room temperature for 1 h, and subsequently handled like the supernatants were. Proteins were separated on a 12% SDS-polyacrylamide gel in a Hoefer SE 260 electrophoretic cell (Amersham Pharmacia Biotech) alongside a Full-Range Rainbow Molecular Weight Marker (GE Life Sciences), transferred to an Immobilon-P polyvinylidene difluoride (PVDF) membrane (Millipore) with a Hoefer miniVE system (Amersham Pharmacia Biotech) and probed with an affinity-purified rabbit polyclonal antibody (anti-FLAG from Sigma-Aldrich, anti-human CD40 (H-120) IgG or anti-human CD40 (C-20) IgG from Santa Cruz Biotechnology) following the protocol detailed in Current Protocols in Molecular Biology, Chapter 10 (Wiley Interscience). The blot was developed with the Enhanced Chemiluminescence (ECL) Western Blotting Detection System (Amersham Pharmacia Biotech).

In the N-deglycosylation experiment, samples were treated for 1 h with Peptide-N-Glycosylase (PNGase) F (BIO-RAD) and loaded side by side to untreated samples for comparison.

In the assay for presence of the CD40 variant missing exon 5, culture medium of del5-CD40-FLAG transfected cells was concentrated 70-fold with Amicon Ultra filter columns (Millipore) before Western blot analysis.

## **2.09 - CELL FRACTIONATION**

Cell fractionation was carried out on HEK-293 and B-LCLs in a HAEREUS ultracentrifuge (courtesy of Dr P. Zucchelli, Ospedale Maggiore, Bologna) as described previously by Lehninger et al. [124], but purifying only up to the 80,000 rpm fraction. Equal quantities of total protein from all fractions were loaded on an SDS-PAGE gel and Western blotting was performed as detailed in Section 2.08.

## **2.10 - IMMUNOFLUORESCENCE STAINING AND CONFOCAL MICROSCOPY**

In order to colocalize CD40 in specific cell compartments, we assayed HEK-40F stable transfectants for different markers. Cells were allowed to grow on sterilized coverslips for 24h, then fixed with 2% paraformaldehyde in PBS at RT for 30' and blocked with 50mM NH<sub>4</sub>Cl in PBS at RT for 15'. Coverslips were washed with a permeabilization buffer, consisting of 0.2% Tween20 (Sigma-Aldrich) in PBS, and stained by incubation at 4°C for 60 min with the appropriate antibodies. We used a 1:400 dilution of mouse anti-human CD40 monoclonal antibody LOB-11 (Santa Cruz Biotechnology), a 1:100 dilution of rabbit anti-human Calnexin antibody [AF18] (Abcam), and a 1:1000 dilution of rabbit anti-human Giantin antibody, Alexa Fluor 488 conjugated (Abcam). CD40 and Calnexin staining required a second incubation with Alexa Fluor® 568 Goat Anti-Mouse IgG (H+L) (Invitrogen) and Alexa Fluor® 488 Goat Anti-Rabbit IgG (H+L) (Invitrogen), respectively, both at a dilution of 1:200. For recycling compartment staining, Transferrin from human serum, Alexa Fluor® 488 conjugated (Invitrogen) was added 1:100 to the culture medium for 60 min immediately prior to cell fixation.

Staining of B-LCLs were performed following the same protocol, but employing anti-CD40 (LOB-11) along with transferrin for the control sample, and along with rabbit polyclonal anti-PDI (Protein Disulfide Isomerase; H-160) IgG (Santa Cruz Biotechnology) for control and Pt.3 samples.

Cells were visualized on a FV300 confocal microscope (Olympus). Images were captured using the 60X objective with the appropriate filter set.

## 3. RESULTS AND DISCUSSION

### 3.01 – CHARACTERIZATION OF HIGM-3 PATIENTS

In the present work we have studied four patients diagnosed with type 3 HIGM. Patient 1 (Pt.1), born from consanguineous Italian parents, and Pt.2, belonging to a multiply related Saudi Arabian family, were previously described by our group [106]. Pt.3 and Pt.4 were more recently diagnosed at the Pediatric Clinic of the University of Brescia [107-108]. All patients entered medical care at an early pediatric age because of severe or recurrent respiratory tract infections. They all shared normal counts of circulating B cells and a profound reduction of IgG and IgA serum levels, whereas IgM were present at normal or high levels. Systematic evaluation of differentiation markers liable to be aberrant in hypogammaglobulinemia patients with normal/high levels of IgM detected normal CD40L expression and lack of mutations in the *AICDA* gene, but flow cytometry profiles showed absence (or, in the case of Pt.4, near absence) of CD40 expression on the surface of peripheral blood B lymphocytes (Fig. 3.01). PCR amplification and nucleotide sequence analysis of each exon, including flanking intronic splice sites and the branch site, revealed mutations in the *TNFRSF5* gene of all four patients (Fig. 3.02), allowing the investigators to assign them to the HIGM-3 group.

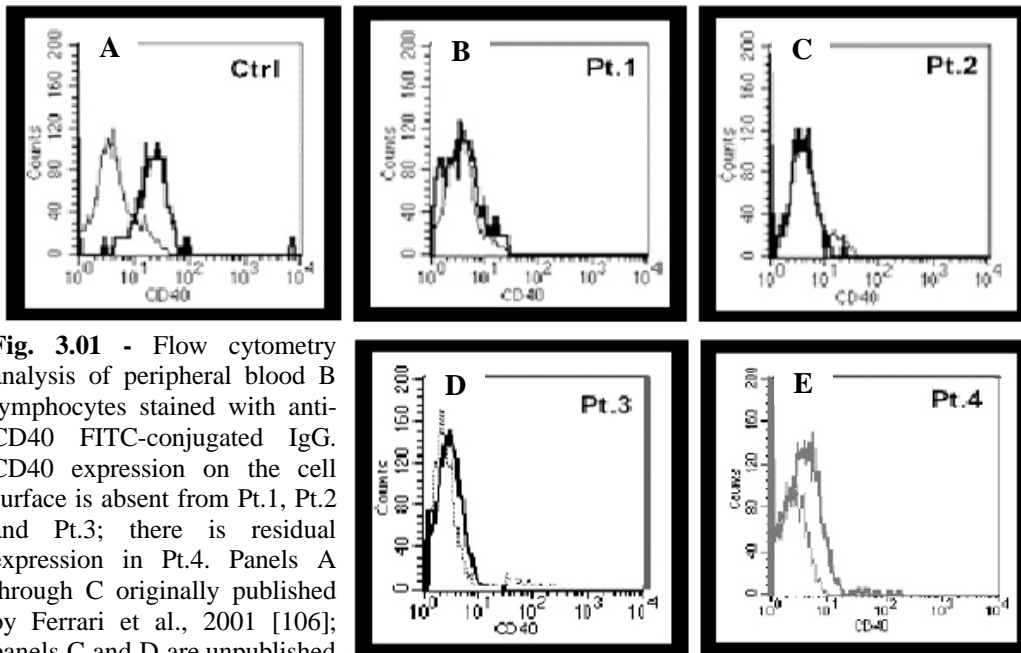


**Fig. 3.01** - Flow cytometry analysis of peripheral blood B lymphocytes stained with anti-CD40 FITC-conjugated IgG. CD40 expression on the cell surface is absent from Pt.1, Pt.2 and Pt.3; there is residual expression in Pt.4. Panels A through C originally published by Ferrari et al., 2001 [106]; panels C and D are unpublished data from Lanzi G and Giliani S [127]. Reproduced by kind permission from the authors.

Pt.1 had a single homozygous change (A455T) at the fifth base pair position of exon 5, purportedly resulting in a silent mutation at codon Thr136, but effectively disrupting an Exonic Splicing Enhancer (ESE), a cis-element that promotes inclusion of specific exons [124] through binding of serine/arginine-rich splicing factors [125]. Direct sequence analysis of the mutant cDNA product and exon-trapping experiments confirmed this mutation to be responsible for the systematic splicing out of the entire exon 5 during mRNA maturation [106].

Pt.2 was homozygous for a T294C nucleotide transition in exon 3, resulting in a Cys to Arg substitution at residue 83, within CRD2.

Pt.3 displayed a homozygous intronic A to T transition 2 nucleotides upstream of exon 4 which scrambles the correct splice site and, according to cDNA nucleotide sequence analysis, promotes the use of a cryptic splice acceptor site 6 nt downstream [126]. The result of this variation on the aminoacid sequence is a deletion of Asn86 and Leu87, along with a Gly88Arg substitution, also within CRD2.

Pt.4 was homozygous for the deletion of bases 174 to 176 (ATA) within exon 2, causing the deletion of Ile33 from the peptide sequence of CRD1.

Due to the patients' condition and/or availability, in the present work we had no access to fresh PBMC samples, but we could resort to B-LCLs derived from Pt.1, Pt.2 and Pt.3 and had limited accessibility to B-LCLs derived from Pt.4 since they were developed by a partner research group led by Dr. S. Giliani, at the Pediatric Clinic of the University of Brescia [127].

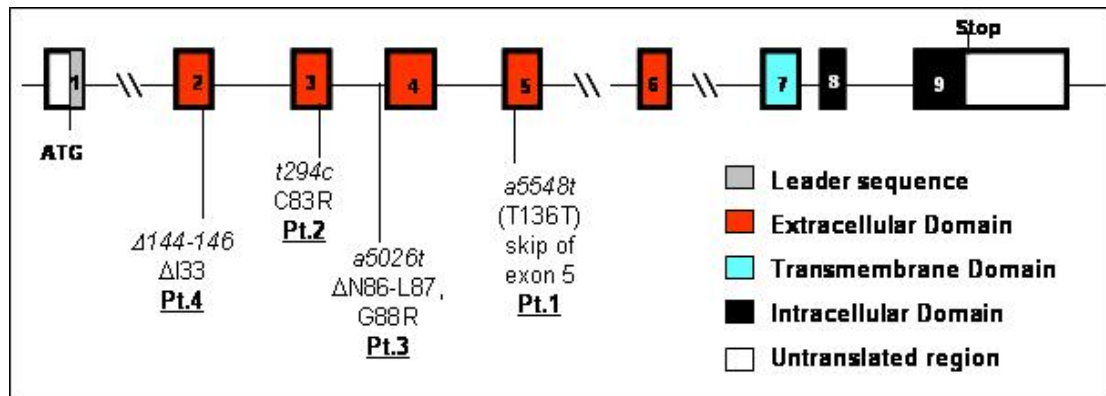


**Fig. 3.02** - Schematic representation of the *TNFRSF5* gene. Boxes identify the various exons. The position of disease-causing mutations identified in patients with CD40 deficiency is indicated respective to the transcript (in *italic*) and to the peptide sequence.

### **3.02 - IDENTIFICATION OF CD40 TRANSCRIPT VARIANTS IN B-LCLs**

Though CD40 expression is still poorly understood, its mouse ortholog offers clear evidence of a complex post-transcriptional regulation driven by alternative splicing, and some indication exists that a similar mechanism also occurs in man [16]. These findings, and the additional evidence that two out of four HIGM-3 patients owe their condition to defective splicing, prompted us to address the problem of identifying CD40 transcript variants by setting up a fast and sensible method based on semi-quantitative RT-PCR combined with capillary gel electrophoresis.

We split the CD40 transcript into four partially overlapping amplicons covering all exon-exon junctions, optimizing their length for electrophoresis in an AB3730 automated sequence analyzer. The forward oligonucleotide of each

primer pair was conjugated with a different fluorescent dye, so that all PCR products from individual cDNA samples could be assayed simultaneously in a single capillary and discriminated by their emission wavelength. As outlined in Fig. 3.03, amplicon A, marked with a FAM fluorescent dye, spans exon-exon junctions 1-2, 2-3 and 3-4; amplicon B (VIC) spans junctions 3-4 and 4-5; amplicon C (NED) spans junctions 4-5, 5-6 and 6-7; amplicon D (PET) spans junctions 6-7, 7-8 and 8-9. The positioning of the primers within distinct CD40 exons and the relevant size of the intervening introns prevented contamination from genomic DNA derived products.

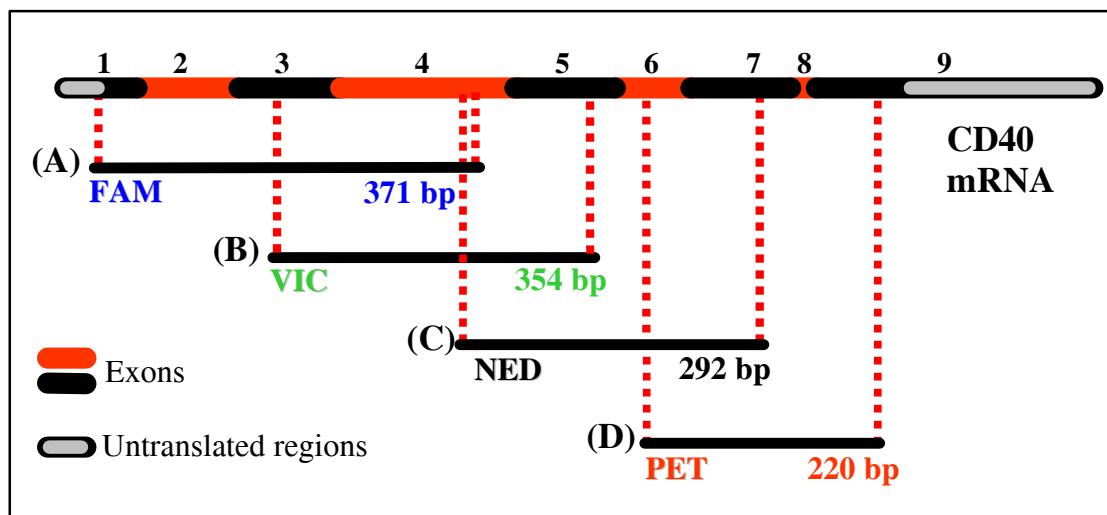


**Fig. 3.03** - CD40 transcript was split into four partially overlapping amplicons, each spanning a specific set of exon-exon junctions and marked with a different fluorescent dye.

We analyzed transcripts from B-LCLs derived from the four patients, along with a control B-LCL derived from a healthy donor. cDNA was prepared from total RNA by using an oligo-d(T) primer. To perform semi-quantitative RT-PCR,  $\beta$ -actin was used as a reference to normalize the samples and the number of PCR cycles was kept low. Only a small part of the reaction was necessary for capillary gel electrophoresis. The readout of each channel (either FAM, VIC, NED or PET emission) was plotted with *GeneMapper* software as a series of discrete peaks characterized by a position on the x-axis (or “size”), corresponding to the length of the PCR products, and by an intensity (or

“height”), approximately proportional to the relative abundance of the amplicons originating from any given primer pair.

The control sample showed a main peak on each channel matching the expected length of the amplicon from the full-length transcript (Fig. 3.04). Head-on comparison of the readouts from the various samples allowed us to discriminate easily transcript length variations in the patients. The plot of Pt.4 evidenced a main peak 3 nt smaller than the control on the FAM channel only, consistent with the known codon deletion within exon 2. Pt.3 displayed a main peak 6 nt smaller than the control both on the FAM and on the VIC channel, which implies a deletion somewhere within exon 3 or 4, in agreement with previously known data. Pt.2, of course, showed no size variation in any amplicon, since its point mutation does not affect RNA length. Pt.1, consistently with the systematic exclusion of exon 5 from the transcript, lacked the 292 nt peak matching full-length amplicon C on the NED channel, but displayed two smaller peaks which pointed out the presence of PCR products spanning 198 and 136 nucleotides. Their size perfectly agrees with the length of the amplicons that would have been obtained from a transcript in which, respectively, splicing out of exon 5 or of both exons 5 and 6 had occurred.

Strikingly, these two peaks, though weaker in intensity, were quite evident on the NED channel of the other samples as well, along with an even lower one at 230 nt on the x-axis, corresponding to the PCR product that would have originated from a transcript missing exon 6 only. Similarly, on the PET channel the main peak of every sample is flanked by two very low peaks: one matches the size of a variant originating from an alternative splice acceptor site 5 nt within exon 8, while the other agrees with the use of an alternative splice donor site contained in intron 7, 12 nt downstream of exon 7. The FAM channel of the control sample also reveals an additional faint signal falling short of the main peak by exactly 79 nucleotides, the precise length of exon 2. This peak overlaps with the main peak of the NED channel; since sometimes high signals on one channel are detected on other channels as well, we had to

rule out this possibility by repeating the analysis and loading the PCR products of each primer pair on different capillaries (Fig. 3.09 B).

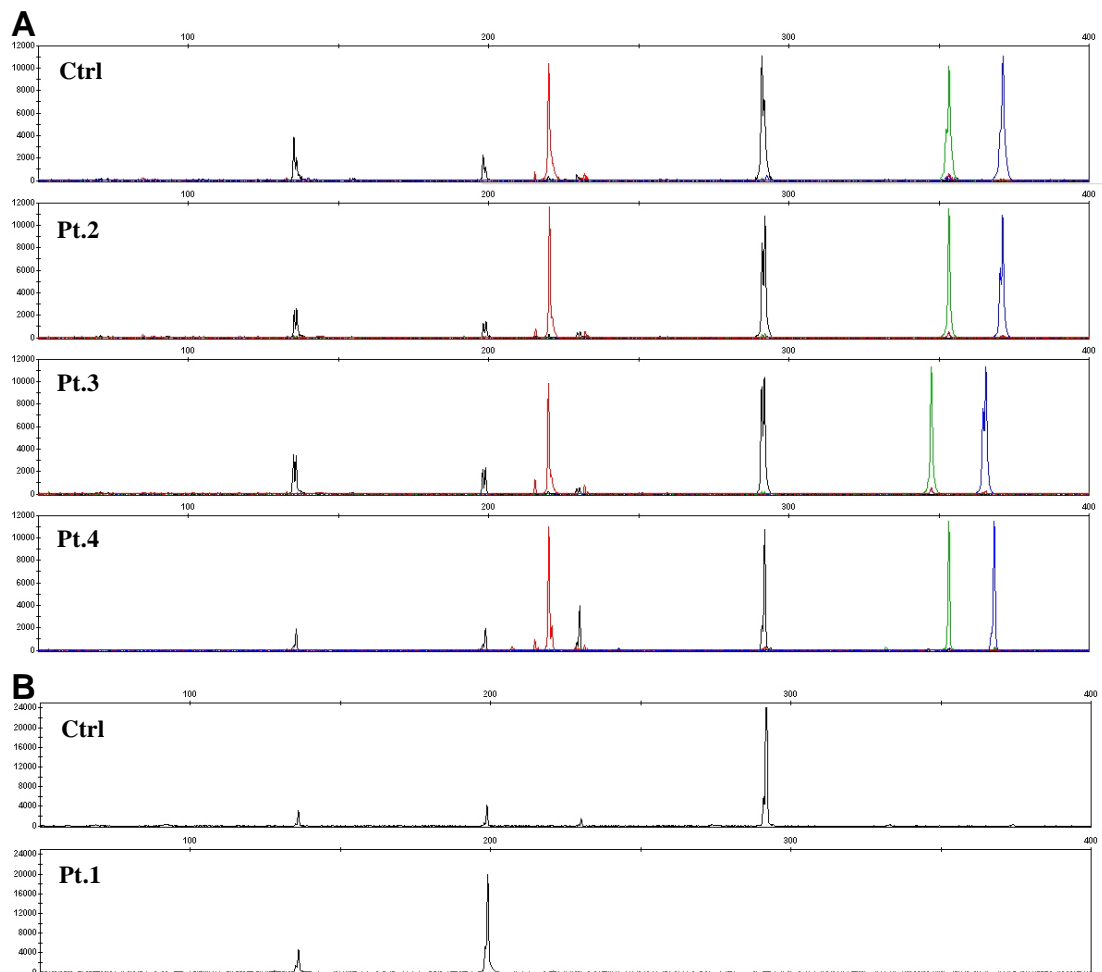


**Fig. 3.04** - Comparison between the plots resulting from *GeneMapper* analysis of CD40 transcripts from B-LCL samples. A) Readouts from Pt.2, Pt.3, Pt.4 and the healthy control displayed on all four channels mark some of the different peak sizes of mutants Pt.2 and Pt.3, and the recurrence of splicing variants in all samples. B) Readout from Pt.1 on the NED channel highlights the absence of full-length transcripts and the concurrent increase in the intensity of the peaks representing splicing out of exon 5 and exons 5 and 6. Ctrl = control sample.

In order to check these CD40 variants we queried either the human Expressed Sequence Tags (ESTs) database or the ASAP (Alternative Splicing Annotation Project) database (<http://bioinfo.mbi.ucla.edu/ASAP/>), created by an automated method for discovering tissue-specific regulation of alternative splicing through a genome-wide analysis of the UniGene clusters of human ESTs. The ESTs in UniGene contain all the CD40 mRNA variants revealed by our method of analysis.

The identity of every variant was further confirmed by inserting the PCR products into Topo-TA vectors and analyzing the nucleotide sequence of the resulting clones. Other extremely low peaks could be seen in the plots apart from those mentioned above, but they were sensibly discounted as either fluorescence artefacts or subliminal products if they both failed to occur in repeated experiments and were never found in any of the clones we screened.

Though the peak intensities displayed in the readouts are related to the abundance of the appropriate amplicons, this technique is essentially qualitative and shouldn't be used to measure differences in absolute expression levels between samples. In order for the assay to be at its most reliable, the highest peak of each plot must be kept within a certain range of values by diluting the sample, while normalizing the data against a reference gene is prone to yield off-scale readings where even small variations are concerned. Over a number of experiments with the B-LCLs, however, we have observed that the most repeatable quantitative aspect of our assay was the ratio between peak heights within the same sample rather than their absolute intensity value. Since alternative splicing ultimately means increasing certain transcript variants at the loss of others, all in all using peak ratios appealed to us as an appropriate quantitative method to compare samples, because it reflects the actual biological effect of the phenomenon it describes. All these considerations notwithstanding, in our experiments semi-quantitative RT-PCR has always been performed to obtain a homogeneous array of samples, so that the optimal dilution of each specimen for the electrophoretic run would be in its own right an indication, though by no means an accurate measure, of its transcription level. Furthermore, it would allow this technique to be effectively combined with QRT-PCR if more accurate measurements were desired.

The sensibility and efficiency of the method employed to study CD40 transcript variants was validated on CD45, a gene that exhibits a known alternative splicing pattern (see Appendix A).

### 3.03 - DETECTION OF CD40 SPLICING VARIANTS IN SUBPOPULATIONS OF HUMAN B LYMPHOCYTES

Analysis of the B-LCLs brought forth evidence of a series of CD40 splicing products common to all samples, even including the control. Since CD40 signalling pathway is known to be constitutively activated in EBV-transformed cell lines [54, 128, 129], logic demanded that we should assay B cells from a fresh blood sample to find out whether the same pattern of PCR products could also be observed in normal B lymphocytes, and whether it would show any variation between resting and activated cells.

We purified three B cell subtypes, based on their surface markers:

- 1) **CD19<sup>+</sup>** cells at large, designated as **total B lymphocytes**;
- 2) **CD19<sup>+</sup>27<sup>+</sup>** cells, or **memory B cells**, a part of which has already undergone CD40/CD40L activation in a germinal centre;
- 3) **CD19<sup>+</sup>27<sup>-</sup>** cells, representing pre-germinal centre **mature B cells**.

All cells were separated using MACS<sup>®</sup> Technology. Applying the B cell Negative Isolation Kit to PBMCs obtained from a buffy coat yielded a 98% purified CD19<sup>+</sup> population by depletion of non-B cell types (we choose to avoid B cell positive selection because we had already established that engagement of CD19 with the anti-CD19 magnetic beads contained in the positive isolation kit would have caused induction of CD40 and CD19 itself, altering the desired experimental conditions).

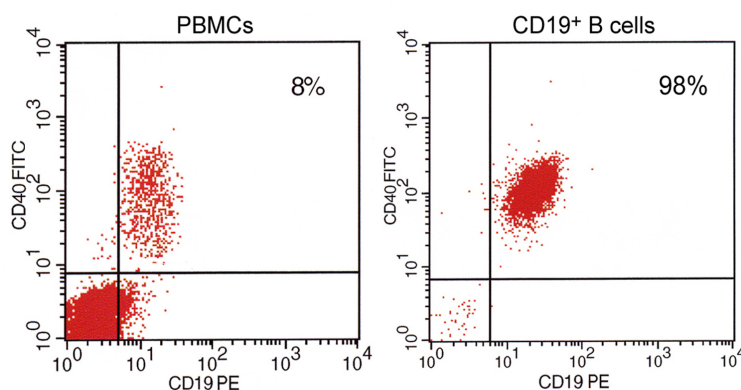


**Fig. 3.05** - Flow cytometry analysis with FITC-conjugated anti-CD40 and PE-conjugated anti-CD19 antibodies. 8% of total PBMCs separated on Ficoll-Paque density gradient are B cells (left). Selection with MACS B cell Negative Isolation Kit yields a 98% pure population of CD19<sup>+</sup>40<sup>+</sup> B lymphocytes (right).

Mature and memory B cells were then sorted from CD19<sup>+</sup> cells via positive selection with anti-CD27 magnetic beads. Purity of the cell fractions was verified through flow cytometry profiling with fluorescence-conjugated antibodies directed against CD40 and CD19 (Fig. 3.05).

To further diversify those three cell populations into a wide range of possible activation states, we cultured them for 24 h with either anti-CD40 [E5-A] antibody + IL-4, to activate the CD40 signalling pathway, or SAC + IL-2, to stimulate the BCR. We collected total RNA from a fraction of each sample before stimulation and 24 h afterwards. QRT-PCR for *AICDA*, one of the main targets induced by CD40 activation, was performed on cDNAs from total, mature and memory B cells stimulated with IL-4/anti-CD40, using  $\beta$ -actin as an endogenous control. As reported in Fig. 3.06, *AICDA* expression levels did increase after 24 h of stimulation for all cell fractions, confirming proper activation of the CD40 signalling pathway.

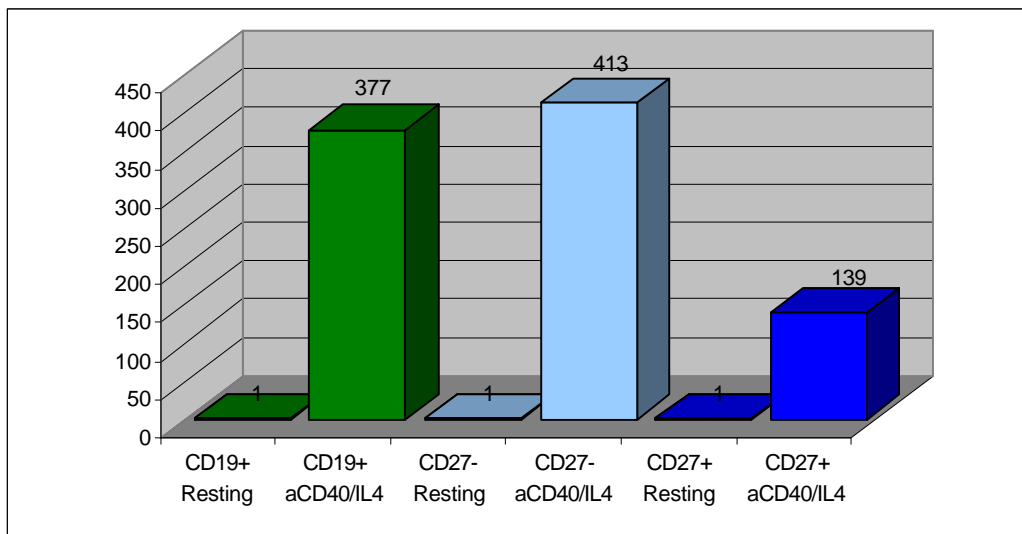


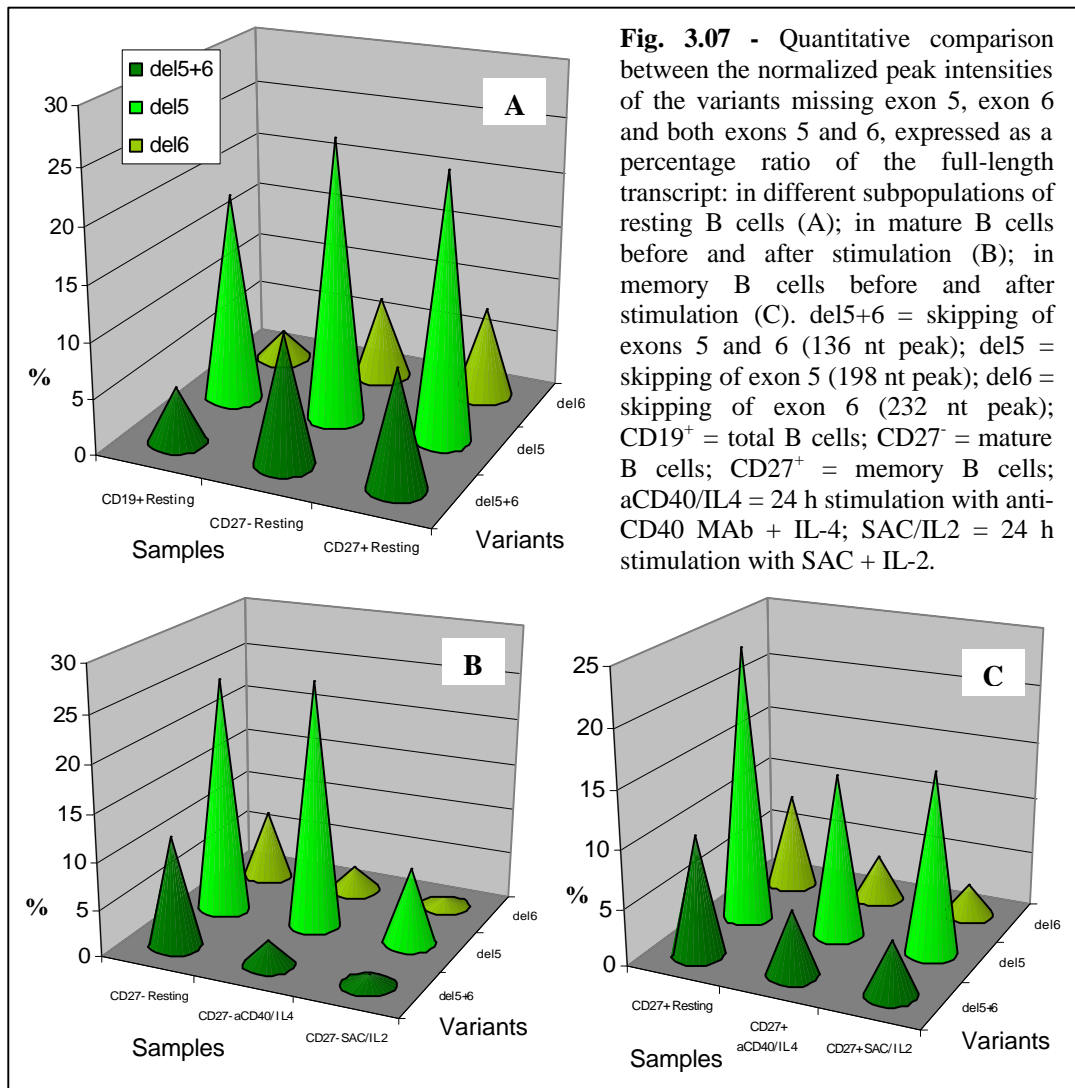
**Fig. 3.06** - CD40 activation of B cell fractions after 24 h of stimulation with anti-CD40 IgG + IL-4, as determined by *AICDA* expression. Relative expression levels for each activated fraction were calculated with the  $\Delta\Delta C_t$  method [130] baselined for the threshold cycle of the respective resting fraction. CD19<sup>+</sup> = total B cells; CD27<sup>-</sup> = mature B cells; CD27<sup>+</sup> = memory B cells; aCD40/IL4 = anti-CD40 MAb + IL-4.

We assayed CD40 splicing variant patterns from all B lymphocyte samples with the same house protocol employed for B-LCL analysis. Peak

sizing data confirmed the presence of all PCR products already observed in the control B-LCL sample. No new products were found, and neither was there any evidence of qualitative splicing pattern variations between the different B cell activation states considered.

As for quantitative variations, they could only be described for the isoforms appearing on the NED channel, since all other splicing variants were too close to the detection limit to support any reliable analysis. For each sample we recalculated the intensity of the three shorter isoforms (i.e. skipping of exon 5, of exon 6, or of both exons 5 and 6) as a ratio of the full-length transcript. This effectively allowed us to directly compare the abundance of these variants between specimens which differ in the absolute expression level of CD40. In fact, in semi-quantitative RT-PCR we detected a slight increase in overall CD40 expression after engagement of BCR or CD40 itself, in agreement with current observations on CD40 upregulation [131].

By plotting side by side the relative values obtained for resting B cells from the total, mature and memory subpopulations, we could observe that the proportions among the three variants and between them and the full-length transcript were quite conserved in the different cell types (Fig. 3.07 A). Moreover, by plotting the resting fraction of each cell type next to its activated states we could evaluate the effects of CD40 and BCR stimulation in every subpopulation. Memory, CD27<sup>+</sup> B cells display a sensible reduction of all three variants (Fig. 3.07 B); since CD40 overall expression showed a tendency to increase in the stimulated samples, this signifies that activation specifically bolsters the full-length variant rather than increasing the general level of CD40 transcription. Mature, CD27<sup>-</sup> B cells show a decrease in the variants missing exon 6 upon activation of the CD40 receptor, and a reduction of all three variants upon activation of the BCR (Fig. 3.07 C). This implies a selective increase in both the full-length and the skipping of exon 5 variants in the case of CD40 stimulation, or in the full-length transcript alone in the case of BCR stimulation.



It is interesting to note that if we choose a basic sampling of B lymphocyte populations, namely non-treated CD19<sup>+</sup>, CD19<sup>+</sup>27<sup>-</sup> and CD19<sup>+</sup>27<sup>+</sup>, and then compare peak sizing data with the information gathered on the B-LCL samples (Fig. 3.08), a faint signal for a PCR product matching the aberrant length of amplicon A in Pt. 3 can be seen on the FAM channel of most other samples. Its absence from some of the samples is likely to be an issue of detection limit: this PCR product was so scarce in all samples but Pt.3 that we overlooked it during our previous analysis of the B-LCLs alone, since it did not appear in any of the clones we sequenced except those obtained from Pt.3. With more data to draw upon, recurrence of this peak bears indication that the cryptic splice acceptor site systematically used in Pt.3 also works for a very

limited proportion of transcripts in normal B cells, hypothetically because of random errors in exon recognition by the splicing machinery.

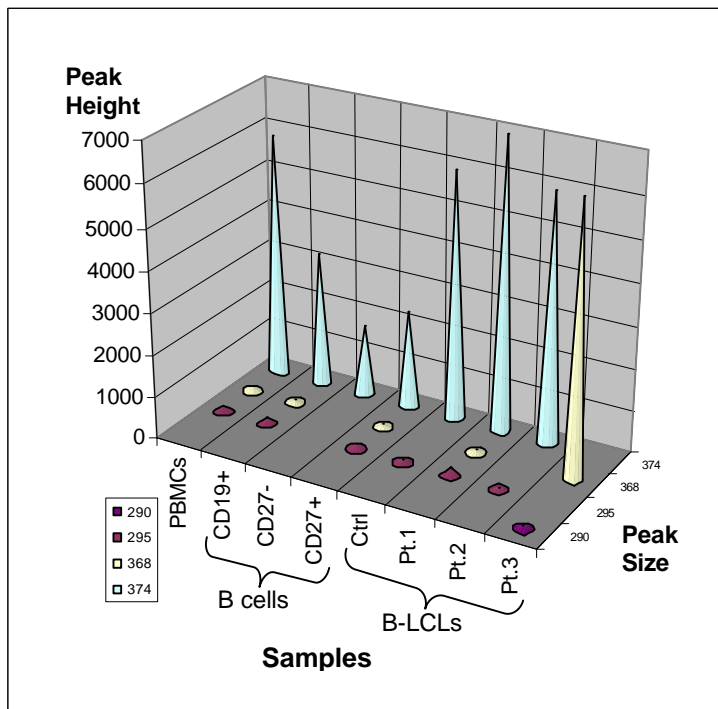


**Fig. 3.08** - Comparison between the FAM channel peaks from subpopulations of resting B cells and from B-LCLs highlights the recurrence of a low signal matching the main peak of Pt.3, i.e. a transcript using a cryptic splice acceptor site 6 nt within exon 4. Peak heights are reported as read by *GeneMapper*, and no normalization was made between the two sample groups.

### 3.04 - DETECTION OF CD40 TRANSCRIPT VARIANTS IN SEVERAL DIFFERENT HUMAN TISSUES

While to the best of our knowledge the relevance of CD40 in HIGM-3 syndrome only concerns its presence on B lymphocytes and antigen presenting cells, this receptor is also widely expressed in non-hematopoietic cells, mostly with a pro-inflammatory role [8, 11]. In order to investigate the splicing behaviour of CD40 in a comprehensive range of cell types, we applied our transcript variant analysis to a panel of pre-normalized, serial diluted cDNAs from 24 different human tissues and developmental stages, commercially available from OriGene Technologies. Initially we tested the panel for CD40 expression in a QRT-PCR, using  $\beta$ -actin as a reference housekeeping gene and

the expression level from PBLs as a baseline value for the  $\Delta\Delta C_t$  calculation method. Relative expression levels in all other tissues, albeit detectable, were very low, with the exception of the brain that showed transcription levels more than ten times higher than PBLs (Fig. 3.09 A). This data fits in well with the numerous reports on the abundance of CD40 expression in the microglia [132].

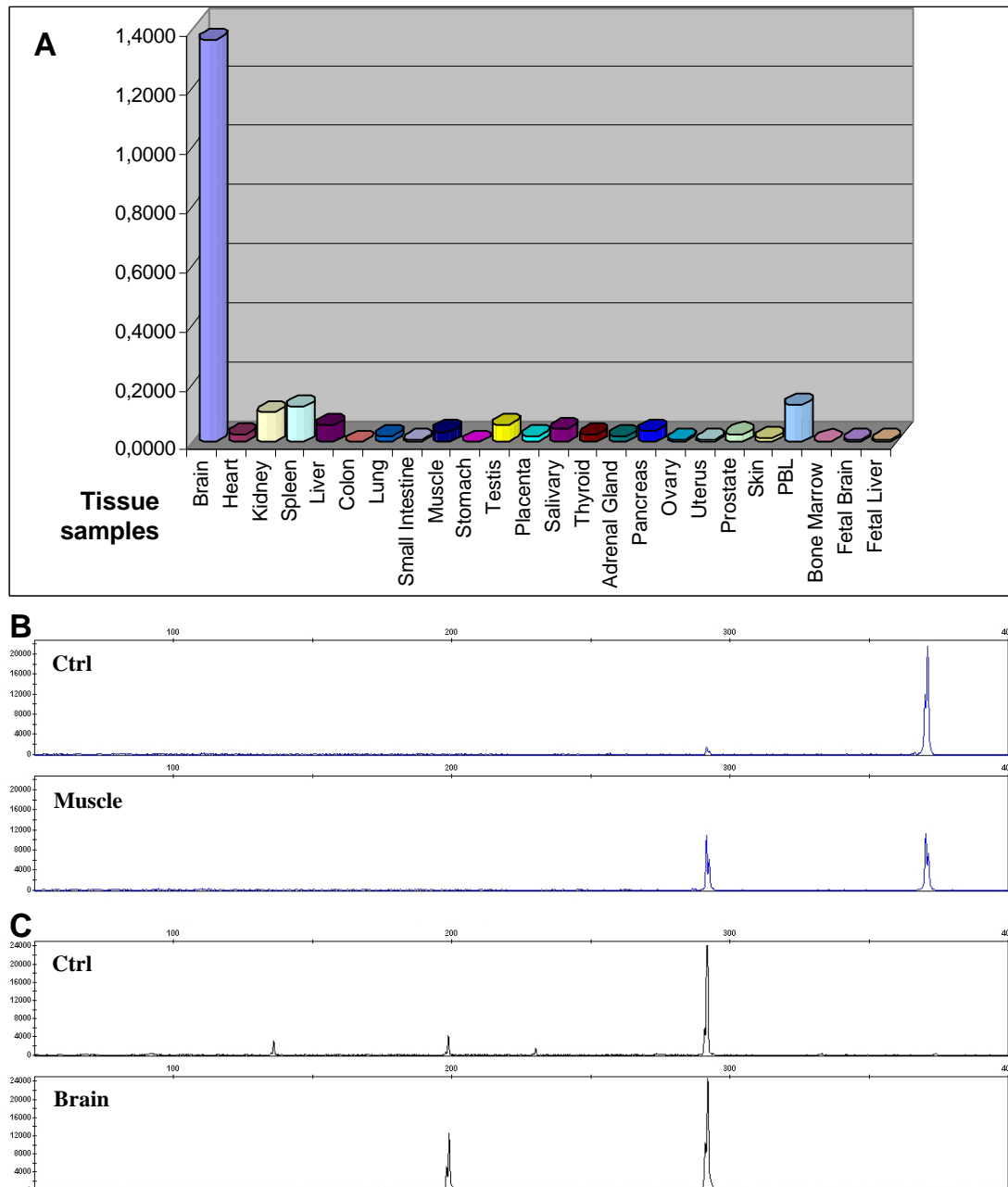


**Fig. 3.09** - A) CD40 expression levels in a range of different human tissues/developmental stages, calculated with the  $\Delta\Delta C_t$  method baselined for the threshold cycle of Peripheral Blood Lymphocytes (PBLs). B) Comparison between *GeneMapper* plots from muscle and control B-LCL samples on the FAM channel highlights the marked incidence of skipping of exon 2 in the former sample. C) Comparison between *GeneMapper* plots from brain and control B-LCL samples on the NED channel reveals absence of the transcripts missing exon 6 or both exons 5 and 6 in brain.

We had to exclude uterus, prostate, skin, bone marrow and fetal tissues from the splicing variant analysis on account of their expression levels being so modest they would bring the less represented splicing variants well below the detection limit of our assay. It should be noted here that no indication was given by the supplier on tissue handling prior to RNA extraction, therefore most samples are likely to be contaminated by the CD40-expressing endothelial cells of capillary blood vessels.

Splicing variant analysis of the gene expression panel revealed the same products and patterns already observed in the previous experiments, with two noteworthy exceptions: muscle and brain (Fig. 3.09 B and C). The muscle showed comparable levels of full-length amplicon A and skipping of exon 2 on the FAM channel. The brain, despite its general high level of CD40 expression, displayed no detectable variants missing exon 6 on the NED channel, either alone or in conjunction with exon 5.

### **3.05 - SIX CD40 SPLICING VARIANTS ARE CONSERVED THROUGHOUT DIFFERENT CELL TYPES**

Overall, other than the canonical full-length transcript and the defective mRNAs from affected individuals, combining the data from the previous experiments we identified at least six CD40 splicing variants frequently recurring above the detection threshold of our assay. Their identity and the predicted outcome of their translation are summarized in Fig. 3.10.

**Skipping of exon 2** leads to a frameshift, generating a premature termination codon (PTC) at the beginning of exon 3. According to state-of-the-art literature on mRNA regulation, the position of this PTC is very likely to direct the transcript toward nonsense-mediated mRNA decay [133]. Furthermore, the predicted protein would be barely 1 aminoacid longer than the

signal peptide, a product which makes no sense and which is far too unstable to be effectively translated. Either way, this variant implies a co-transcriptional or co-translational control of CD40 expression. Muscle tissue could provide a good model to investigate this kind of regulation, since splicing out of exon 2 appeared to occur nearly as often as its inclusion in the full-length transcript (Fig. 3.09 B).

The use of an **alternative 5' splice site in intron 7** adds 12 nt to the canonical 5' end of exon 7, resulting in a Lys216 to Ser mutation and in the insertion of 4 residues (Glu-Ser-Ser-Glu) at positions 217-220. Predicting the outcome of this variation on protein stability/receptor function would prove difficult, since it occurs immediately beneath the transmembrane domain (entirely coded within exon 7), but upstream of the signal-transducing cytoplasmic tail of CD40.

The use of an **alternative 3' splice site in exon 8** causes a frameshift, which generates a stop codon 21 nt downstream of the new exon-exon junction. Provided it does not undergo nonsense-mediated RNA decay, this transcript will translate into a protein lacking the cytoplasmic tail and therefore incapable of signal transduction.

**Skipping of exon 5** leads to a frameshift and to the formation of a PTC within exon 7. Translation would produce a protein retaining two and a half of the four CRDs from the extracellular portion of the receptor, but ending with a frameshift-generated sequence of 26 aa which bears no homology to any other known human protein accessible through a BLAST query. Transmembrane and intracellular domains are completely missing. From the information gathered, three hypotheses on this splicing variant can be surmised: its product could be a soluble, and possibly secreted, isoform of CD40 still retaining some ligand-binding capability; its product could be misfolded and/or degraded; the transcript could be subjected to nonsense-mediated RNA decay. The two latter conjectures would indicate a post-translational or co-transcriptional regulation of CD40 expression, while the former suggests a product with a distinct biological role.

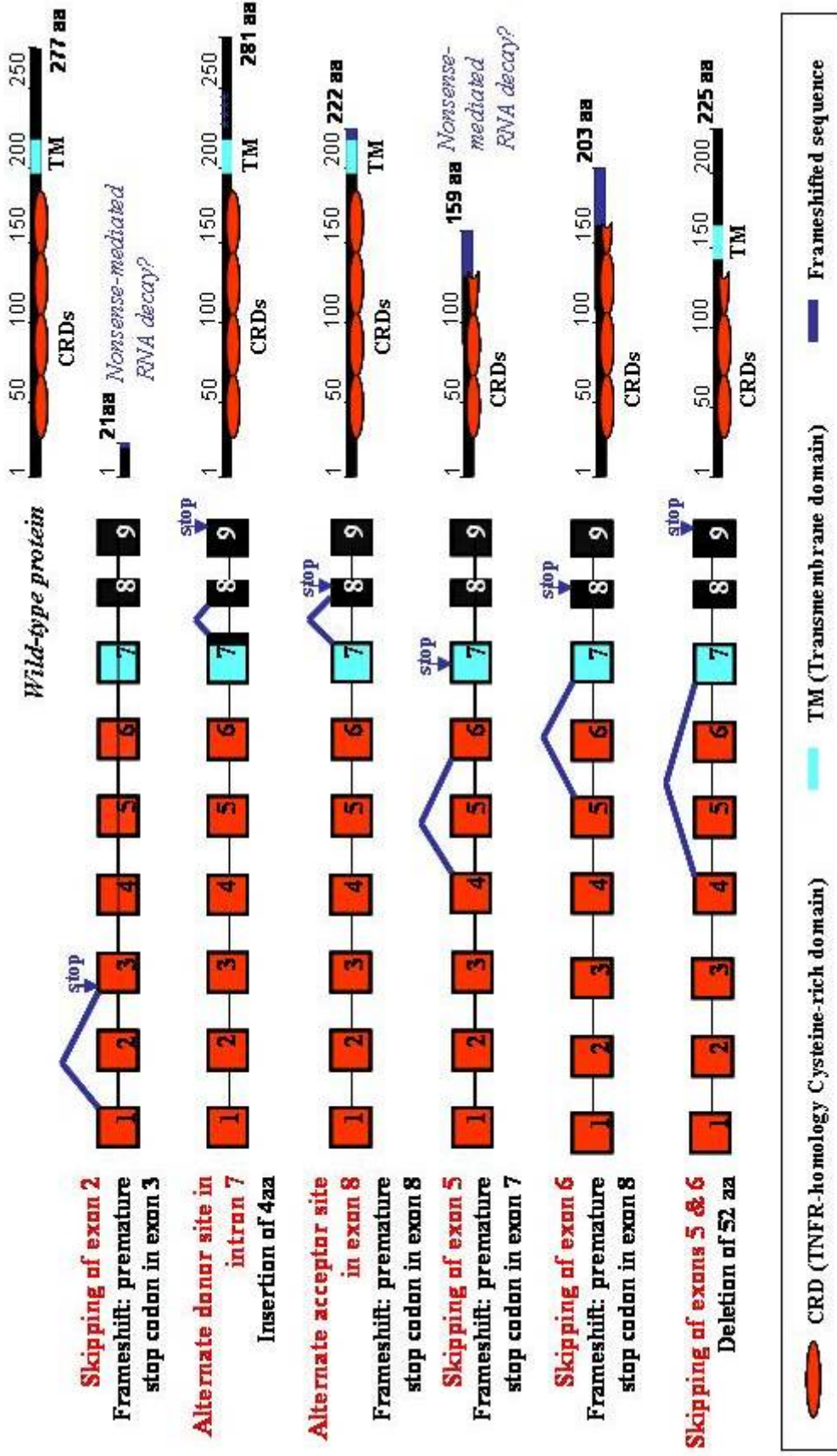
**Skipping of exon 6** also leads to a frameshift and to the formation of a PTC within exon 8. It would encode a product similar to the variant missing exon 5, but with a more extended CRD region fused to 38 frameshift-generated residues. The effective outcome of translation would also contemplate the same hypotheses exposed for skipping of exon 5. The presence of three CRDs instead of two does not necessarily mean greater protein stability, since TNFR superfamily members are known to have a number of CRDs ranging from one to six [34]. Position of the PTC near the 3' end of exon 8, though, would make nonsense-mediated RNA decay unlikely for this transcript.

**Skipping of both exons 5 and 6** causes the downstream sequence to remain in-frame, with a deletion 156 nt encompassing the region coding for CRD4 and half of CRD3. Unless foiled by misfolding and degradation, this transcript can generate a protein retaining the whole transmembrane and cytoplasmic domains, which would reasonably represent an isoform of CD40 with the same membrane localization but impaired binding capability. Functional binding of a TNF-like ligand to a receptor with non-canonical, incomplete CRDs has already been described for BAFF/BR3 [134].

Some of these splicing variations are not mutually exclusive and could occur within the same transcript; when a single pair of PCR primers was used to amplify the entire ORF from CD40 cDNA, though, this was never observed.

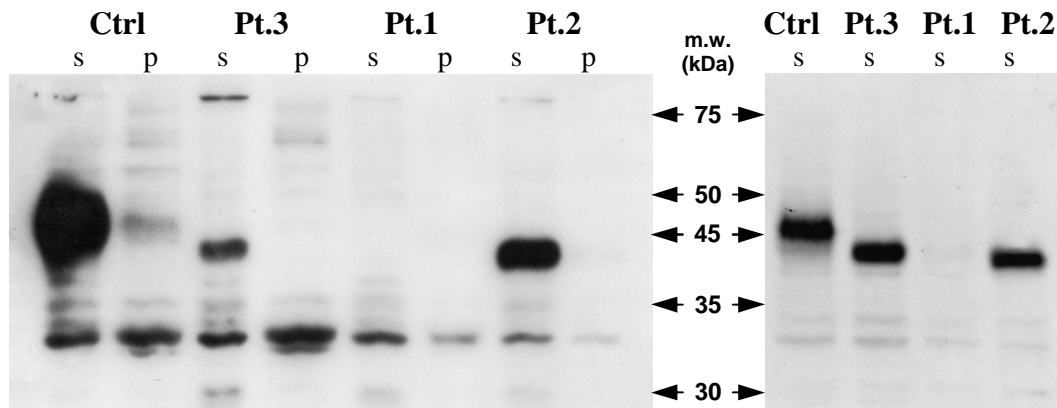
Most of the alternatively spliced variants are weakly expressed, making analysis of their physiological function difficult. For this reason, further efforts in our investigations focused on the two most abundant isoforms, namely those generated by skipping of exon 5 and by skipping of both exons 5 and 6. While cloning the PCR products from the control B-LCL to confirm their sequence, these two were the only variants to be found in more than 1% of the clones. We also took advantage of the fact that Pt.1 chiefly expresses these two specific variants in a wt-CD40 knockout environment, providing a good model for this kind of analysis.

Fig. 3.10 - *TNFRSF5* mRNA splicing variants and protein isoforms.



### 3.06 - DETECTION OF THE CD40 PROTEIN

Detection of the CD40 protein was performed by Western Blot on lysates from Pt.1, Pt.2, Pt.3 and control B-LCLs, using either anti-CD40 (C-20), a polyclonal IgG raised against the intracytoplasmatic C-terminus of the receptor, or anti-CD40 (H-120), recognizing the extracellular CRDs (Fig. 3.11).



**Fig. 3.11** - Western blots showing B-LCL lysates probed with anti-CD40 (H-120) IgG, directed against the extracellular domains of CD40 (left) or with anti-CD40 (C-20) IgG, directed against the C-terminal, intracellular region of CD40 (right). Analysis of the pellet fraction, containing nuclei and cell debris, revealed only traces of the CD40 protein, hence it was discontinued unless otherwise noted. Anti-CD40 (H-120) IgG showed a remarkably different affinity among the CD40 variants, whereas anti-CD40 (C-20) recognized all of them equally well. Both antibodies failed to reveal any of the expected CD40 products in Pt.1 lysate. s=supernatant, p=pellet

The same amount of total proteins was loaded from each sample. In the supernatant fraction of the control lysate, containing membranes and soluble proteins, both antibodies revealed with similar efficiency the 45 kDa band characteristic of CD40. The pellet from the lysate, containing nuclei and cell debris, shows just a trace of CD40, probably due to contamination with the supernatant fraction. In the lysate from Pt.1 B-LCL only faint bands at a small molecular weight were detected. Since they were present in all lysates, they are likely to be the result of aspecific binding, but lacking a CD40 knock-out as a negative control we could not rule out the possibility that they could be CD40 isoforms or degradation products. Lysates from Pt.2, Pt.3 and B-LCLs were positive, but for a band at a molecular weight slightly smaller (35 kDa) than the expected. Their aminoacid sequence variations by themselves were too small to

account for the observed weight difference, unless they somehow hampered protein maturation. Indeed, anti-CD40 (H-120) IgG showed weaker recognition of the mutant proteins than anti-CD40 (C-20), suggesting that these sequence variations affected the modification of the CRDs.

*In silico* prediction of post-translational modifications identified two putative N-glycosylation sites (centered around Asn153 and Asn180) in the extracellular region. We removed all N-linked oligosaccharides by treating lysates from Pt.2, Pt.3 and control B-LCLs with PNGase F; the same test was eventually repeated for Pt.4 at the Pediatric Clinic of the University of Brescia with identical results (data withheld by the investigators). Complete N-deglycosylation brought the molecular weight of the mutant and wild-type proteins on the same level, evidencing incomplete glycosylation of the mutants during maturation (Fig. 3.12). This defect is probably caused by a misfolding of the CRDs that prevents exposure of the correct Asn residues for oligosaccharide modification. Failure to undergo proper glycosylation is predicted to thwart protein folding even further and check its maturation at the Endoplasmic Reticulum (ER)/Golgi level, which would explain why the mutant proteins fail to be exposed on the plasma membrane.

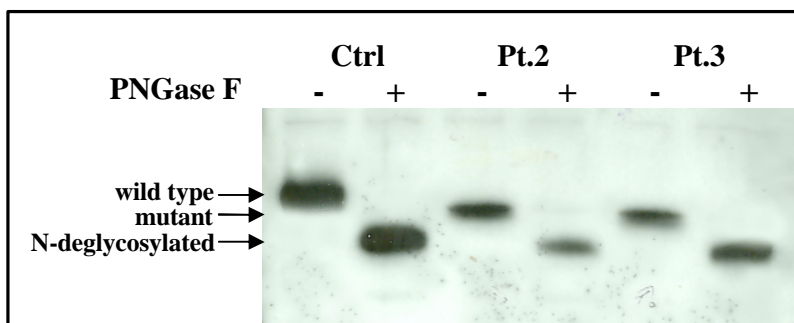


**Fig. 3.12** - After 1 hour digestion with PNGase F, which removes N-linked oligosaccharides, the protein scaffold assumes the same weight in both the control and the patients.

Confocal microscopy on B-LCLs derived from Pt.3 confirmed retention of the mutant protein in the ER, as defined by staining with an anti-PDI antibody, while on control B-LCLs CD40 was correctly localized on the cell surface (Fig. 3.13).

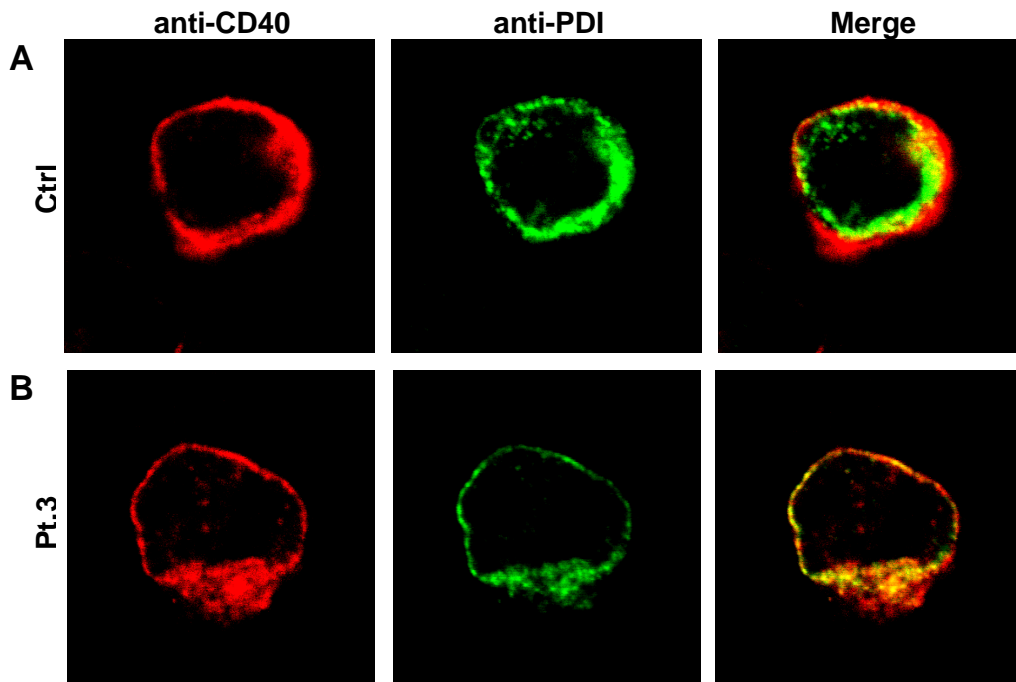


**Fig. 3.13** - Immunofluorescence staining of control (A) and Pt.3 (B) B-LCLs for CD40 (left panels) and ER (middle panels). Mutant protein from Pt.3 tends to accumulate on one side of the cell. Merging the channels (right panels) shows colocalization of Pt.3 mutant CD40 and the ER, while the wild-type protein correctly becomes localized on the plasma membrane.

These observations demonstrate the importance of glycosylation in CD40 functional maturation. Since the N-glycosylated residues Asn153 and Asn180 are encoded respectively within exon 5 and exon 6, the putative CD40 isoforms originating from transcripts lacking one or both of these exons would arguably undergo an inefficient maturation as well. Even if a small fraction managed to fold productively, it could prove difficult to detect, since it would probably bind anti-CD40 (H-120) IgG with low affinity, and only the in-frame variant would be recognized by anti-CD40 (C-20).

### **3.07 - RECOMBINANT CONSTRUCTS AND STABLE CELL LINES EXPRESSING CD40 AND ITS VARIANTS ALLOW CONSIDERATIONS ON PROTEIN STABILITY**

In order to facilitate CD40 products recognition in Western blot, to better pinpoint their localization in cells, and in general as an aid to understanding CD40, we cloned the most relevant variants into three different sets of mammalian expression vectors: pcDNA3, pEGFP-N1 and pFLAG-N1. All plasmids guarantee good expression levels since the heterologous gene is placed under the transcriptional control of the highly efficient IE-CMV promoter.

We elected to clone cDNAs obtained from the wild-type full length transcript (wt-CD40), from Pt.3 full-length transcript (pt3-CD40), from Pt.4 full-length transcript (pt4-CD40), and from the wild-type transcripts missing exon 5 (del5-CD40) or both exons 5 and 6 (del5+6-CD40). Since in Western blot analysis Pt.2 behaved exactly as Pt.3, we saw fit to delay development of constructs containing Pt.2 CD40 until we could gather more data on Pt.3. CD40 transcriptional state of Pt.1 is reproduced by vectors del5-CD40 and del5+6-CD40.

**pcDNA3 constructs** were used to express unmodified gene products from the individual CD40 variants.

In **pEGFP-N1 constructs** the C-terminal end of the CD40-derived peptides was fused with the Enhanced Green Fluorescence Protein (EGFP), which allows direct visualization of the heterologous products in live cells via fluorescence microscopy. EGFP was joined at the C-terminus of the CD40 products because modification of the N-terminus was predicted to interfere with folding. A large drawback is that EGFP takes up a large part of the chimeric protein, particularly where the short del5-CD40 isoform is concerned: the fluorescent moiety comprises 239 residues and weighs 27 kDa, whereas for instance wt-CD40 is only 277 aa long and weighs about 45 kDa in its glycosylated form. This may well affect protein stability, and almost surely prevents TRAFs binding and signal transduction.

**pFLAG-N1 constructs** express the CD40 variants as fusion proteins with a C-terminal FLAG<sup>®</sup> epitope tag. This small octapeptide is very unlikely to adversely affect folding or protein stability, and allows indirect detection of the recombinant products with an anti-FLAG MAb.

All vectors were used for transient expression in HEK-293 mammalian cells. RT-PCR confirmed that all heterologous genes were transcribed correctly and efficiently by the host cells.

Expression of the EGFP-tagged variants was easily verified through fluorescence microscopy (Fig. 3.17). Western Blot analysis with anti-CD40 (H-120) IgG confirmed the correct size of the EGFP-tagged products (Fig. 3.14 B), but failed to detect pcDNA3-based constructs del5-CD40 and del5+6-CD40 altogether (Fig. 3.14 A).

Western Blot analysis of the FLAG-tagged recombinant products with an anti-FLAG MAb revealed expression of all but the del5-CD40-FLAG construct (Fig. 3.14 C), and reblotting with anti-CD40 (H-120) IgG provided identical results. Since according to structure prediction del5-CD40 product should be soluble and possibly secreted, we searched for it in a serum-free culture medium in which HEK-293 cells transfected with del5-CD40-FLAG were grown for 24h. Even concentrating the medium 70-fold, though, we found no trace of it either with anti-FLAG MAb, or by reblotting with anti-CD40 (H-120) IgG (data not shown). Presumably, del5-CD40 is recognized as an aberrant product and downregulated at the translational level, and it was only observed as a fusion peptide with EGFP because the EGFP moiety itself granted stability to the whole protein. This consideration might also hold true for del5+6-CD40 and del5+6-CD40-FLAG.

In order to gain a more robust tool for experiments dealing with protein analysis, we also established two stable cell lines that constitutively expressed wt-CD40-FLAG (designated as HEK-40F) or wt-CD40-EGFP (designated as HEK-40G). HEK-293 cells were used as a host because they do not express endogenous CD40 (Fig. 3.15 panel A), and since they were originally derived

from human embryonic kidney they should carry out protein maturation in the correct species-specific manner.

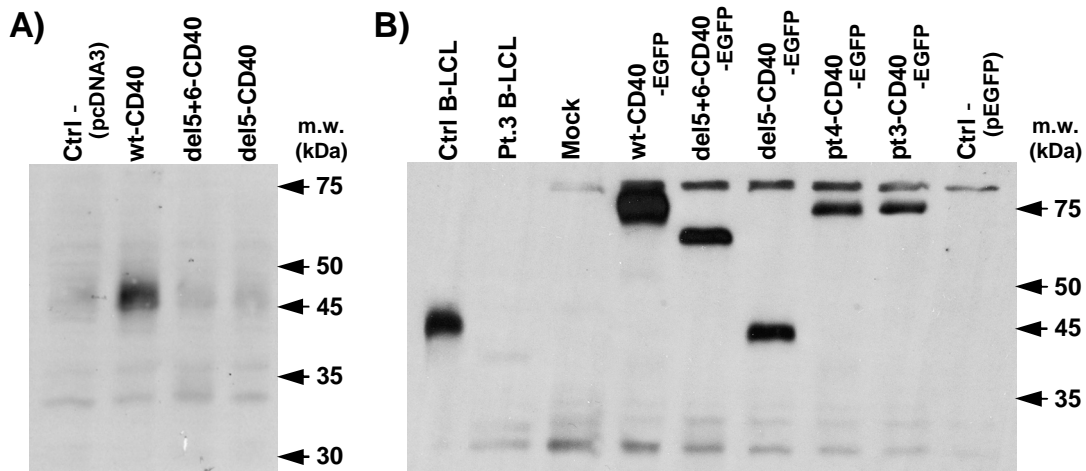
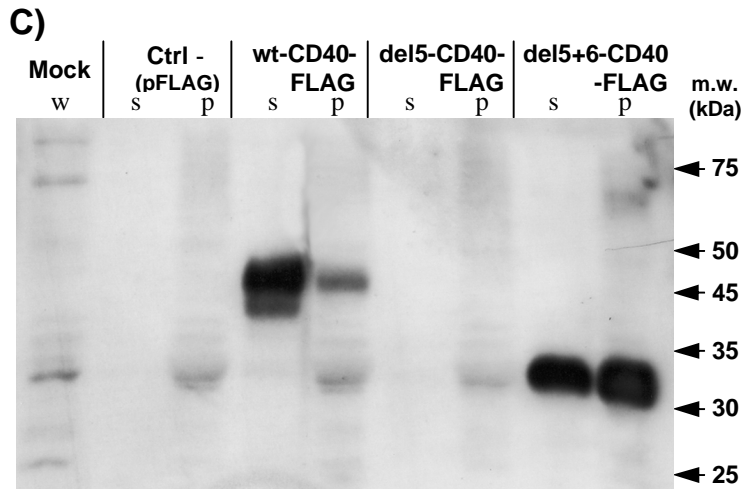


**Fig. 3.14** - Western blots showing lysates from HEK-293 cells transfected with the recombinant vectors: pcDNA3 constructs (A), pEGFP constructs (B) and pFLAG constructs (C). A and B were probed with anti-CD40 (H-120) IgG, since del5-CD40 products lack the correct C-terminus and could not possibly be revealed by anti-CD40 (C-20). Reblotting with anti-CD40 (C-20) confirmed this assumption (data not shown). C was probed with anti-FLAG MAb, and later reprobed with anti-CD40 (H-120) (data not shown). s=supernatant, p=pellet, w=whole lysate, Ctrl-=transfection with appropriate empty vector, Mock=mock transfection (without plasmid DNA)



### **3.08 - EXPOSURE OF THE CD40 VARIANTS ON THE PLASMA MEMBRANE**

We analyzed HEK-293 cells transfected with wt-CD40, wt-CD40-FLAG, del5+6-CD40, del5+6-CD40-FLAG and pt4-CD40-FLAG in a flow cytometer to detect cell surface exposure of the appropriate CD40 variant. Presence of wt-CD40 and wt-CD40-FLAG on the cell surface proved to be fair,

though expression level and number of positive cells were considerably lower compared to the control B-LCL (Fig. 3.15 panel A). del5+6-CD40, del5+6-CD40-FLAG and pt4-CD40-FLAG all displayed poor surface expression, with del5+6-CD40 being barely detectable and del5+6-CD40-FLAG showing the greatest CD40 exposure among the three (Fig. 3.15 panels B through E). On one hand, this seems to indicate that the FLAG epitope does help stabilize the del5+6-CD40 peptide, which is an interesting result *per se* since the C-terminal end of a TNFR family member is not supposed to influence stability of the whole protein to such extent. On the other hand, this proves that the CD40 mutation of Pt.4 is leaky and does not prevent surface exposure completely.

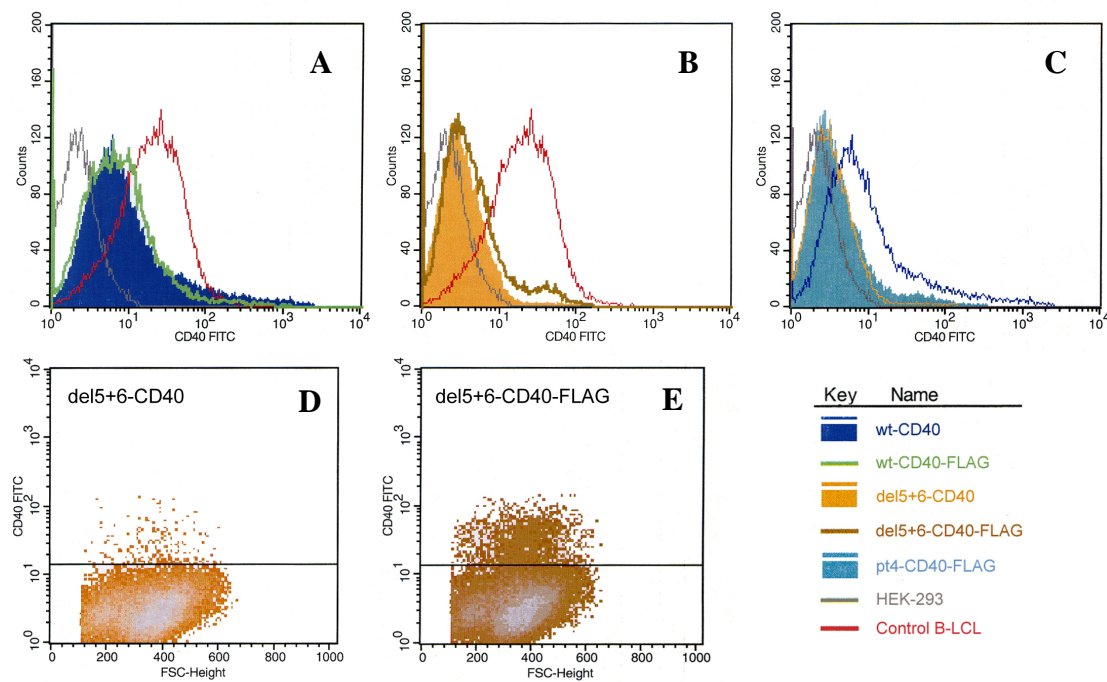


**Fig. 3.15** - Flow cytometry analysis of HEK-293 transfectants with FITC-conjugated anti-CD40. A) Histogram plot of wt-CD40 and wt-CD40-FLAG shows surface expression levels halfway between control B-LCLs and non-transfected HEK-293 cells. Non-transfected HEK-293 cells proved to be a good negative control because staining with either anti-CD40 or anti-IgG antibodies produced perfectly overlapping profiles (data not shown). B and C) Histogram plots of del5+6-CD40 compared with del5+6-CD40-FLAG and pt4-CD40-FLAG, respectively. D and E) Density plots of del5+6-CD40 and del5+6-CD40-FLAG.

Given that cytofluorimetric analysis successfully detected del5+6-CD40 on the cell surface, failure to do so in Western Blot probably depended on poor translation efficiency combined with suboptimal affinity of the polyclonal

antibodies for the variant peptides; hence the need to evaluate FLAG-tagged proteins and test anti-CD40 IgGs from different sources.

Since systematic splicing-out of exon 5 makes del5+6-CD40 the only possible membrane isoform in Pt.1 cells, the hitherto-unexpected observation of del5+6-CD40 on the transfectants surface prompted us to carry out in-depth cytofluorimetric investigations on Pt.1 B-LCLs. Staining with anti-CD40 [E5-A] IgG, which was raised against a different epitope than those recognized by the antibodies previously used in flow cytometry or Western blot, showed a definite signal on the surface of Pt.1 B-LCL (Fig. 3.16), marking the exposure of a CD40 variant. This result might have a deeper significance: according to product specifications, anti-CD40 [E5-A] IgG performs as an activating ligand for CD40 (and its efficiency has already been observed on B cells, as detailed in Fig. 3.06). Whatever it is the exact CD40 variant it recognizes, its binding could feasibly exert a biological effect, possibly through cross-linking and clustering of the CD40 isoform. High levels of the variant missing exons 5 and 6 revealed in Pt.1 transcript analysis, together with structural predictions suggesting the retention of pre-ligand association capability, offer strong indications that del5+6-CD40 might be exactly the antigen detected by the anti-CD40 [E5-A] antibody.

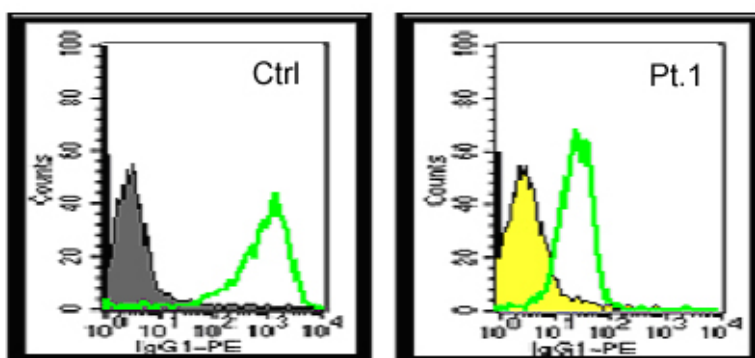


**Fig. 3.16** - Flow cytometry analysis of Pt.1 vs. control B-LCLs stained with an anti-CD40 [E5-A] activating antibody and a PE-conjugated secondary IgG.

**3.09 - LOCALIZATION OF THE CD40 PROTEIN VARIANTS WITHIN CELL COMPARTMENTS**

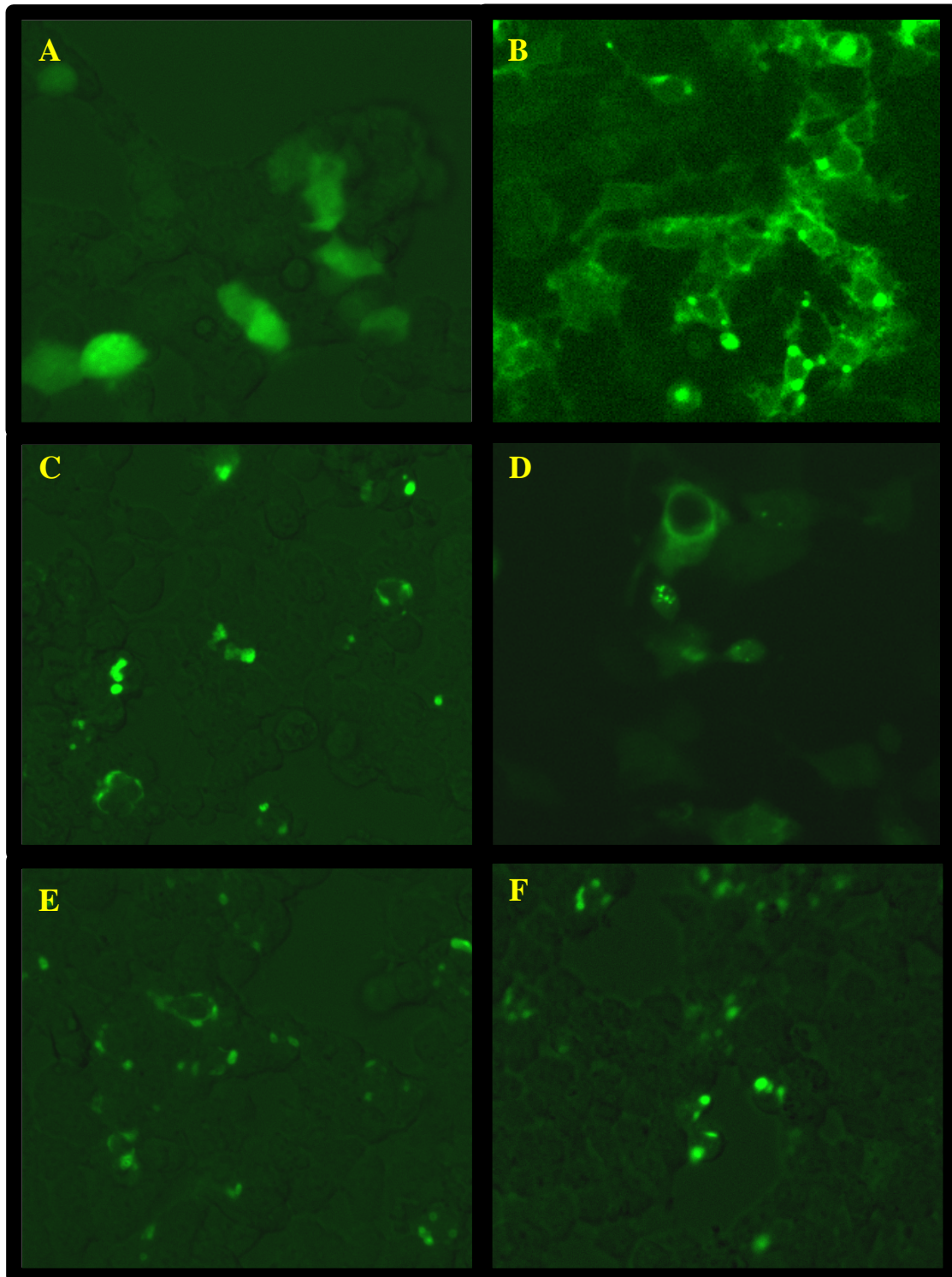


**Fig. 3.17** - Fluorescence microscopy of live HEK-293 cells transfected with: A) pEGFP-N1 (control vector); B) wt-CD40-EGFP; C) del5+6-CD40-EGFP; D) del5-CD40-EGFP; E) pt3-CD40-EGFP; F) pt4-CD40-EGFP. All images were captured on an inverted microscope with a 20x objective, overlaying fluorescence and transmitted light in order to outline the cells.

Fluorescence microscopy performed on HEK-293 cells 24 h post transfection (p.t.) with the EGFP-tagged constructs provided us an overview on the behaviour of the CD40 variants in live cells (Fig. 3.17). wt-CD40-EGFP could be seen defining the plasma membrane even in the outstretched cell processes, and formed inclusion bodies in cells where expression of the heterologous protein was greater/more prolonged (confirmed by observation at later times p.t., data not shown). del5-CD40-EGFP displayed a diffuse cytoplasmic distribution, which in a few cases coalesced in a punctate pattern. del5+6-CD40-EGFP, pt3-CD40-EGFP and pt4-CD40-EGFP accumulated in a small number of inclusion bodies in the perikaryal area. pt4-CD40-EGFP showed a tendency to form more discrete granules resembling vesicular deposits, whereas the other two recombinant proteins sometimes spread to outline part of the nucleus in a manner reminiscent of cis-Golgi.

Through ultracentrifugation we isolated different cell fractions from HEK-293 cells transfected with wt-CD40-FLAG or del5+6-CD40-FLAG (Fig. 3.18 A). Both CD40 isoforms were present in the fractions corresponding to mitochondria/lysosomes/peroxysomes and microsomes/small vesicles, and were indeed more abundant in these compartments than in the cell membrane. The nuclear fraction of HEK-293 transfectants appeared to contain small amounts of CD40, particularly where del5+6-CD40-FLAG is concerned. Though this result would agree with the nuclear localization of CD40 proposed by Lin-Lee *et al.* [135], we never observed CD40 isoforms within the nuclei of B-LCLs, and neither did we find any trace of them in the nuclei of transfected HEK-293 cells by EGFP fluorescence or, in later experiments, indirect immunofluorescence.

Surprisingly, fractionation of the control B-LCL also showed that the mitochondria/lysosomes/peroxysomes and the microsomes/small vesicles fractions were particularly enriched in CD40 with respect to the plasma membrane fraction (Fig. 3.18 B). Since plasma membrane is the site normally associated with CD40 function, consistent intracellular presence of the protein

indicates some form of post-translational control on CD40 expression, either through internalization or by retention in the ER/Golgi vesicles.

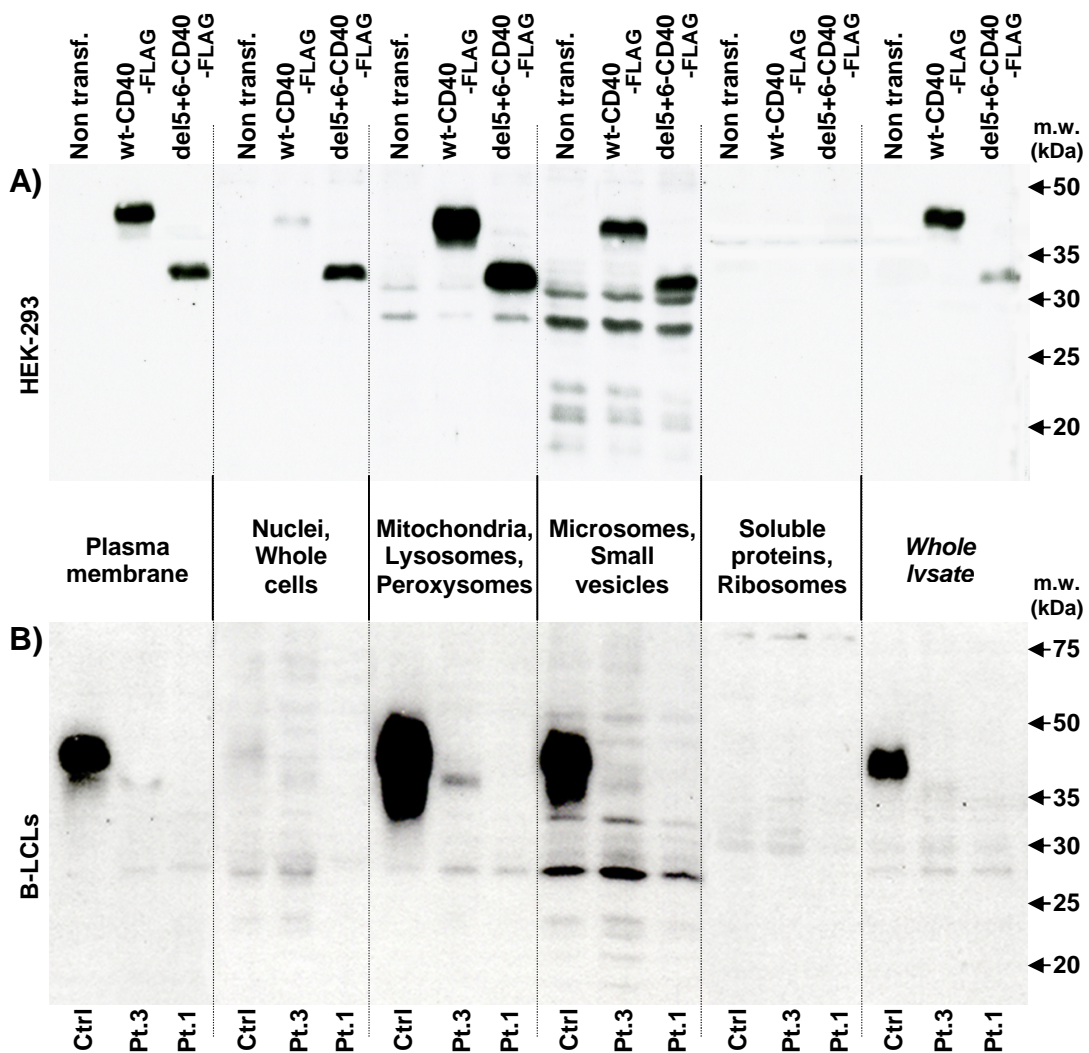


**Fig. 3.18** - Western blot with anti-CD40 (H-120) antibody after cell fractionation of HEK-293 transfectants (A) and B-LCLs (B). Non-transfected HEK-293 cells were used as a negative control.

We performed confocal microscopy on HEK-40F to identify the exact intracellular compartment in which CD40 accumulates. Fluorescence staining with anti-CD40 (LOB-11) IgG located wt-CD40-FLAG partly on the cell membrane, and partly in a single intracytoplasmic region near the nucleus. It did not colocalize with either Calnexin, an ER marker, or Giantin, a cis-Golgi marker (Fig. 3.19 A and B). On closer examination, the intracytoplasmic accumulation of CD40 and the Golgi structures evidenced by Giantin appeared juxtaposed (Fig. 3.19 row C), as if CD40 was retained in a nearby intracellular

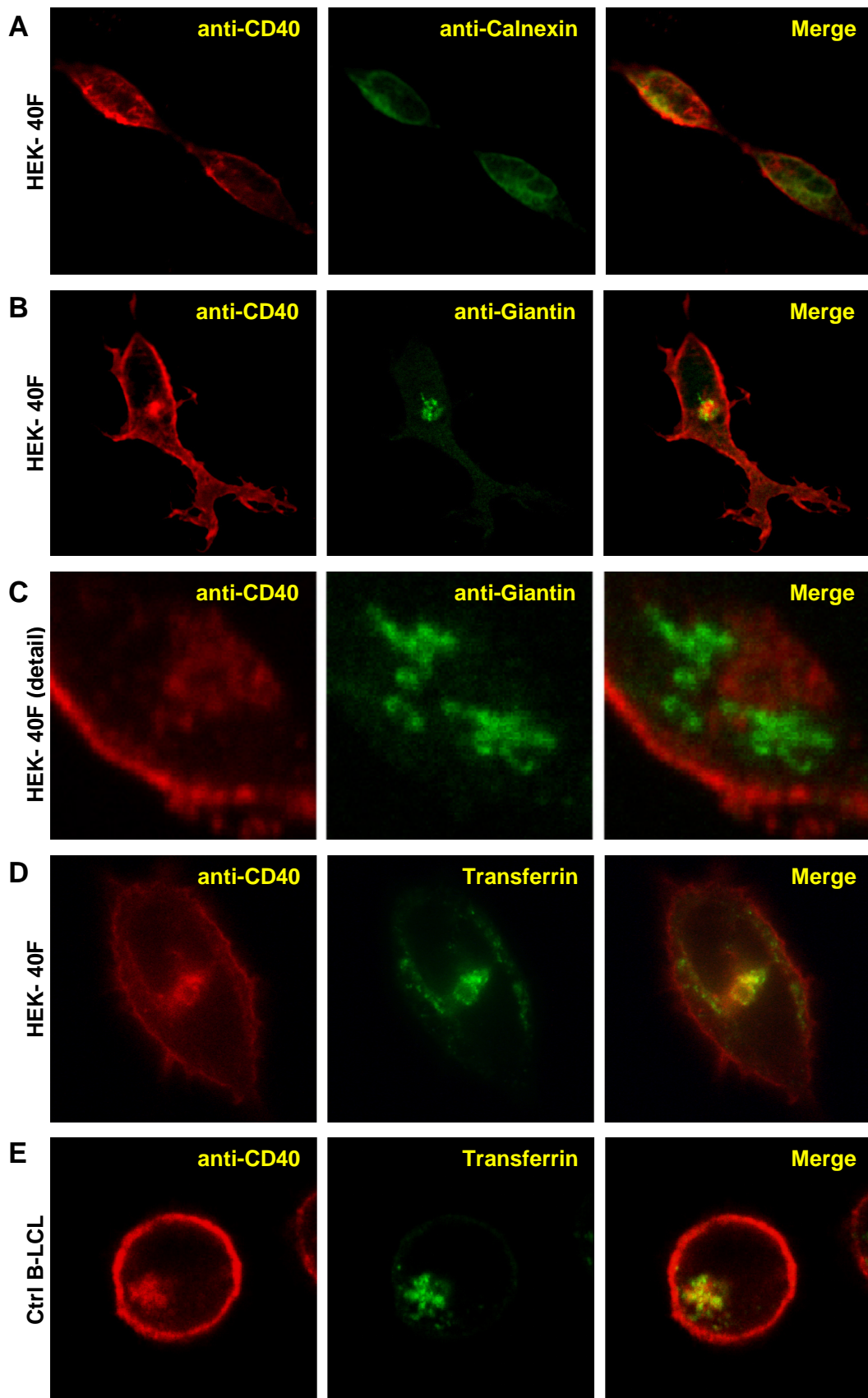


**Fig. 3.19** - Confocal microscopy analysis on HEK-40F cells (A-D) and B-LCLs (E). CD40 is stained in red (left panels), while the green staining (middle panels) is associated with Calnexin/ER (A), Giantin/Golgi (B, and detail of cytoplasmic accumulation of CD40 in C), or Transferrin/recycling compartment (D and E).

membrane compartment. In fact, by incorporation of fluorescein-conjugated human serum transferrin in live cells prior to fixation, we finally localized the CD40 intracytoplasmic fraction within the recycling compartment (Fig. 3.19 D). Further IF analysis also confirmed the presence of CD40 in the recycling compartment of control B-LCLs (Fig. 3.19 E).

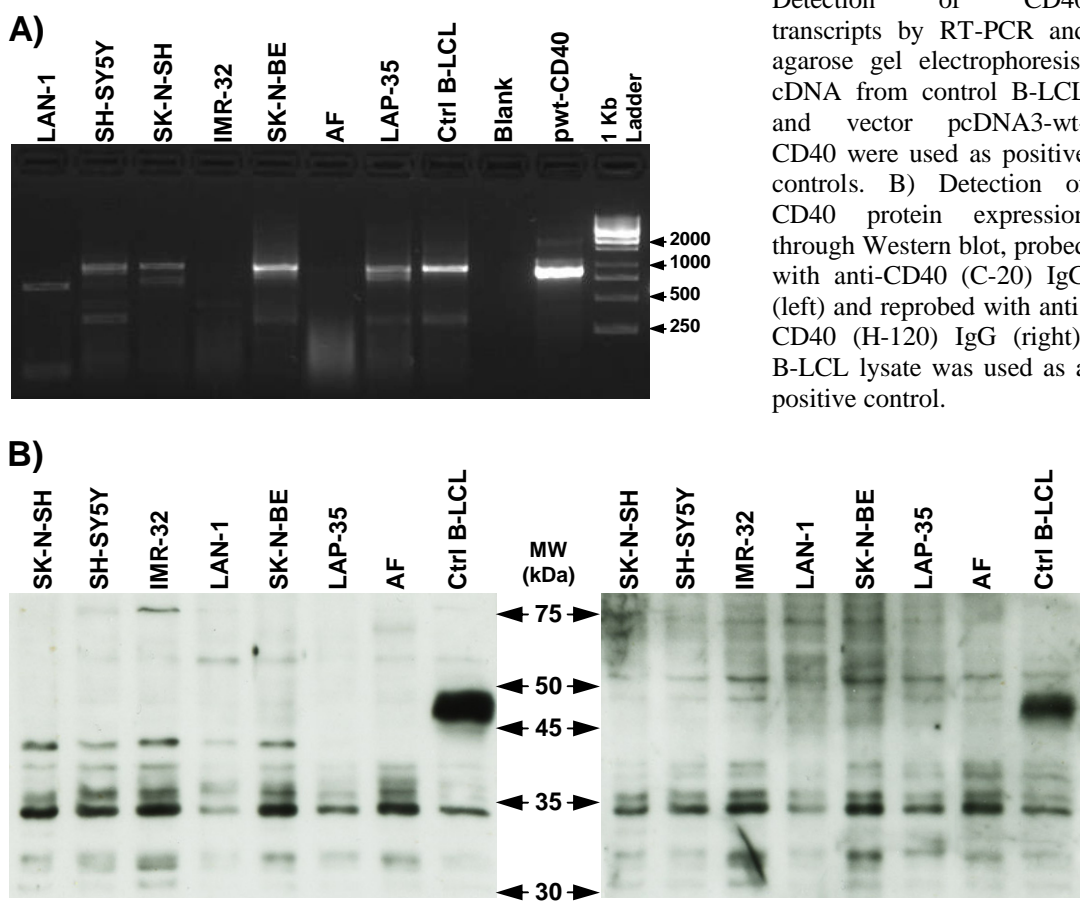
### **3.10 - ANALYSIS OF CD40 SPLICING IN NEUROBLASTOMA CELL LINES**

The information gathered from the CD40 splicing variants assays highlighted the peculiarity of brain tissue as regards expression level and splicing pattern, and prompted us to extend our analysis to cells from the central nervous system. Additional spur to follow this lead came from the fact that Pt.1 shows signs of mental retardation, though her situation is unclear and environmental conditions may have played a significant part in her impairment.

It is widely accepted in literature the importance of CD40 as a critical pro-inflammatory factor in the microglia [132, 136], but there is contrasting evidence about its presence on neuronal cells proper [137-138]. Given the difficulties involved in cultivating pure populations of these cell types *in vitro*, we set up a preliminary analysis using several cell lines derived from transformed human neural tissue: neuroblastoma in the case of LAN-1, SH-SY5Y, SK-N-SH, IMR-32, SK-N-BE and AF cells; neuroectodermal tumor in the case of LAP-35 cells. Semi-quantitative RT-PCR carried out with primers encompassing the entire open reading frame of CD40 revealed no detectable levels of CD40 transcripts in IMR-32 and AF cells, while LAN-1 displayed a single band about 100 bp shorter than the expected full-length amplicon (Fig. 3.20 A). Isolation of this aberrant band followed by nucleotide sequence analysis and querying of the BLAST database ascertained it to be an aspecific amplicon originating from the transcript of Ribosomal Protein L3, which is known to have enhanced expression in many neoplastic cells [139]. Therefore,

to all accounts, LAN-1 cells are CD40 transcription negative along with IMR-32 and AF cells. All cell lines were analyzed with our assay for transcript variants; LAN-1, IMR-32 and AF cells were negative even with respect to these partial transcripts, while all other lines displayed the usual splicing pattern common to B cells and most other tissues. Unlike cDNA from normal brain, both skipping of exon 6 alone and skipping of exons 5 and 6 together were detected.

**Fig. 3.20** - Analysis of CD40 expression in cell lines derived from transformed neural tissue. A) Detection of CD40 transcripts by RT-PCR and agarose gel electrophoresis; cDNA from control B-LCL and vector pcDNA3-wt-CD40 were used as positive controls. B) Detection of CD40 protein expression through Western blot, probed with anti-CD40 (C-20) IgG (left) and reprobbed with anti-CD40 (H-120) IgG (right); B-LCL lysate was used as a positive control.



In contrast with RT-PCR results, Western blot analysis with either anti-CD40 (H-120) or anti-CD40 (C-20) IgG indicated that none of these cell lines featured detectable levels of CD40 receptor, whether they were transcription positive or not (Fig. 3.20 B). The number of low-molecular weight bands detected by both antibodies seemed to be the outcome of aspecific binding rather than product degradation, since they also appeared in transcription-

negative samples. Together, RT-PCR and Western Blot data suggest a tight regulation of protein expression at the post-transcriptional level.

## 4. CONCLUSIONS

The task to understand the complexities of CD40 regulation is a challenging one. We still do not know the identity of many of its intracellular partners and the effects of its expression under different circumstances. The ability of the CD40 protein to reach cell compartments other than the plasma membrane prompts us to investigate how localization affects its function, whether exposing different roles and novel interactions, or in a merely regulatory way.

Recent studies reveal that a number of proteins, especially G protein coupled receptors, are expressed 'inefficiently' at the site normally associated with their biological action [140]. In some cases, large amounts of receptor may be destroyed without ever reaching the plasma membrane: engagement with the cellular quality control system regulates the delicate balance between either exposure on the cell surface or retention/degradation in the ER. Our results suggest that functional levels of CD40 are also subjected to a similar control at the post-translational level. In further studies we propose to follow CD40 trafficking within cell vesicles and to identify its possible interactions with chaperone molecules, similarly to what was recently described for the CTLA-4 coreceptor in T cells [141].

The identification of several CD40 splicing variants also broadens the range of ways in which CD40 expression can be regulated. Even mutations in

Pt.1 and Pt.3 apparently do not generate totally new non-endogenous transcripts, but rather impose severe limitations to the range of pre-existent splicing solutions. In some instances, alternative splicing may simply act as a restraint on gene expression by generating non productive variants, and this seems to be the purpose of extensive skipping of exon 2 revealed in the muscle tissue. In other cases, alternative isoforms could be actually translated into functional proteins. We gathered some evidence about the relative stability and surface expression of the del5+6-CD40 variant in transfected cells; though we were unable to isolate it from normal CD40-expressing cells by Western blot, flow cytometry of Pt.1 B-LCL revealed a surface antigen binding anti-CD40 IgG which, according to RNA transcription data, probably is del5+6-CD40 itself. The role of this transmembrane isoform has still to be defined. Since its extracellular domains are predictably sufficient to allow multimerization and pre-ligand assembly, it could be cross-linked by extracellular ligands and somehow modulate CD40 intracellular signalling, or simply act as a decoy. Through cotransfection with different constructs, in proposed investigations we shall also address the possibility that del5+6-CD40 could decrease the signalling response through association with wild-type CD40 in heteromers marked by reduced ligand binding ability or inefficient transduction.

Although the present work stems from B cells analysis, neuroblastoma cell lines also offer an easy-to-handle model to characterize post-transcriptional regulation of CD40, since many of them display a remarkable discrepancy between transcription and protein expression. Furthermore, neuroblastoma cell lines that lack CD40 transcripts altogether may provide a servicable negative model for future studies.

Last but not least, our experimental outline pursues the synergy with the clinical aspects of CD40 research. Screening HIGM patients for the presence of additional CD40 splicing defects, apart from its intrinsic diagnostic value, could clarify the involvement of SR proteins in B cell specific developmental and functional processes.

## **APPENDIX A**

### **ANALYSIS OF CD45 ISOFORMS VALIDATES A RAPID AND SENSITIVE METHOD FOR THE SCREENING OF TRANSCRIPT VARIANTS.**

CD45 is a transmembrane glycoprotein expressed on leukocytes [142]. Alternative splicing of three variable exons (4, 5 and 6 or A, B and C) allows the production of eight possible isoforms. In rodent cells, all of these have been isolated [143-145], while in humans only five have been identified: from highest to lowest molecular weight (m.w.), they are CD45R-ABC, AB, BC, B and 0 or null (Fig. A.01) [146-147]. The splicing is cell-type specific and activation dependent. B lymphocytes express mainly the high m.w. isoform, CD45RABC, while T cells express a panel of different isoforms ranging from the smallest one (null), found also on thymocytes, to the largest one (ABC) [148]. T cell activation leads to a programmed shift from high to low m.w. isoforms: a complex interplay of Exonic Splicing Enhancers (ESE) and Silencers (ESS) enables activation-induced exon repression [149], in which down-regulation of CD45RA expression and concomitant up-regulation of CD45R0 are the prominent features [150].

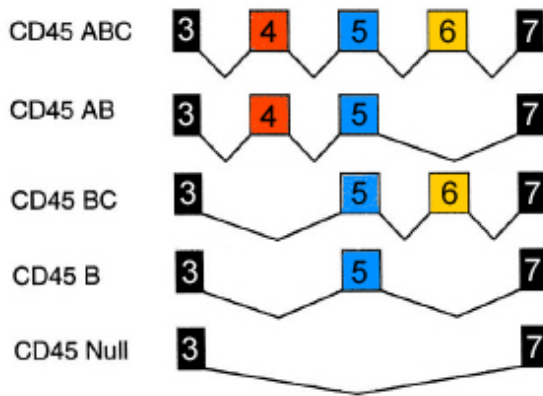


**Fig. A.01** - Schematic representation of the alternatively spliced human CD45 transcripts. Of the eight possible combinations, only 5 were found in man, while all eight are commonly present in mouse cells [151]. CD45RABC, RAB and RBC are designated as the high m.w. isoforms, while CD45RB and R0 as the low m.w. isoforms.

In order to validate the assay we devised for CD40 splicing variants analysis, we applied it to CD45 transcripts obtained from T cells selected for their surface expression of high or low m.w. isoforms, and eventually activated in vitro with Phorbol 12-Myristate 13-Acetate (PMA) and Ionomycin (Ion).

T cell subpopulations were isolated from the Ficoll-Paque purified PBMC fraction of a buffy coat using MACS Separation Technology (Miltenyi) according to the supplier's protocols.

Naive CD4<sup>+</sup> T lymphocytes ("T-ly Naive") were obtained via negative selection from PBMCs using the Naive CD4<sup>+</sup> T Cell Isolation Kit (Miltenyi).

CD45RA<sup>+</sup> T lymphocytes ("T-ly RA") were obtained via positive selection from the naive T cell fraction using FITC-conjugated CD45RA antibodies in conjunction with the Anti-FITC MultiSort Kit (both from Miltenyi).

CD45RO<sup>+</sup> T lymphocytes ("T-ly RO") were obtained via positive selection from PBMCs using CD45RO Microbeads (Miltenyi).

All fractions were assayed through flow cytometry analysis with anti-CD45RA-FITC and either anti-CD4-PE to evaluate the proportion of RA vs. R0 T cells, or anti-CD19-PE to detect residual B cells. Separated T-ly Naive and T-ly RO were roughly 20% and 10% of total PBMCs, respectively, whereas T-ly RA made up 70% of the T-ly Naive fraction. As expected, all T cell fractions revealed a wide distribution of CD45 isoforms, with T-ly Naive and

T-ly RA enriched in the CD45RA surface antigen, and T-ly RO in the CD45RO. No trace of B cell contamination was found.

Part of the T-ly Naive and T-ly RA cells were cultured for 24 h in RPMI medium supplemented with 10% FBS, 100 ng/ml of PMA and 1 µg/ml ionomycin (PMA/ion) to elicit an activation response [152]. Stimulated T cells were designated with the descriptor 'PMA/ion'.

cDNA was obtained from each fraction as described for CD40 in Sections 2.05. Accordingly, samples were diluted 1:20 in ddH<sub>2</sub>O and loaded on the ABI Prism 3730 DNA Analyzer after 30 PCR cycles with an annealing step at 58°C, using 1 unit of FastStart Taq DNA Polymerase (Roche) in the presence of 3 mM MgCl<sub>2</sub> and 0.4µM of each PCR primer. The forward primer (45tr\_2F: 5'-GGACACAGAAGTATTTGTGACAGG-3'), conjugated with a FAM dye, was designed to hybridize with exon 2, and the reverse primer (45tr\_6R: 5'-AAAGGTGCTGGCTGTACTCCT-3') with exon 6, thus spanning the whole region interested by the RA/RO alternative splicing. In order to set an internal standard for relative titration of the isoforms, we readjusted the reaction as a multiplex PCR by adding 0.4µM each of PCR primers 45tr\_8F (5'-AGCTACTACTCCATCTAAGCC-3'), FAM-conjugated, and 45tr\_9-10R (5'-ACTTTTCAACCCCTGGTG-3'). Choosing the control primers on exon 8 and on the exon 9-10 junction, for which no splicing was ever documented, provided us with an internal reference of the total presence of CD45 transcripts, and at the same time prevented contamination from genomic DNA PCR products. Moreover, using the same fluorochrome for both primer pairs allowed us to forego considerations on the comparative intensities of different dyes, while still being able to distinguish the internal control amplicon from the splicing variants by its characteristic peak size.

Therefore, with a single PCR we were able to detect and quantify all CD45 splicing variants (Fig. A.02). The identity of every PCR product was successfully verified through cloning and direct sequence analysis, as detailed in Section 2.05 for CD40 transcripts.

From the qualitative point of view, *GeneMapper* plots revealed a 2-6 nt discrepancy between the expected and observed size of each peak (Table A.01). According to the software documentation, such variations are within the normal running parameters of *GeneMapper* and depend on fluorochrome conjugates, Taq DNA polymerase efficiency and amplicon length. Since these size variations were constant for each peak in the course of repeated experiments, this bias did not ultimately affect the precision of our assay, and each peak could be unambiguously assigned to a specific CD45 splicing variant.

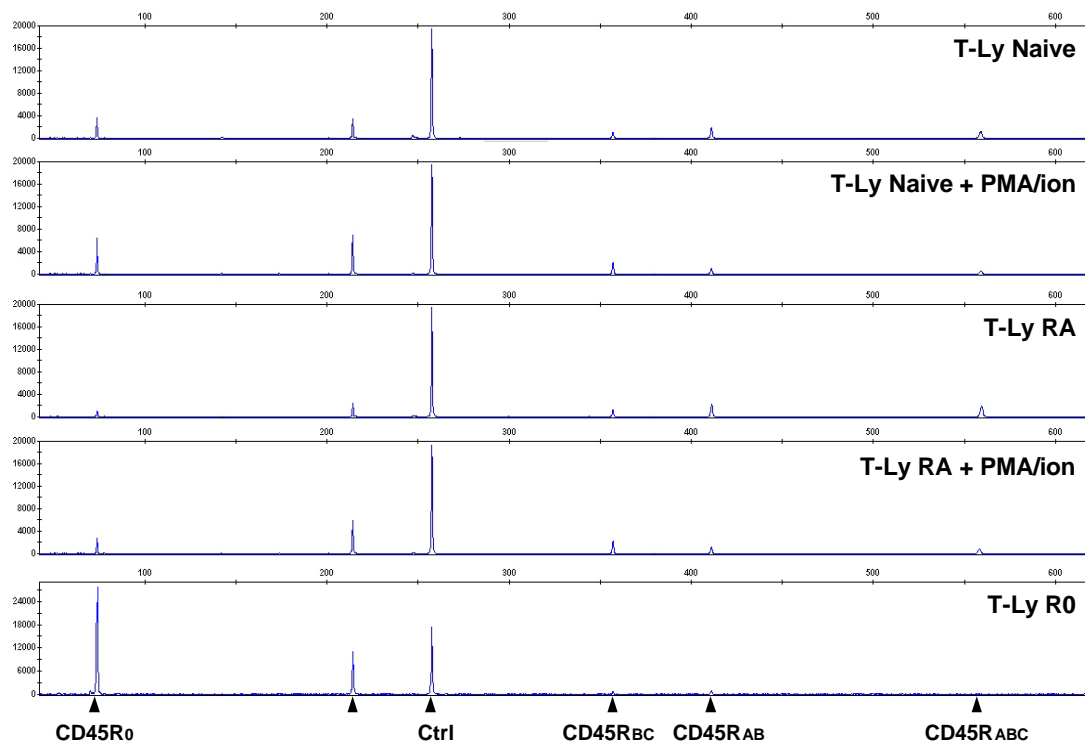


**Fig. A.02** - *GeneMapper* plot of the CD45 transcripts from the different T cell fractions.

In T-ly R0 only the peaks corresponding to the low m.w. isoforms (CD45R0 and RB) were detected. The intensity of CD45R0 appears greater than the internal control because its shorter size entails greater PCR efficiency. Similarly, though we found all isoforms in T-ly Naïve and T-ly RA as expected, the peaks corresponding to CD45R0/RB were higher than those of the heavier isoforms: again, this is due to amplification efficiency. In fact, by performing the PCR with the less processive AmpliTaq Gold DNA polymerase

(Applied Biosystems), we observed the profile of the peaks change according to their size: low m.w. isoforms appeared even higher and high m.w. even lower, in an almost linear fashion (data not shown). This implies that direct comparison of the peak intensities within each sample is not a legitimate method to calculate the RA/R0 ratio, as the absolute quantity of the RA isoforms will be displayed as being lower than R0 isoforms due to PCR efficiency, though very likely the reverse is true. We could instead track changes in the relative levels of each isoform among different samples, e.g. stimulated vs. resting. We normalized the intensity of the control peaks across all samples and calculated the heights of the splicing variant-associated peaks in each sample as a percentage ratio of the control amplicon (Table A.01).

**Table A.01**

Included Exons	Peak Size (nt)		Normalized Peak Heights (%)				
	Expected	Observed	T-Ly Naive	T-Ly Naive + PMA/ion	T-Ly RA	T-Ly RA + PMA/ion	T-Ly R0
<b>Ctrl</b>	260	258	100%	100%	100%	100%	100%
<b>CD45RABC</b>	562	559	6,2	2,6	9,7	4,2	0
<b>CD45RAB</b>	418	412	9,6	4,7	11,7	6,0	3,4
<b>CD45RBC</b>	364	358	5,3	10,1	6,5	11,5	2,5
<b>CD45RB</b>	220	214	17,7	34,5	12,2	29,4	66,1
<b>CD45R0</b>	79	74	18,4	32,0	5,4	13,5	183,1

According to this relative quantification method, 24 h stimulation with PMA + ion led to a marked increase in the low m.w. CD45R0 and RB isoforms and a concomitant decrease in the CD45RA isoforms (ABC, AB) for both T-Ly Naive and T-ly RA cells (Fig. A.03). We could also describe a rise in the levels of CD45RBC: it may reflect a tendency of activated T cells to preferentially skip CD45 exon 4 rather than exon 6 when they begin to shift their splicing pattern toward low m.w. isoforms, as reported by various investigators [153-154].

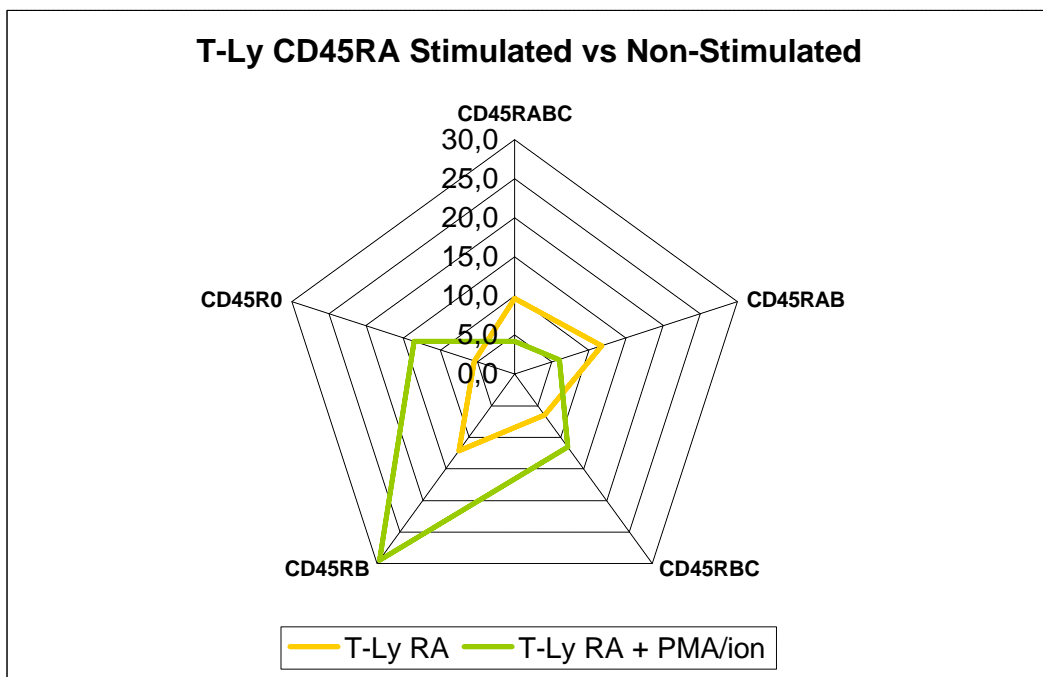
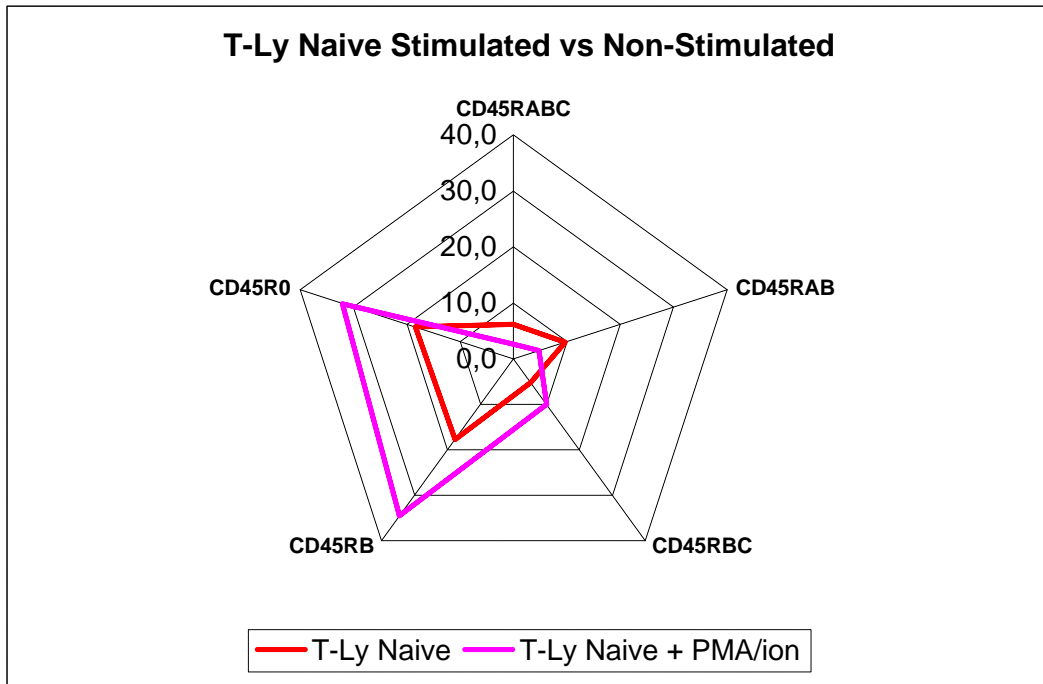


**Fig. A.03** - Comparison between the relative expression levels of CD45 splicing isoforms in stimulated and resting Naive CD4<sup>+</sup> T cells (A) and CD45RA<sup>+</sup> T cells (B).

As expected, non-stimulated T-ly RA cells were enriched in RA isoforms compared to T-ly Naive cells (Fig. A.04), while the T-ly R0 fraction had practically no high m.w. CD45 isoforms compared to all other fractions (Fig. A.05).

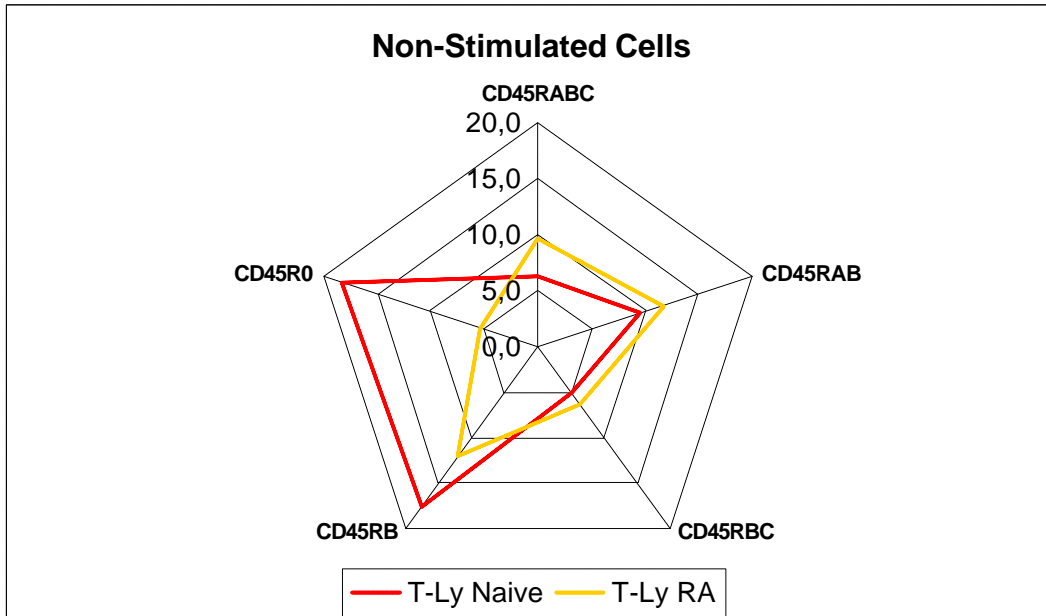


**Fig. A.04** - Comparison between the relative expression levels of CD45 splicing isoforms in resting Naive CD4<sup>+</sup> T cells and CD45RA<sup>+</sup> T cells.

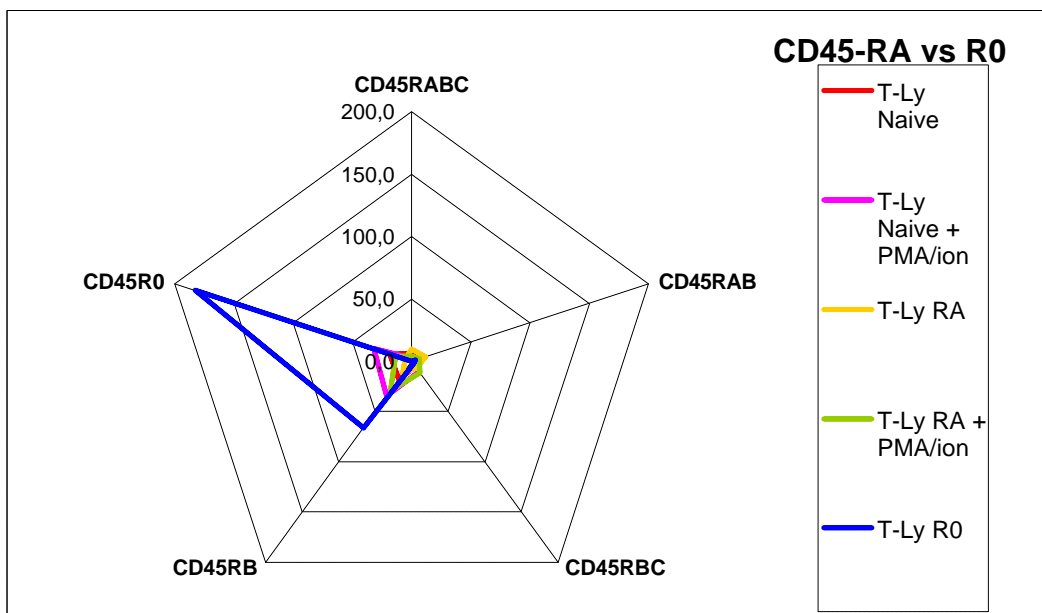


**Fig. A.05** - Relative expression levels of CD45 splicing isoforms in resting CD45R0<sup>+</sup> T cells.

Observations based on these relative measurements agree with the variations in CD45 isoforms expression described in literature [149, 151, 153, 154], effectively validating our transcript analysis method even with respect to quantitative considerations.

## REFERENCES

1. Janeway, Charles A.; Travers, Paul; Walport, Mark; Shlomchik, Mark. 2001. *Immunobiology* 5th ed. New York and London: Garland Science.
2. Koho, H., Paulie, S., Ben-Aissa, H., Jonsdottir, I., Hansson, Y., Lundblad, M. L. and Perlmann, P., 1984. Monoclonal antibodies to antigens associated with transitional cell carcinoma of the human urinary bladder. I. Determination of the selectivity of six antibodies by cell ELISA and immunofluorescence. *Cancer Immunol Immunother.* 17, 165-172.
3. Allen RC, Armitage RJ, Conley ME, Rosenblatt H, Jenkins NA, Copeland NG, Bedell MA, Edelhoff S, Disteché CM, Simoneaux DK, Fanslow WC, Belmont J, Spriggs MK. 1993. CD40 ligand gene defects responsible for X-linked hyper-IgM syndrome. *Science* 259:990–993
4. Aruffo A, Farrington M, Hollenbough D, Li X, Milatovich A, Nonoyama S, Bajorath J, Grosmaire LS, Stenkamp R, Neubauer M, Roberts RL, Noelle RJ, Ledbetter JA, Francke U, Ochs HD. 1993. The CD40 ligand, gp39, is defective in activated T cells from patients with X-linked hyper-IgM syndrome. *Cell* 72:291–300
5. DiSanto JP, Bonnefoy JY, Gauchat JF, Fischer A, De Saint Basile G. 1993. CD40 ligand mutations in x-linked immunodeficiency with hyper-IgM. *Nature* 361:541–543
6. Fuleihan R, Ramesh N, Loh R, Jabara H, Rosen RS, Chatila T, Fu SM, Stamenkovic I, Geha RS. 1993. Defective expression of the CD40 ligand in X chromosome-linked immunoglobulin deficiency with normal or elevated IgM. *Proc Natl Acad Sci U S A* 90:2170–2173
7. Korthäuer U, Graf D, Mages HW, Brière F, Padayachee M, Malcolm S, Ugazio AG, Notarangelo LD, Levinsky RJ, KroczeK RA. 1993. Defective expression of T-cell CD40 ligand causes X-linked immunodeficiency with hyper-IgM. *Nature* 361:539–541

8. van Kooten, C. and Banchereau, J., 2000. CD40-CD40 ligand. *J Leukoc Biol.* 67, 2-17.
9. Xu, J., Foy, T. M., Laman, J. D., Elliott, E. A., Dunn, J. J., Waldschmidt, T. J., Elsemore, J., Noelle, R. J., Flavell, R. A. (1994) Mice deficient for the CD40 ligand. *Immunity* 1, 423–431.
10. Kawabe, T., Naka, T., Yoshida, K., Tanaka, T., Fujiwara, H., Suematsu, S., Yoshida, N., Kishimoto, T., Kikutani, H. (1994) The immune responses in CD40-deficient mice: impaired immunoglobulin class switching and germinal center formation. *Immunity* 1, 167–178.
11. Schonbeck, U. and Libby, P., 2001. The CD40/CD154 receptor/ligand dyad. *Cell Mol Life Sci.* 58, 4-43.
12. Stamenkovic, I., Clark, E. A., Seed, B. (1989) A B-lymphocyte activation molecule related to the nerve growth factor receptor and induced by cytokines in carcinomas. *EMBO J.* 8, 1403–1410.
13. Torres, R. M., Clark, E. A. (1992) Differential increase of an alternatively polyadenylated mRNA species of murine CD40 upon B lymphocyte activation. *J. Immunol.* 148, 620–626.
14. Grimaldi, J. C., Kozak, C. A., Chang, R., Clark, E. A., Howard, M., Cockayne, D. A. (1992) Genomic structure and chromosomal mapping of the murine CD40 gene. *J. Immunol.* 149, 3921–3926.
15. Lafage-Pochitaloff, M.; Herman, P.; Birg, F.; Galizzi, J.-P.; Simonetti, J.; Mannoni, P.; Banchereau, J. 1994. Localization of the human CD40 gene to chromosome 20, bands q12-q13.2. *Leukemia* 8: 1172-1175.
16. Tone M, Tone Y, Fairchild PJ, Wykes M, Waldmann H. 2001. Regulation of CD40 function by its isoforms generated through alternative splicing. *Proc Natl Acad Sci U S A.* Feb 13;98(4):1751-6.
17. Braesch-Andersen, S., Paulie, S., Koho, H., Nika, H., Aspenstrom, P. and Perlmann, P., 1989. Biochemical characteristics and partial amino acid sequence of the receptor-like human B cell and carcinoma antigen CDw40. *J Immunol.* 142, 562-567.
18. Singh, J., Garber, E., Van Vlijmen, H., Karpusas, M., Hsu, Y. M., Zheng, Z., Naismith, J. H., Thomas, D. (1998) The role of polar interactions in the molecular recognition of CD40L with its receptor CD40. *Protein Sci.* 7, 1124–1135.
19. Naismith, J. H., Sprang, S. R. 1998. Modularity in the TNF-receptor family. *Trends Biol. Sci.* 23, 74–79.
20. Karpusas, M., Hsu, Y. M., Wang, J. H., Thompson, J., Lederman, S., Chess, L., Thomas, D. 1995. 2A crystal structure of an extracellular fragment of human CD40 ligand. *Structure* 3, 1031–1039.

21. Bajorath, J. 1998. Detailed comparison of two molecular models of the human CD40 ligand with an X-ray structure and critical assessment of model-based mutagenesis and residue mapping studies. *J. Biol. Chem.* 273, 24603–24609.
22. Björck, P., Braesch-Andersen, S. and Paulie, S., 1994. Antibodies to distinct epitopes on the CD40 molecule co-operate in stimulation and can be used for the detection of soluble CD40. *Immunology.* 83, 430-437.
23. Sakata, N., Hamelmann, E., Siadak, A. W., Terada, N., Gerwins, P., Aruffo, A., Johnson, G. L. and Gelfand, E. W., 2000. Differential regulation of CD40-mediated human B cell responses by antibodies directed against different CD40 epitopes. *Cell Immunol.* 201, 109-123.
24. Barr, T. A. and Heath, A. W., 2001. Functional activity of CD40 antibodies correlates to the position of binding relative to CD154. *Immunology.* 102, 39-43.
25. Fanslow, W. C., Srinivasan, S., Paxton, R., Gibson, M. G., Spriggs, M. K. and Armitage, R. J., 1994. Structural characteristics of CD40 ligand that determine biological function. *Semin Immunol.* 6, 267-278.
26. Pound, J. D., Challa, A., Holder, M. J., Armitage, R. J., Dower, S. K., Fanslow, W. C., Kikutani, H., Paulie, S., Gregory, C. D. and Gordon, J., 1999. Minimal cross-linking and epitope requirements for CD40-dependent suppression of apoptosis contrast with those for promotion of the cell cycle and homotypic adhesions in human B cells. *Int Immunol.* 11, 11-20.
27. Ellmark P, Furebring C, Borrebaeck CA. 2003. Pre-assembly of the extracellular domains of CD40 is not necessary for rescue of mouse B cells from anti-immunoglobulin M-induced apoptosis. *Immunology.* Apr;108(4):452-7.
28. Werneburg, B. G., Zoog, S. J., Dang, T. T., Kehry, M. R. and Crute, J. J., 2001. Molecular characterization of CD40 signaling intermediates. *J Biol Chem.* 18, 18.
29. Haswell, L. E., Glennie, M. J. and Al-Shamkhani, A., 2001. Analysis of the oligomeric requirement for signaling by CD40 using soluble multimeric forms of its ligand, CD154. *Eur J Immunol.* 31, 3094-3100.
30. Baccam, M. and Bishop, G. A., 1999. Membrane-bound CD154, but not CD40-specific antibody, mediates NF- $\kappa$ B-independent IL-6 production in B cells. *Eur J Immunol.* 29, 3855-3866.
31. Papoff, G., Hausler, P., Eramo, A., Pagano, M. G., Di Leve, G., Signore, A. and Ruberti, G., 1999. Identification and characterization of a ligand-independent oligomerization domain in the extracellular region of the CD95 death receptor. *J Biol Chem.* 274, 38241-38250.
32. Siegel, R. M., Chan, F. K., Chun, H. J. and Lenardo, M. J., 2000. The multifaceted role of Fas signaling in immune cell homeostasis and autoimmunity. *Nat Immunol.* 1, 469-474.

33. Chan, F. K., Chun, H. J., Zheng, L., Siegel, R. M., Bui, K. L. and Lenardo, M. J., 2000. A domain in TNF receptors that mediates ligand-independent receptor assembly and signaling. *Science*. 288, 2351-2354.
34. Locksley, R. M., Killeen, N. and Lenardo, M. J., 2001. The TNF and TNF receptor superfamilies: integrating mammalian biology. *Cell*. 104, 487-501.
35. Malmborg Hager AC, Ellmark P, Borrebaeck CA, Furebring C. 2003. Affinity and epitope profiling of mouse anti-CD40 monoclonal antibodies. *Scand J Immunol*. Jun;57(6):517-24.
36. Hostager, B. S., Catlett, I. M. and Bishop, G. A., 2000. Recruitment of CD40 and tumor necrosis factor receptor-associated factors 2 and 3 to membrane microdomains during CD40 signaling. *J Biol Chem*. 275, 15392-15398.
37. Pham, L. V., Tamayo, A. T., Yoshimura, L. C., Lo, P., Terry, N., Reid, P. S. and Ford, R. J., 2002. A CD40 Signalosome anchored in lipid rafts leads to constitutive activation of NFkappaB and autonomous cell growth in B cell lymphomas. *Immunity*. 16, 37-50.
38. Vidalain, P. O., Azocar, O., Servet-Delprat, C., Rabourdin-Combe, C., Gerlier, D. and Manie, S., 2000. CD40 signaling in human dendritic cells is initiated within membrane rafts. *Embo J*. 19, 3304-3313.
39. Malapati, S. and Pierce, S. K., 2001. The influence of CD40 on the association of the B cell antigen receptor with lipid rafts in mature and immature cells. *Eur J Immunol*. 31, 3789-3797.
40. Dykstra, M., Cherukuri, A. and Pierce, S. K., 2001. Rafts and synapses in the spatial organization of immune cell signaling receptors. *J Leukoc Biol*. 70, 699-707.
41. Grassme, H., Bock, J., Kun, J. and Gulbins, E., 2002a. Clustering of CD40 ligand is required to form a functional contact with CD40. *J Biol Chem*. 277, 30289-30299.
42. Goldstein, M. D., Cochrane, A., Watts, T. H. 1997. Cyclic-AMP modulates downstream events in CD40-mediated signal transduction, but inhibition of protein kinase A has no direct effect on CD40 signaling. *J. Immunol*. 159, 5871-5880.
43. Grammer, A. C., Swantek, J. L., McFarland, R. D., Miura, Y., Geppert, T., Lipsky, P. E. 1998. TNF receptor-associated factor-3 signaling mediates activation of p38 and Jun N-terminal kinase, cytokine secretion, and Ig production following ligation of CD40 on human B cells. *J. Immunol*. 161, 1183-1193.
44. Purkerson, J. M., Parker, D. C. 1998. Differential coupling of membrane Ig and CD40 to the extracellularly regulated kinase signaling pathway. *J. Immunol*. 160, 2121-2129.

45. 39. Craxton, A., Shu, G., Graves, J. D., Saklatvala, J., Krebs, E. G., Clark, E. A. 1998. p38 MAPK is required for CD40-induced gene expression and proliferation in B lymphocytes. *J. Immunol.* 161, 3225–3236.
46. Cheng, G., Cleary, A. M., Ye, Z. S., Hong, D. I., Lederman, S., Baltimore, D. 1995. Involvement of CRAF1, a relative of TRAF, in CD40 signaling. *Science* 267, 1494–1498.
47. Xu, Y., Cheng, G., Baltimore, D. 1996. Targeted disruption of TRAF3 leads to postnatal lethality and defective T-dependent immune responses. *Immunity* 5, 407–415.
48. McWhirter, S. M., Pullen, S. S., Holton, J. M., Crute, J. J., Kehry, M. R., Alber, T. 1999. Crystallographic analysis of CD40 recognition and signaling by human TRAF2. *Proc. Natl. Acad. Sci. USA* 96, 8408–8413.
49. Ishida, T., Tojo, T., Aoki, T., Kobayashi, N., Ohishi, T., Watanabe, T., Yamamoto, T., Inoue, J. 1996. TRAF5, a novel tumor necrosis factor receptor-associated factor family protein, mediates CD40 signaling. *Proc. Natl. Acad. Sci. USA* 93, 9437–9442.
50. Nakano, H., Sakon, S., Koseki, H., Takemori, T., Tada, K., Matsumoto, M., Munechika, E., Sakai, T., Shirasawa, T., Akiba, H., Kobata, T., Santee, S. M., Ware, C. F., Rennert, P. D., Taniguchi, M., Yagita, H., Okumura, K. 1999. Targeted disruption of *Traf5* gene causes defects in CD40- and CD27-mediated lymphocyte activation. *Proc. Natl. Acad. Sci. USA* 96, 9803–9808.
51. Kashiwada, M., Shirakata, Y., Inoue, J. I., Nakano, H., Okazaki, K., Okumura, K., Yamamoto, T., Nagaoka, H., Takemori, T. 1998. Tumor necrosis factor receptor-associated factor 6 (TRAF6) stimulates extracellular signal-regulated kinase (ERK) activity in CD40 signaling along a ras-independent pathway. *J. Exp. Med.* 187, 237–244.
52. Hu, H. M., O'Rourke, K., Boguski, M. S., Dixit, V. M. 1994. A novel RING finger protein interacts with the cytoplasmic domain of CD40. *J. Biol. Chem.* 269, 30069–30072.
53. Mosialos, G., Birkenbach, M., Yalamanchili, R., VanArsdale, T., Ware, C., Kieff, E. 1995. The Epstein-Barr virus transforming protein LMP1 engages signaling proteins for the tumor necrosis factor family. *Cell* 80, 389–399.
54. Kilger, E., Kieser, A., Baumann, M., Hammerschmidt, W. 1998. Epstein-Barr virus-mediated B-cell proliferation is dependent upon latent membrane protein 1, which simulates an activated CD40 receptor. *EMBO J.* 17, 1700–1709.
55. Hatzivassiliou, E., Miller, W. E., Raab-Traub, N., Kieff, E., Mosialos, G. 1998. A fusion of the EBV latent membrane protein-1 (LMP1) transmembrane domains to the CD40 cytoplasmic domain is similar to LMP1 in constitutive activation of epidermal growth factor receptor expression, nuclear factor-kappa B, and stress-activated protein kinase. *J. Immunol.* 160, 1116–1121.

56. Hsing, Y., Hostager, B. S., Bishop, G. A. 1997. Characterization of CD40 signaling determinants regulating nuclear factor-kappa B activation in B lymphocytes. *J. Immunol.* 159, 4898–4906.
57. Schauer, S. L., Bellas, R. E., Sonenshein, G. E. 1998. Dominant signals leading to inhibitor kappaB protein degradation mediate CD40 ligand rescue of WEHI 231 immature B cells from receptor-mediated apoptosis. *J. Immunol.* 160, 4398–4405.
58. Hanissian, S. H., Geha, R. S. 1997. Jak3 is associated with CD40 and is critical for CD40 induction of gene expression in B cells. *Immunity* 6, 379–387.
59. Karras, J. G., Wang, Z., Huo, L., Frank, D. A., Rothstein, T. L. 1997. Induction of STAT protein signaling through the CD40 receptor in B lymphocytes: distinct STAT activation following surface Ig and CD40 receptor engagement. *J. Immunol.* 159, 4350–4355.
60. Mizuno T, Rothstein TL. 2005. B cell receptor (BCR) cross-talk: CD40 engagement creates an alternate pathway for BCR signaling that activates I kappa B kinase/I kappa B alpha/NF-kappa B without the need for PI3K and phospholipase C gamma. *J Immunol.* May 15;174(10):6062-70.
61. Khanna, R., Cooper, L., Kienzle, N., Moss, D. J., Burrows, S. R., Khanna, K. K. 1997. Engagement of CD40 antigen with soluble CD40 ligand up-regulates peptide transporter expression and restores endogenous processing function in Burkitt's lymphoma cells. *J. Immunol.* 159, 5782–5785.
62. Hu, B. T., Lee, S. C., Marin, E., Ryan, D. H., Insel, R. A. 1997. Telomerase is up-regulated in human germinal center B cells in vivo and can be re-expressed in memory B cells activated in vitro. *J. Immunol.* 159, 1068–1071.
63. Gulino AV, Notarangelo LD. 2003. Hyper IgM syndromes. *Curr Opin Rheumatol.* Jul;15(4):422-9.
64. Kenter AL. 1999 The liaison of isotype class switch and mismatch repair: an illegitimate affair. *J Exp Med*, 190:307–310.
65. Schrader CE, Edelmann W, Kucherlapati R, Stavnezer J. 1999. Reduced isotype switching in splenic B-cells from mice deficient in mismatch repair enzymes. *J Exp Med*, 190:323–330.
66. Mizuta R, Iwai K, Shigeno M, Mizuta M, Uemura T, Ushiki T, Kitamura D. 2003. Molecular visualization of immunoglobulin switch region RNA/DNA complex by atomic force microscope. *J Biol Chem*, 278:4431–4434.
67. Petersen S, Casellas R, Reina-San-Martin B, Chen HT, Difilippantonio MJ, Wilson PC, Hanitsch L, Celeste A, Muramatsu M, Pilch DR, Redon C, Ried T, Bonner WM, Honjo T, Nussenzweig MC, Nussenzweig A. 2001. AID is required to initiate Nbs1/gamma-H2AX focus formation and mutations at sites of class switching. *Nature*, 6:660–665.

68. Tian M, Alt FW. 2000. Transcription-induced cleavage of immunoglobulin switch regions by nucleotide excision repair nucleases in vitro. *J Biol Chem*, 275:24163–24172.
69. Ballantyne, J., Henry, D. L., Muller, J. R., Briere, F., Snapper, C. M., Kehry, M., Marcu, K. B. 1998. Efficient recombination of a switch substrate retrovector in CD40-activated B lymphocytes: implications for the control of CH gene switch recombination. *J. Immunol.* 161, 1336–1347.
70. Jeannin, P., Delneste, Y., Lecoanet-Henchoz, S., Gretener, D., Bonnefoy, J. Y. 1998. Interleukin-7 (IL-7) enhances class switching to IgE and IgG4 in the presence of T cells via IL-9 and sCD23. *Blood* 91, 1355–1361.
71. Jeannin, P., Lecoanet, S., Delneste, Y., Gauchat, J. F., Bonnefoy, J. Y. 1998. IgE versus IgG4 production can be differentially regulated by IL-10. *J. Immunol.* 160, 3555–3561.
72. Dubois, B., Vanbervliet, B., Fayette, J., Massacrier, C., Van Kooten, C., Briere, F., Banchereau, J., Caux, C. 1997. Dendritic cells enhance growth and differentiation of CD40-activated B lymphocytes. *J. Exp. Med.* 185, 941–951.
73. Fayette, J., Dubois, B., Vandenabeele, S., Bridon, J. M., Vanbervliet, B., Durand, I., Banchereau, J., Caux, C., Briere, F. 1997. Human dendritic cells skew isotype switching of CD40-activated naive B cells towards IgA1 and IgA2. *J. Exp. Med.* 185, 1909–1918.
74. Cerutti, A., Schaffer, A., Shah, S., Zan, H., Liou, H. C., Goodwin, R. G., Casali, P. 1998. CD30 is a CD40-inducible molecule that negatively regulates CD40-mediated immunoglobulin class switching in non-antigenselected human B cells. *Immunity* 9, 247–256.
75. Papavasiliou FN, Schatz DG. 2002. Somatic hypermutation of immunoglobulin genes: merging mechanisms for genetic diversity. *Cell*, 109:S35–S44.
76. Zeng X, Winter DB, Kasmer C, Kraemer KH, Lehmann AR, Gearhart PJ. 2001. DNA polymerase eta is an A-T mutator in somatic hypermutation of immunoglobulin variable genes. *Nat Immunol*, 2:537–541.
77. Papavasiliou FN, Schatz DG. 2000. Cell-cycle-regulated DNA double stranded breaks in somatic hypermutation of immunoglobulin genes. *Nature*, 408:216–221.
78. Jacobs H, Bross L. 2001. Towards an understanding of somatic hypermutation. *Curr Opin Immunol*, 13:208–218.
79. Rothstein, T. L., Wang, J. K. M., Panka, D. J., Foote, L. C., Wang, Z., Stanger, B., Cui, H., Ju, S. T., Marshak-Rothstein, A. 1995. Protection against Fas-dependent Th1-mediated apoptosis by antigen receptor engagement in B cells. *Nature* 374, 163–165.
80. Galibert, L., Burdin, N., Barthelemy, C., Meffre, G., Durand, I., Garcia, E., Garrone, P., Rousset, F., Banchereau, J., Liu, Y. J. 1996. Negative selection of

- human germinal center B cells by prolonged BCR crosslinking. *J. Exp. Med.* 183, 2075–2085.
81. Rathmell, J. C., Townsend, S. E., Xu, J. C., Flavell, R. A., Goodnow, C. C. 1996. Expansion or elimination of B cells in vivo: dual roles for CD40 and Fas (CD95)-ligands modulated by the B cell antigen receptor. *Cell* 87, 319–329.
  82. Brodeur, S. R.; Angelini, F.; Bacharier, L. B.; Blom, A. M.; Mizoguchi, E.; Fujiwara, H.; Plebani, A.; Notarangelo, L. D.; Dahlback, B.; Tsitsikov, E.; Geha, R. S. 2003. C4b-binding protein (C4BP) activates B cells through the CD40 receptor. *Immunity* 18: 837-848.
  83. Stout, R. D., Suttles, J. 1996. The many roles of CD40 in cell-mediated inflammatory responses. *Immunol. Today* 17, 487–492.
  84. Grewal, I. S., Flavell, R. A. 1996. A central role of CD40 ligand in the regulation of CD41 T cell responses. *Immunol. Today* 17, 410–414.
  85. Banchereau, J., Steinman, R. M. 1998. Dendritic cells and the control of immunity. *Nature* 392, 245–252.
  86. Stout, R. D., Suttles, J., Xu, J., Grewal, I. S., Flavell, R. A. 1996. Impaired T cell-mediated macrophage activation in CD40 ligand-deficient mice. *J. Immunol.* 156, 8–11.
  87. Mackey, M. F., Barth, R. J., Jr., Noelle, R. J. 1998. The role of CD40/CD154 interactions in the priming, differentiation, and effector function of helper and cytotoxic T cells. *J. Leukoc. Biol.* 63, 418–428.
  88. Van Essen, D., Kikutani, H., Gray, D. 1995. CD40 ligand-transduced co-stimulation of T cells in the development of helper function. *Nature* 378, 620–623.
  89. Poudrier, J., van Essen, D., Morales-Alcelay, S., Leanderson, T., Bergthorsdottir, S., Gray, D. 1998. CD40 ligand signals optimize T helper cell cytokine production: role in Th2 development and induction of germinal centers. *Eur. J. Immunol.* 28, 3371–3383.
  90. Buhlmann, J. E., Foy, T. M., Aruffo, A., Crassi, K. M., Ledbetter, J. A., Green, W. R., Xu, J. C., Shultz, L. D., Roopesian, D., Flavell, R. A., Fast, L., Noelle, R. J., Durie, F. H. (1995) In the absence of a CD40 signal, B cells are tolerogenic. *Immunity* 2, 645–653.
  91. Oxenius, A., Campbell, K. A., Maliszewski, C. R., Kishimoto, T., Kikutani, H., Hengartner, H., Zinkernagel, R. M., Bachmann, M. F. 1996. CD40-CD40 ligand interactions are critical in T-B cooperation but not for other anti-viral CD41 T cell functions. *J. Exp. Med.* 183, 2209–2218.
  92. Borrow, P., Tishon, A., Lee, S., Xu, J., Grewal, I. S., Oldstone, M. B., Flavell, R. A. 1996. CD40L-deficient mice show deficits in antiviral immunity and have an impaired memory CD81 CTL response. *J. Exp. Med.* 183, 2129–2142.

93. Hayward, A. R., Levy, J., Facchetti Notarangelo, L., Ochs, H. D., Etzioni, A., Bonnefoy, J. Y., Cosyns, M., Weinberg, A. 1997. Cholangiopathy and tumors of the pancreas, liver, and biliary tree in boys with X-linked immunodeficiency with hyper-IgM. *J. Immunol.* 158, 977–983.
94. Hess, S., Engelmann, H. 1996. A novel function of CD40: induction of cell death in transformed cells. *J. Exp. Med.* 183, 159–167.
95. Young, L. S., Eliopoulos, A. G., Gallagher, N. J., Dawson, C. W. 1998. CD40 and epithelial cells: across the great divide. *Immunol. Today* 19, 502–506.
96. Hirano, A., Longo, D. L., Taub, D. D., Ferris, D. K., Young, L. S., Eliopoulos, A. G., Agathangelou, A., Cullen, N., Macartney, J., Fanslow, W. C., Murphy, W. J. 1999. Inhibition of human breast carcinoma growth by a soluble recombinant human CD40 ligand. *Blood* 93, 2999–3007.
97. Henn, V., Slupsky, J. R., Grafe, M., Anagnostopoulos, I., Forster, R., Muller-Berghaus, G., Kroczeck, R. A. 1998. CD40 ligand on activated platelets triggers an inflammatory reaction of endothelial cells. *Nature* 391, 591–594.
98. Galy AHM, Spits H. 1992. CD40 functionally expressed on human thymic epithelium. *J Immunol*, 149:775.
99. Foy TM, Page DM, Waldschmidt TJ, Schoneveld A, Laman JD, Masters SR, Tygrett L, Ledbetter JA, Aruffo A, Claassen E, Xu JC, Flavell RA, Oehen S, Hedrick SM, Noelle RJ. 1995. An essential role for gp39, the ligand for CD40, in thymic selection. *J Exp Med*, 182:1377.
100. Datta, S. K., Kalled, S. L. 1997. CD40-CD40 ligand interaction in autoimmune disease. *Arthritis Rheum.* 40, 1735–1745.
101. Larsen, C. P., Pearson, T. C. 1997. The CD40 pathway in allograft rejection, acceptance, and tolerance. *Curr. Opin. Immunol.* 9, 641–647.
102. Larsen, C. P., Elwood, E. T., Alexander, D. Z., Ritchie, S. C., Hendrix, R., Tucker-Burden, C., Cho, H. R., Aruffo, A., Hollenbaugh, D., Linsley, P. S., Winn, K. J., Pearson, T. C. 1996. Long-term acceptance of skin and cardiac allografts after blocking CD40 and CD28 pathways. *Nature* 381, 434–438.
103. Bhushan A, Covey LR. 2001. CD40:CD40L interaction in X-linked and non X-linked hyper-IgM syndromes. *Immunol Res*, 24:311–324.
104. Weller S, Faili A, Garcia C, et al. 2001. CD40-CD40L independent Ig gene hypermutation suggests a second B-cell diversification pathway in humans. *Proc Natl Acad Sci U S A*, 98:1166–1170.
105. Leone V, Tommasini A, Andolina M, et al. 2002. Elective bone marrow transplantation in a child with X-linked hyper-IgM syndrome presenting with acute respiratory distress syndrome. *Bone Marrow Transplant*, 30:49–52.
106. Ferrari S, Giliani S, Insalaco A, Al-Ghoniaim A, Soresina AR, Loubser M, Avanzini MA, Marconi M, Badolato R, Ugazio AG, Levy Y, Catalan N,

- Durandy A, Tbakhi A, Notarangelo LD, Plebani A. 2001. Mutations of CD40 gene causes an autosomal recessive form of immunodeficiency with hyper IgM. *Proc Natl Acad Sci U S A* 98:12614–12619.
107. Kutukculer N, Moratto D, Aydinok Y, Lougaris V, Aksoylar S, Plebani A, Genel F, Notarangelo LD. 2003. Disseminated cryptosporidium infection in an infant with hyper-IgM syndrome caused by CD40 deficiency. *J Pediatr*. Feb;142(2):194-6.
  108. Giliani S, Ferrari S, Lanzi G, Caraffi S; unpublished data.
  109. Kutukculer N, Aksoylar S, Kensoy S, Cetingul N, Notarangelo LD 2003. Outcome of hematopoietic stem cell transplantation in hyper-IgM syndrome caused by CD40 deficiency. *J Pediatr* 143:141–142.
  110. Etzioni A, Ochs HD. 2004. The hyper IgM syndrome - an evolving story. *Pediatr Res*. Oct;56(4):519-25.
  111. Conley ME, Larche M, Bonagura VR, Lawton III AR, Buckley RH, Fu SM, Coustan-Smith E, Herrod HG, Campana D 1994. Hyper IgM syndrome associated with defective CD40-mediated B cell activation. *J Clin Invest* 94:1404–1409.
  112. Durandy A, Hivroz C, Mazerolles F, Schiff C, Bernard F, Jouanguy E, Revy P, DiSanto JP, Gauchat JF, Bonnefoy JY, Casanova JL, Fischer A 1997. Abnormal CD40 mediated activation pathway in B lymphocytes from patients with hyper-IgM syndrome and normal CD40 ligand expression. *J Immunol* 158:2576–2584.
  113. Revy P, Muto T, Levy Y, Geissmann F, Plebani A, Sanal O, Catalan N, Forveille M, Dufourcq-Labelouse R, Gennery A, Tezcan I, Ersoy F, Kayserili H, Ugazio AG, Brousse N, Muramatsu M, Notarangelo LD, Kinoshita K, Honjo T, Fischer A, Durandy A 2000. Activation-induced cytidine deaminase (AID) deficiency causes the autosomal recessive form of the Hyper- IgM syndrome (HIGM2). *Cell* 102:565–575.
  114. Muto T, Muramatsu M, Taniwaki M, et al. 2000. Isolation tissue distribution and chromosomal localization of the human activation-Induced cytidine deaminase (hAID) gene. *Genomics*, 15:85–88.
  115. Okazaki IM: Kinoshita K., Muramatsu M. et al. 2002. AID enzyme-induced hypermutation in an actively transcribed gene in fibroblasts. *Science*, 296:20033–20036.
  116. Durandy A, Honjo T 2001. Human genetic defects in class-switch recombination (hyper- IgM syndromes). *Curr Opin Immunol* 13:543–548.
  117. Rada C, Williams GT, Nilsen H, Barnes DE, Lindahl T, Neuberger MS 2002. Immunoglobulin isotype switching is inhibited and somatic hypermutation perturbed in UNG-deficient mice. *Curr Biol* 12:1748–1755.
  118. Imai K, Slupphaug G, Lee WI, Revy P, Nonoyama S, Catalan N, Yel L, Forveille M, Kavli B, Krokan HE, Ochs HD, Fischer A, Durandy A 2003.

- Human uracil-DNA glycosylase deficiency associated with profoundly impaired immunoglobulin class-switch recombination. *Nat Immunol* 4:1023–1028.
119. Zonana J, Elder ME, Schneider LC, et al. 2000. A novel X-linked disorder of immune deficiency and hypohidrotic ectodermal dysplasia is allelic to incontinentia pigmenti and due to mutations in IKK-gamma (NEMO). *Am J Hum Genet*, 67:1555–1562.
  120. Doffinger R, Smahi A, Bessia C, et al. 2001. X-linked anhidrotic ectodermal dysplasia with immunodeficiency is caused by impaired NFkB signaling. *Nat Genet*, 27:277–285.
  121. Orange JS, Brodeur SR, Jain A, et al. 2002. Deficient natural killer cell cytotoxicity in patients with IKK-gamma/NEMO mutations. *J Clin Invest*, 109:1501–1509.
  122. Marconi M, Plebani A, Avanzini MA, Maccario R, Pistorio A, Duse M, Stringa M, Monafò V. 1998. IL-10 and IL-4 co-operate to normalize in vitro IgA production in IgA-deficient (IgAD) patients. *Clin Exp Immunol*. Jun;112(3):528-32.
  123. Lehninger, Albert L.; Nelson, David L.; Cox, Michael M. 2004. Principles of Biochemistry 4th ed. New York: W H Freeman & Co.
  124. Liu, H.X., Cartegni, L., Zhang, M.Q., Krainer, A.R. 2001. A mechanism for exon skipping caused by nonsense or missense mutations in BRCA1 and other genes. *Nat. Genet.* 27, 55–58.
  125. Graveley BR. 2000. Sorting out the complexity of SR protein functions. *RNA*. Sep;6(9):1197-211.
  126. Ferrari S, Giliani S, Caraffi S, Lanzi G; unpublished data.
  127. Lanzi G, Giliani S; unpublished data.
  128. Lu KT, Dryer RL, Song C, Covey LR. 2005. Maintenance of the CD40-related immunodeficient response in hyper-IgM B cells immortalized with a LMP1-regulated mini-EBV. *J Leukoc Biol*. Sep;78(3):620-9.
  129. Wu S, Xie P, Welsh K, Li C, Ni CZ, Zhu X, Reed JC, Satterthwait AC, Bishop GA, Ely KR. 2005. LMP1 protein from the Epstein-Barr virus is a structural CD40 decoy in B lymphocytes for binding to TRAF3. *J Biol Chem.*, Sep 30;280(39):33620-6.
  130. Dorak MT (Ed): Real-Time PCR (Advanced Methods Series). Oxford: Taylor & Francis, 2006. (<http://www.dorak.info/genetics/realtime.html>)
  131. Chai H, Yan S, Wang H, Zhang R, Lin PH, Yao Q, Chen C. 2006. CD40 ligand increases expression of its receptor CD40 in human coronary artery endothelial cells. *Surgery*. Aug;140(2):236-42.

132. Carson MJ, Reilly CR, Sutcliffe JG, Lo D. 1998. Mature microglia resemble immature antigen-presenting cells. *Glia*. Jan;22(1):72-85.
133. Maquat, L. E. 1995. When cells stop making sense: effects of nonsense codons on RNA metabolism in vertebrate cells. *RNA* 1, 453–465.
134. Gordon NC, Pan B, Hymowitz SG, Yin J, Kelley RF, Cochran AG, Yan M, Dixit VM, Fairbrother WJ, Starovasnik MA. 2003. BAFF/BLyS receptor 3 comprises a minimal TNF receptor-like module that encodes a highly focused ligand-binding site. *Biochemistry*. May 27;42(20):5977-83.
135. Lin-Lee YC, Pham LV, Tamayo AT, Fu L, Zhou HJ, Yoshimura LC, Decker GL, Ford RJ. 2006. Nuclear localization in the biology of the CD40 receptor in normal and neoplastic human B lymphocytes. *J Biol Chem.*, Jul 7;281(27):18878-87.
136. Tan J, Town T, Paris D, Placzek A, Parker T, Crawford F, Yu H, Humphrey J, Mullan M. Activation of microglial cells by the CD40 pathway: relevance to multiple sclerosis. *J Neuroimmunol*. 1999 Jun 1;97(1-2):77-85.
137. Tan J, Town T, Mori T, Obregon D, Wu Y, DelleDonne A, Rojiani A, Crawford F, Flavell RA, Mullan M. CD40 is expressed and functional on neuronal cells. *EMBO J*. 2002 Feb 15;21(4):643-52.
138. Odeberg J, Piao JH, Samuelsson EB, Falci S, Akesson E. Low immunogenicity of in vitro-expanded human neural cells despite high MHC expression. *J Neuroimmunol*. 2005 Apr;161(1-2):1-11.
139. Ou J H, T S Yen, Y F Wang, W K Kam, and W J Rutter Cloning and characterization of a human ribosomal protein gene with enhanced expression in fetal and neoplastic cells. *Nucleic Acids Res*. 1987. November 11; 15(21): 8919–8934.
140. Conn PM, Knollman PE, Brothers SP, Janovick JA. Protein folding as posttranslational regulation: evolution of a mechanism for controlled plasma membrane expression of a G protein-coupled receptor. *Mol Endocrinol*. 2006 Dec;20(12):3035-41.
141. Valk E, Leung R, Kang H, Kaneko K, Rudd CE, Schneider H. T cell receptor-interacting molecule acts as a chaperone to modulate surface expression of the CTLA-4 coreceptor. *Immunity*. 2006 Nov;25(5):807-21.
142. Trowbridge, I. S., and M. L. Thomas. 1994. CD45: an emerging role as a protein tyrosine phosphatase required for lymphocyte activation and development. *Annu. Rev. Immunol*. 12:85.
143. Barclay, A. N., D. I. Jackson, A. C. Willis, and A. F. Williams. 1987. Lymphocyte specific heterogeneity in the rat leucocyte common antigen (T200) is due to differences in polypeptide sequences near the NH<sub>2</sub>-terminus. *EMBO J*. 6:1259.

144. Saga, Y., J. S. Tung, F. W. Shen, and E. A. Boyse. 1987. Alternative use of 5' exons in the specification of Ly-5 isoforms distinguishing hematopoietic cell lineages. *Proc. Natl. Acad. Sci. USA* 84:5364.
145. Saga, Y., J. S. Lee, C. Saraiya, and E. A. Boyse. 1990. Regulation of alternative splicing in the generation of isoforms of the mouse Ly-5 (CD45) glycoprotein. *Proc. Natl. Acad. Sci. USA* 87:3728.
146. Ralph, S. J., M. L. Thomas, C. C. Morton, and I. S. Trowbridge. 1987. Structural variants of human T200 glycoprotein (leukocyte-common antigen). *EMBO J.* 6:1251.
147. Streuli, M., L. R. Hall, Y. Saga, S. F. Schlossman, and H. Saito. 1987. Differential usage of three exons generates at least five different mRNAs encoding human leukocyte common antigens. *J. Exp. Med.* 166:1548.
148. ten Dam GB, Zilch CF, Wallace D, Wieringa B, Beverley PC, Poels LG, Screatton GR. 2000. Regulation of alternative splicing of CD45 by antagonistic effects of SR protein splicing factors. *J Immunol.* May 15;164(10):5287-95.
149. Tong A, Nguyen J, Lynch KW. 2005. Differential expression of CD45 isoforms is controlled by the combined activity of basal and inducible splicing-regulatory elements in each of the variable exons. *J Biol Chem.* Nov 18;280(46):38297-304.
150. Akbar, A. N., L. Terry, A. Timms, P. C. Beverley, and G. Janossy. 1988. Loss of CD45R and gain of UCHL1 reactivity is a feature of primed T cells. *J. Immunol.* 140:2171.
151. Ratech H, Denning S, Kaufman RE. 1997. An analysis of alternatively spliced CD45 mRNA transcripts during T cell maturation in humans. *Cell Immunol.* May 1;177(2):109-18.
152. Lynch KW, Weiss A. 2000. A model system for activation-induced alternative splicing of CD45 pre-mRNA in T cells implicates protein kinase C and Ras. *Mol Cell Biol.* Jan;20(1):70-80.
153. Fukuhara K, Okumura M, Shiono H, Inoue M, Kadota Y, Miyoshi S, Matsuda H. 2002. A study on CD45 isoform expression during T-cell development and selection events in the human thymus. *Hum Immunol.* May;63(5):394-404.
154. McNeill L, Cassady RL, Sarkardei S, Cooper JC, Morgan G, Alexander DR. 2004. CD45 isoforms in T cell signalling and development. *Immunol Lett.* Mar 29;92(1-2):125-34.

## ACKNOWLEDGEMENTS

This is perhaps the hardest part... who should I thank, and in which order? Luckily, this subject has already been extensively covered by Daniel Pennac (should I thank him too?), you won't find him among the references of this work but you really *ought* to go and find him among the shelves of your favorite bookshop.

Of course everything I talked about in these pages wouldn't have happened without Simona, Cesare, Roberta, Michela, and everyone from the Unit of Medical Genetics, well met and ill met. Please give a big hand for my ex-colleagues and all-time friends at the Unit of Microbiology too, they deserve it for all the patience and support they lent me! Though, if it comes to that, the Golden Globulin for patience goes to all my friends at home, my girlfriend, my parents and relatives, who had to put up with my insouciant attitude during the month-and-a-half I spent entrenched in my room to write down this three-years-worth mumble-jumble of experiments, suppositions, delusions and revelations. I must confess I've had some *excellent* company during this time of self-imposed seclusion: I wouldn't have made it without some soul-soothing strokes from the likes of Morrissey, Kate Bush, Air, Van der Graaf. But most of all, I wouldn't have made it *at all* without he whose very name is the quintessence of genetics. He whose sympathetic example guided me out of the abyss where depression and madness lie. He whose deeds did not exactly help

me cope with my own deadlines. He whose tales, even beyond the grave, helped me pull through the darkest moments. He whose words are written in large, friendly letters, which spell

# ***DON'T PANIC***

upon the blighted night of the soul.